PULSATILE FLOW IN A UNIFORMLY POROUS TUBE

Dissertation for the Degree of Ph. D.

MICHIGAN STATE UNIVERSITY
FRANCIS MARTIN SKALAK

1975

This is to certify that the

thesis entitled

Pulsatile Flow in a
Uniformly Porous Tube

presented by

Francis Martin Skalak

has been accepted towards fulfillment
of the requirements for
Ph.D. degree in Applied Mathematics

C-Y Wang
Major professor

Date July 23, 1975

ABSTRACT

PULSATILE FLOW IN A UNIFORMLY POROUS TUBE

By

Francis Martin Skalak

This work studies the fluid dynamics of pulsatile flow in a porous tube under the following assumptions: a) The flow is laminar, b) The flow is axisymmetric, c) The transverse or angular velocity component is zero, d) Density is constant, e) The tube is uniformly porous, f) The viscosity is constant, g) An unsteady periodic pressure is imposed at the ends of the tube, h) The flow is fully developed.

Under these assumptions the Navier-Stokes equations are reduced to two ordinary differential equations. The first equation, which represents the steady component of velocity, is nonlinear and contains the crossflow Reynolds number, $R = \frac{Va}{\nu}$, where V is the velocity at which the fluid is being injected or extracted, a is the radius of the tube, and ν is the viscosity, as a parameter. The second equation, which represents the unsteady component of velocity, is linear, is coupled to the first but not conversely and contains as parameters the crossflow Reynolds number and the Strouhal number, $\alpha = \frac{a}{2}\sqrt{\frac{\omega}{\nu}}$, where ω is frequency.

To examine the solution of the boundary value problem for the nonlinear equation a scheme was used to transform it into an initial value problem. The resulting equation was examined theoretically and solved numerically. The numerical integration was carried out by means of a Taylor series and a fourth order Runge-Kutta method.

The boundary value problem for the linear equation was solved numerically by a shooting method. Again the numerical solution was found by using a Taylor series and a fourth order Runge-Kutta method. Perturbation solutions for large and small values of the Reynolds number and Strouhal number were also studied by using series methods and the method of matched asymptotic expansions.

For the nonlinear equation giving the steady component of velocity the following results were obtained: a) It was shown theoretically that this equation had two solutions for $R < 4$, four possible solutions for $R > 4$ and no solutions at $R = 4$. The qualitative behavior of each type of solution was also characterized. b) All the theoretical solutions were obtained numerically including two new solutions for large suction.

For the linear equation giving the unsteady component of velocity the following results were obtained: a) Numerical solutions for various values of the Strouhal number and for those values of R for which the steady equation had a solution

were found. b) Suction can cause resonance like effects for small frequency pressure gradients. c) The annular effect occurs but only at higher frequences than in the case of a nonporous tube. d) Asymptotic solutions were found for large and small values of R and α. The results were compared to the numerical solutions and agreement was generally found to be good.

The corresponding two dimensional problem for steady flow is also considered. It is shown theoretically that there is only one type of solution for injection but that three types are possible for suction. Each type of solution is obtained numerically and the results examined in terms of velocity profiles and skin friction at the wall.

PULSATILE FLOW IN A UNIFORMLY POROUS TUBE

By

Francis Martin Skalak

A DISSERTATION

Submitted to

Michigan State University

in partial fulfillment of the requirement

for the degree of

DOCTOR OF PHILOSOPHY

Department of Mathematics

1975

To my Mother and to my fiancée, Bernadette Broniak,
for their encouragement and moral support

ACKNOWLEDGEMENTS

First of all I wish to especially thank Professor C.-Y. Wang whose guidance and suggestions were invaluable in the preparation of this work.

I would also like to thank Jill Shoemaker for all the work she did in preparing the manuscript.

Finally, I would like to thank the Department of Mathematics for their financial support while I was pursuing my degree.

TABLE OF CONTENTS

LIST OF TABLES

LIST OF FIGURES

LIST OF SYMBOLS

a - radius of the tube; point on ξ-axis (Sections 1.3 and A.2); point on λ-axis (Section 3.2)

a_0 - point on ξ-axis

a_0^2 - parameter εs^2

a_1 - point on ξ-axis (Section 1.3); error weight (Section 2.1)

a_2 - error weight

a_3 - error weight

A - coefficient of linear part of pressure gradient

A_0 - determinant of a linear system of equations

b - non-dimensionalized length; point on ξ-axis; point on λ-axis (Section 3.2)

b_0 - real constant

$b_0, b_1, b_2, \ldots$ - complex coefficients of a power series

B - coefficient of linear part of pressure gradient (Section 1.2); real constant (Section 3.2); parameter $\sqrt{-s^2}$ (Section 4.3)

c - point on ξ-axis

$c_0, c_1, c_2, \ldots$ - gauge functions

C - coefficient of unsteady part of pressure gradient (Section 1.2); real constant (Sections 1.3 and 3.4)

C_1 - real constant (Sections 1.3, 2.2, and 3.4); complex constant (Section 4.3)

C_2 - real constant (Sections 1.3 and 2.2); complex constant (Section 4.3)

$C_0(z), C_1(z), \ldots$ - coefficients of the Fourier series for pressure

c_1^0 - real constant

c_2^0 - real constant

d - real constant, $\frac{Ba^2}{4\sqrt{V}}$, (Section 1.2); point on ξ-axis (Section 1.3); one half width of channel (Section A.1)

D - real constant (Section 2.1); complex constant (Sections 4.3 and 4.4)

D_a - real constant

$f(\eta)$ - similarity function for the steady component of velocity in tube and channel flow.

$f_0, f_1, f_2, \ldots$ - functions of order one used in asymptotic expansions for $f(\eta)$

$F(r)$ - related to radial velocity by equation 1.2.6

$F(\lambda)$ - $f(\eta)$ in inner variable

$F_0, F_1, F_2, \ldots$ - functions of order one used in aymptotic expansion for $F(\lambda)$

$g(\xi)$ - transformation of $f(\eta)$ as defined by equation 1.3.1

$g_1(\xi)$ - a function of order one used in an asymptotic expansion for $f(\eta)$

g_1 - computed value of $g(\xi)$ at step size h

g_2 - computed value of $g(\xi)$ at step size $2h$

$G(r)$ - component of velocity in axial direction

h - step size for numerical integration

$h(\eta)$ - non-dimensional form of $H(r)$

$h_0, h_1, h_2, \ldots$ - functions of order one used in asymptotic expansion for $h(\eta)$

h_R - real part of $h(\eta)$

h_i - imaginary part of $h(\eta)$

h_p - particular solution for $h_0(\eta)$

$H(r)$ - complex valued function giving unsteady component of velocity

$H(\lambda)$ - $h(\eta)$ in inner variable

$H_0, H_1, H_2, \ldots$ - functions of order one used in aymptotic expansions for $H(\lambda)$

$H_0(r), H_1(r), \ldots$ - coefficients of the Fourier series for the axial velocity

i - $\sqrt{-1}$

J_0 - Bessel function of the first kind of order zero

J_1 - Bessel function of the first kind of order one

k - real constant (Sections 1.2 and A.1); integer constant (Section 3.2)

$k_0, k_1, k_2, \ldots$ - function of order one used in asymptotic expansions for $h(\eta)$

K - real constant; $\frac{-Ra^2A}{4V^2}$ for the tube; $\frac{Rk}{b^4}$ for the channel

$\bar{K}$ - constant of integration

K_1 - constant, $\frac{K}{\lambda b^2}$

$K_0, K_1, K_2, \ldots$ - functions of order one used in asymptotic expansion for $H(\lambda)$

ℓ - real constant

$\ell_0, \ell_1, \ell_2, \ldots$ - functions of order one used in asymptotic expansions for $h(\eta)$

$L_0, L_1, L_2, \ldots$ - functions of order one used in the asymptotic expansion for $H(\lambda)$

$L_1, L_2, \ldots$ - complex constants

m - integer constant

p - pressure

p_0 - pressure outside porous wall

p_i - pressure inside porous wall

$P_1(z,t)$ - arbitrary function

r - radial distance, modulus of a complex number (Section 4.4)

R - crossflow Reynolds number, $\frac{Va}{\nu}$ for tube, $\frac{Vd}{\nu}$ for the channel

R_i - inlet Reynolds number for steady flow in a non-porous tube, $\frac{2wa}{\nu}$

s - variable of integration

s^2 - complex parameter, $\frac{i\omega a^2}{4\nu}$

t - time

u - non-dimensionalized form of $G(r)$; velocity along channel (Section A.1)

u_0 - a non-dimensionalized component of velocity in channel flow

v - velocity through a porous medium (Section 1.2); velocity toward wall in channel flow (Section A.1)

v_r - radial velocity

v_z - axial velocity

V - velocity at which fluid injected or extracted

w - mean axial flow velocity for steady flow in a non-porous tube

$w(\eta)$ - function used to compute $\frac{\partial h}{\partial C_1}$ and $\frac{\partial h}{\partial C_2}$

x - coordinate along the channel

y - coordinate toward wall of channel

Y_0 - Bessel function of second kind of zero order

Y_1 - Bessel function of second kind of first order

z - axial coordinate

α - real constant (Sections 1.3 and A.2); Strouhal number. $\frac{a}{2}\sqrt{\frac{\omega}{\nu}}$ (Chapter IV)

$\alpha_0, \alpha_1, \ldots$ - gauge functions

β - real constant

$\beta_0, \beta_1, \beta_2, \ldots$ - coefficients in asymptotic expansion

$\gamma_0, \gamma_1, \gamma_2, \ldots$ - gauge functions

δ - width of inner region; error bound (Section 2.1)

$\bar{\delta}$ - exponentially small gauge function

ϵ - small parameter

ζ - variable of order one

η - non-dimensionalized distance, $\frac{r^2}{a^2}$ for tube, y/d for channel

η_t - change over point in solving for $h(\eta)$ numerically

η^* - constant, 0.262

θ - phase lag, argument of complex number (Section 4.4)

λ - parameter $2/R$ (Section 1.3), inner variable

$\mu_0, \mu_1, \ldots$ - gauge functions

ν - viscosity, small parameter (Sections 4.1, 4.2 and 4.3)

$\nu_0, \nu_1, \nu_2, \ldots$ - gauge functions

ξ - non-dimensionalized length (Sections 1.3 and A.2); variable $\frac{\beta\eta}{\epsilon}$ (Section 3.4)

ρ - density

τ - point between 0 and ξ_t or η_t

τ_{rz} - shear stress

$\varphi(\zeta)$ - function of small order defined in equation 1.3.8

$\varphi(r,t)$ - arbitrary function

$\Psi(r,z,t)$ - stream function

$\omega, \omega_0, \omega_1, \omega_2, \ldots$ - frequency

CHAPTER I

INTRODUCTION AND FORMULATION

Section 1.1. Introduction

The problem of describing the flow of a fluid through a pipe from which fluid is being extracted or into which fluid is being injected is important in the following physcial processes: 1) Transpiration cooling. In this process the walls of a pipe transporting a hot fluid are made of a porous material through which fluid is injected to form a protective layer of cooler fluid at the wall [33]. 2) Flow in a heat pipe. In this type of flow fluid is condensing or evaporating at the wall of the tube. In this process the interface between the condensate and the vapor behaves as a permeable wall [8]. 3) Dialysis of blood in artificial kidneys. In this process water and small solutes are removed from the blood by diffusion across a porous wall [10]. 4) The separation of U-235 from U-238 by gaseous diffusion [3]. 5) Boundary layer control to prevent separation and delay transition to turbulence along an airfoil [18]. Since the region of flow of a fluid around an airfoil can be treated as an infinite domain while the region of flow through a tube must be treated as a finite domain the applications of porous tube flow to this process are limited.

The study of these problems has generally been based on the following assumptions: a) The fluid is incompressible. b) The flow is axisymmetric, laminar, and steady. c) Viscosity is constant. d) The walls of the tube are uniformly porous. e) The flow is fully developed. The significance of these assumptions will be discussed further in the next section but for now we shall recount only the previous work done on these types of flows.

The first treatment of a problem in which the fluid is bounded on more than one side by a porous wall was in a paper by Berman [2] in 1953 in which he examined the flow in a uniformly porous channel where fluid was being extracted or injected at the same rate at both walls. He attacked the problem in terms of similarity solutions. By a similarity solutions we mean that the solution of the governing system of partial differential equations can be obtained by solving a system of ordinary differential equations. In this case Berman was able to reduce the problem to solving a non-linear ordinary differential equation involving the cross-flow Reynolds number defined by $R = \frac{Vd}{\nu}$ where V is the velocity of the fluid at the walls, d is one-half the width of the channel and ν is the viscosity of the fluid, as the only parameter. Berman, and later others, studied the asymptotic and numerical solutions of this equation. Two papers by Terrill [21,22] in 1964 and 1965 summarize most of the results that have been obtained for flow through a uniformly porous

channel. In these papers Terrill reported one and only one similarity solution was found for each value of the crossflow Reynolds number. But in 1970 Raithby [16] found numerically a second similarity solution for large suction. The problem of the number of similarity solutions possible for flow in a uniformly porous channel will be treated in Appendix A. We turn now to previous works on the topic of primary interest, that is, flow through a uniformly porous tube.

This problem was first treated in 1955 by Yuan and Finkelstein [33]. In their paper they examined the problem of flow in a uniformly porous tube by seeking similarity solutions. As in the channel problem examined by Berman they were able to reduce the governing system of partial differential equations to a non-linear ordinary differential equation involving the crossflow Reynolds number, R, as the only parameter. In this case R is defined as $\frac{Va}{\nu}$, where V is the velocity at which the fluid is being injected or extracted, a is the radius of the tube and ν is the viscosity. A positive crossflow Reynolds number indicates suction while a negative crossflow Reynolds number indicates injection. Their method of solution was to look for asymptotic solutions for large and small values of the crossflow Reynolds number. The authors were able to find two regular perturbation expansions. The first was valid for small injection and suction while the second was valid for large injection. However no numerical results were obtained to check the accuracy of their expansions.

Later Morduchow [11] used the method of averages to find an approximate solution to the ordinary differential equation deduced by Yuan and Finkelstein valid for all values of negative Reynolds number. However again no numerical results were obtained and the accuracy of the approximate values obtained by Morduchow was checked by comparison with the asymptotic values obtained by Yuan and Finkelstein.

The first numerical results for this problem were obtained by Eckert, Donoughe, and Moore [6]. In their paper they studied numerical solutions of the ordinary differential equation given by Yuan and Finkelstein. For R, the crossflow Reynolds number, negative only one numerical solution was found, but for R positive two numerical solutions were found at $R = 2$ and $R = 10$ but no numerical solutions were found for $2 < R < 10$. A year later Berman, studying the same equation, found two solutions for $2.05 < R < 2.3$ and $R > 9$ and no solutions for $2.3 < R < 9$. Both Berman and Eckert et al. attributed their failure to find similarity solutions for $2.3 < R < 9$ to the fact that as the Reynolds number increased to 2.3 the skin friction at the wall drops to zero which, in conjunction with an adverse pressure gradient, results in separation of the flow from the wall. This situation of multiple solutions or no solutions for suction contrasted sharply with the case of channel flow where, up to this time, one and only one similarity solution had been found for each value of the corresponding crossflow Reynolds number.

To examine why no similarity solutions were found in tube flow for $2.3 < R < 9$ Weissberg [29] studied the flow at the entrance region of the pipe. He was able to show that for $2.4 < R < 7.6$ and for a parabolic inlet profile fully developed flow could not be achieved. Since Weissberg the problem of flow in the entrance region for a uniformly porous pipe has received considerable interest in the literature. Since in this work we will not be considering the flow in the entrance region we refer the reader to Quaile and Levy [15] for a current list of references on this problem.

In 1962 White [30] studied the solutions of the ordinary differential equation deduced by Yuan and Finkelstein by means of a power series expansion. He was able to predict dual solutions for $0 < R < 2.3$ and $R > 9.1$, but was unable to find any solutions for $2.3 < R < 9.1$. Dual solutions for $2.0 < R < 2.3$ had been predicted previously by Berman by extending Morduchow's method of averages to small values of suction.

In 1969 Terrill and Thomas [24] published a comprehensive study of the theoretical results for similarity solutions for flow through a uniformly porous tube. Numerically they were able to find two solutions for all values of suction and injection except for $2.3 < R < 9.0$. They were able to find asymptotic solutions for large injection and for small suction and injection for the new solutions they had obtained.

Also they were able to obtain a series which was asymptotic to both numerical solutions obtained for large suction. The difference between the series and the two solutions for suction was found to be exponentially small but in this paper they were unable to find these terms. However in a later paper Terrill [23] was able to give the missing terms of the expansion. Since the paper by Terrill and Thomas has the most complete discussion of fully developed steady flow in a uniformly porous tube, several of their results and techniques will be useful in our study of unsteady flow in a porous tube.

Fully developed flows through porous tubes have also been studied by Peng and Yuan [13], Kinney [8], Raithby [16] and others in connection with heat transfer problems. These studies have as far as flow through porous tubes is concerned, mainly reviewed and reworked older results.

In all the above studies of flow through a porous tube the transverse or angular velocity component was assumed to be zero. In 1972, however, Terrill and Thomas [25], extending an older work by Prager [14] examined fully developed flow in a uniformly porous tube with a non-zero angular velocity component. The main point of this work was to examine whether by including a non-zero angular velocity, similarity solutions could be obtained for $2.3 < R < 9.0$. Under this assumption they were able to find in this range two similarity solutions for each value of R. Although this is a very interesting result our study will be restricted to the case where the angular velocity component is zero.

Experimental work has been done recently for fully developed flows in uniformly porous tubes. The case of injection was examined by Bundy and Weissberg [4]. For $-8 < R < 0$ their experimental results agreed well with the theoretical results of the injection solution first studied by Yuan and Finkelstein. The case of small suction was examined experimentally by Quaile and Levy [15]. Although their experiment was designed to verify the entrance region solution, their studies showed that for $0 < R < 1.2$ there was good agreement between the similarity solution originally found by Yuan and Finkelstein and experimental results. For $1.2 < R < 2.3$ the agreement between the theoretical similarity solution and experimental results progressively decreased.

The problem of fully developed pulsatile flow in a rigid impermeable pipe has been discussed in connection with several applications. The most extensive work on this problem has appeared in the study of the circulation of the blood. However pulsatile flows have also been applied to studies in acoustics, surge phenomena in power plants, and supercharging systems in piston engines. This type of flow was first studied experimentally by Richardson and Tyler [17] in 1929. They observed that as the frequency of the pulsatile pressure increased the maximum axial velocity of the fluid shifts from the center to the wall of the tube. Sexl [19] in 1930 studied similarity solutions for fully developed pulsatile flow in a

tube to explain this effect. The ordinary differential equation he obtained, he was able to solve exactly in terms of Bessel functions. The solution explained the phenomenom observed by Richardson and Tyler. Womersley [31] in 1955 and Uchida [26] in 1956 both examined further aspects of the solution obtained by Sexl. It was found that as the frequency increased, the phase lag of the maximum shear stress or skin friction at the wall and axial velocity relative to the pressure gradient increased while the maximum skin friction at the wall decreased.

No previous work has been found in the literature on the effects of suction and injection on pulsatile flow in a tube. The most closely related work is a paper by Wang [28] which discusses pulsatile flow in a uniformly porous channel and in an annulus in which fluid is being injected from one side and extracted at the same rate from the other side.

In this work we will be studying the effects of suction and injection on pulsatile flow. In the next section we state our assumptions about the flow and reduce the governing system of partial differential equations to a system of two ordinary differential equations in a manner analagous to Berman's treatment of flow in a porous channel and Yuan and Finkelstein's treatment of flow in a porous tube. The first equation will be the same as that obtained previously in the study of steady flow in a uniformly porous tube and will give

the steady component of the flow. The second equation, which is coupled to the first, will give the unsteady component of the flow. Since the unsteady component of the flow is coupled to the steady component, but not conversely, we then proceed to examine the following aspects of the steady component of the flow:

1. The number and qualitative behavior of the solutions for each value of the crossflow Reynolds number.
2. The numerical solutions.
3. The asymptotic solutions for large and small values of the crossflow Reynolds number.

With these solutions we are then able to examine the following aspects of the unsteady component of the flow:

1. The numerical solutions.
2. The effects of suction and injection on the skin friction at the wall, the phase shift of the velocity profile and skin friction at the wall relative to the pulsatile pressure gradient, and the annular effect.
3. The asymptotic solutions for large and small values of the crossflow Reynolds number and Strouhal number and the accuracy of these solutions.

Section 1.2. Formulation of the Problem.

Consider flow through a rigid circular tube into which fluid is being injected or from which fluid is being extracted through the walls (see Figure 1.2.1). The following assumptions about the flow will be made:

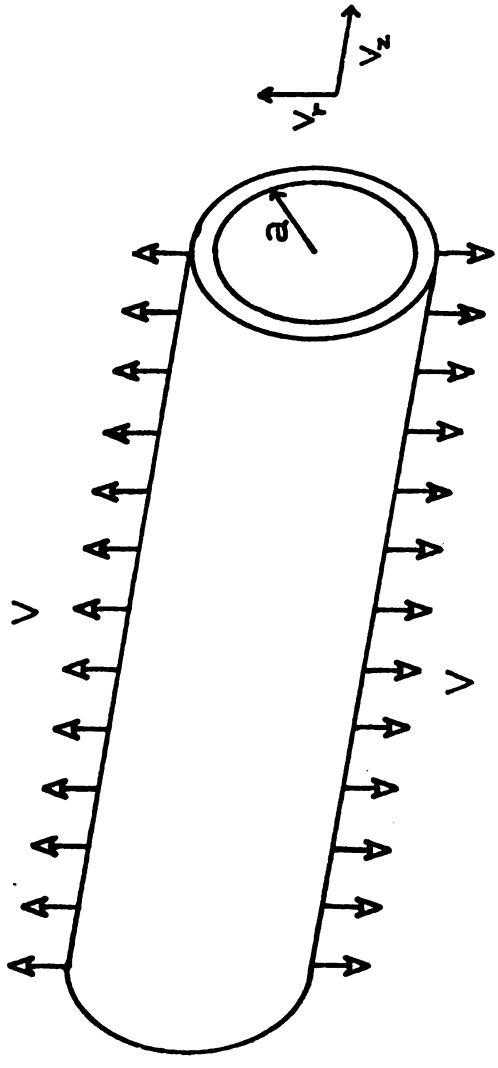

Figure1.2.1. Uniformly porous tube.

a) The flow is laminar. For steady flow in an impermeable tube laminar flow can be maintained up to an inlet Reynolds number, defined by $R_i = \frac{2aw}{\nu}$, where w is the mean axial flow-velocity, a is the radius of the tube, and ν is the viscosity, of around 2000 [18]. The value of R_i at which transition from laminar to turbulent flow occurs in a porous tube has not been thoroughly studied. However the experimental studies of Quaile and Levy [15] indicate that, at least for small suction, transition occurs at a much lower value of R_i. There does not appear to be any experimental data available in the literature on the transition of a flow driven by a pulsatile pressure gradient.
b) The flow is axisymmetric. This assumption means there is no angular dependence in the velocity components.
c) The transverse or angular velocity component is zero. As mentioned previously the effect of including a non-zero angular velocity component on steady flow in a porous tube has been studied by Terrill and Thomas [25] with interesting results. However we will not examine this effect in our study of pulsatile flow in a uniformly porous tube.
d) Density is a constant. This assumption greatly simplifies the continuity equation but makes the solution of limited applicability to a large number of important problems such as filtration where density variations must be considered.
e) The tube is uniformly porous. In the literature this has been taken to mean that the radial velocity at the wall is a constant. The following discussion establishes the soundness

of this condition in the case of injection. From Darcy's Law [32] it is known that the velocity of a fluid through a porous medium is proportional to the pressure difference. That is, $v = k(p_o - p_i)$ where v is the velocity through the porous wall, k is a constant of proportionality, p_o is the pressure outside the porous wall, and p_i is the pressure inside the porous wall. If $p_o >> p_i$ then $v \cong kp_o$. Thus, since p_o could be held constant, the velocity of the fluid at the wall would be approximately constant. However in the case of suction this condition is not so plausible because the pressure at the inside wall of the tube must be larger than the pressure outside the wall in order that fluid be extracted from the flow. However the pressure inside the wall is axially dependent. Thus it would seem that to maintain a constant velocity at the wall the permeability of the wall must also vary accordingly with the axial position. In most physical situations this does not occur. However Quaile and Levy [15] claimed they were able to obtain uniform suction by using a tube with very low permeability in their experiments. Also it has been observed by Kinney [8] that the vapor-liquid interface of a vapor and its condensate could be treated as a porous boundary through which fluid is being extracted with a constant velocity. Thus the condition of constant radial velocity at the wall could be used for both injection and suction.

A problem in which the velocity at the wall has not been assumed to be constant has been discussed by Kozinski, Schmidt and Lightfoot [9]. The governing equation used, however, is the linear Stokes equation which does not exhibit the complicated non-linear phenomena presented in this study.

f) Viscosity is constant.

g) The tube is sufficiently long that the flow is fully developed. By this assumption we mean that end effects and the effects of starting the motion of the fluid from rest will not be considered and also that the radial velocity is a function of the radial distance only.

h) An unsteady periodic pressure is imposed at the ends of the tube. The form of the imposed pressure will be determined by the other assumption on the flow.

We turn now to the mathematical formulation of the problem. In this case the cylindrical coordinate system is the natural one to use. The axisymmetric Navier-Stokes equation in cylindrical coordinates with no angular component of velocity as given by Schlichting [18] become

1.2.1a
$$\frac{\partial v_r}{\partial t} + v_r \frac{\partial v_r}{\partial r} + v_z \frac{\partial v_r}{\partial z} = - \frac{1}{\rho} \frac{\partial p}{\partial r} + \nu\left(\frac{\partial^2 v_r}{\partial r^2} + \frac{1}{r} \frac{\partial v_r}{\partial r} - \frac{v_r}{r^2} + \frac{\partial^2 v_r}{\partial z^2}\right)$$

1.2.1b $$\frac{\partial v_z}{\partial t} + v_r \frac{\partial v_z}{\partial r} + v_z \frac{\partial v_z}{\partial z} = - \frac{1}{\rho} \frac{\partial p}{\partial z} + \nu\left(\frac{\partial^2 v_z}{\partial r^2} + \frac{1}{r} \frac{\partial v_z}{\partial r} + \frac{\partial^2 v_z}{\partial z^2}\right)$$

The continuity equation is given by

1.2.2 $$\frac{\partial v_r}{\partial r} + \frac{v_r}{r} + \frac{\partial v_z}{\partial z} = 0$$

Since we will be examining the skin friction or shear stress at the wall we give also that

1.2.3 $$\tau_{rz} = \rho\nu\left(\frac{\partial v_r}{\partial z} + \frac{\partial v_z}{\partial r}\right)$$

The boundary conditions are

1.2.4 $$v_r(a,z) = V \qquad v_z(a,z) = 0$$

$$\left.\frac{\partial v_z}{\partial r}\right|_{r=0} = 0 \qquad v_r(0,z) = 0$$

Since we are not considering the problem of starting the fluid from rest no initial condition is required.

The continuity equation allows us to define a stream function Ψ such that

1.2.5 a) $$v_r = - \frac{\partial \Psi}{\partial z} \qquad \text{b)} \quad v_z = \frac{1}{r} \frac{\partial}{\partial r} (r\Psi)$$

Since it has been assumed that the radial velocity is a function of r alone and to simplify the form of the equations we write

1.2.6 $$v_r = \frac{F(r)}{r}$$

where $F(r)$ is a function to be determined.

Then from equations 1.2.5a and 1.2.6 we get

1.2.7 $$\psi = \frac{-zF(r)}{r} + \frac{1}{r}\varphi(r,t)$$

where $\frac{\varphi}{r}$ is an arbitrary function of integration. From equations 1.2.5b and 1.2.7 we obtain that

1.2.8 $$v_z = \frac{-zF'(r)}{r} + \frac{1}{r}\frac{\partial\varphi}{\partial r}$$

Substituting equations 1.2.6 and 1.2.8 into equation 1.2.2a one obtains after an integration with respect to r

1.2.9a $$-\frac{1}{\rho}p = \frac{1}{2}\left(\frac{F(r)}{r}\right)^2 - \nu\left(\frac{d}{dr}\left(\frac{F(r)}{r}\right) + \frac{F(r)}{r^2}\right) + P_1(z,t)$$

where $P_1(z,t)$ is an arbitrary function. Substituting equations 1.2.6, 1.2.8 and 1.2.9a into equation 1.2.2b gives

1.2.9b $$\frac{1}{r}\frac{\partial^2\varphi}{\partial r\partial t} + z\left(\frac{-F(r)}{r}\frac{d}{dr}\left(\frac{F(r)}{r}\right) + \left(\frac{F'(r)}{r}\right)^2 + \nu\frac{d^2}{dr^2}\left(\frac{F'(r)}{r}\right)\right.$$
$$\left. + \frac{\nu}{r}\frac{d}{dr}\left(\frac{F'(r)}{r}\right)\right) + \frac{F(r)}{r}\frac{\partial}{\partial r}\left(\frac{1}{r}\frac{\partial\varphi}{\partial r}\right) - \frac{F'(r)}{r^2}\frac{\partial\varphi}{\partial r}$$
$$- \nu\frac{\partial^2}{\partial r^2}\left(\frac{1}{r}\frac{\partial\varphi}{\partial r}\right) - \frac{\nu}{r}\frac{\partial}{\partial r}\left(\frac{1}{r}\frac{\partial\varphi}{\partial r}\right) = -\frac{1}{\rho}\frac{\partial P_1}{\partial z}$$

Since equation 1.2.9b is linear in t and the imposed pressure is periodic we write $\frac{1}{r}\frac{\partial\varphi}{\partial r}$ and $P_1(z,t)$ in terms of Fourier series as follows:

$$\frac{1}{r}\frac{\partial\varphi}{\partial r} = G(r) + \sum_n H_n(r)e^{i\omega_n t}$$

$$P_1(z,t) = C_0(z) + \sum_n C_n(z)e^{i\omega_n t}$$

Since equation 1.2.9b shows that $C_0(z)$ must be quadratic in z and $C_n(z)$ must be linear in z and since the linearity of equation 1.2.9b in t allows us, without loss of generality to restrict our analysis to only one component of the Fourier series we write v_z and p as follows:

1.2.10a $$v_z = \frac{-zF'(r)}{r} + G(r) + H(r)e^{i\omega t}$$

1.2.10b $$\frac{-p}{\rho} = \frac{1}{2}\left(\frac{F(r)}{r}\right)^2 - \nu\left(\frac{d}{dr}\left(\frac{F(r)}{r}\right) + \frac{F(r)}{r^2}\right) - Az^2 - Bz + Cze^{i\omega t} + D + D_a e^{i\omega t}$$

where A,B,C,D and D_a are constants.

To nondimensionalize the problem and simplify the form of the resulting equations we rescale the variables as follows:

$$r = a\eta^{1/2} \qquad F(r) = aVf(\eta) \qquad G(r) = Vu(\eta)$$

$$H(r) = \frac{Ca^2}{4\nu} h(\eta)$$

Equations 1.2.6 and 1.2.10a then become

1.2.11a $$v_r = \frac{Vf(\eta)}{\eta^{1/2}}$$

1.2.11b $$v_z = \frac{-zVf'(\eta)}{a} + Vu(\eta) + \frac{Ca^2}{4\nu} h(\eta)e^{i\omega t}$$

Substituting equations 1.2.11a, 1.2.11b and 1.2.10b into equation 1.2.9b we obtain the following system of ordinary differential equations for the three unknown functions:

1.2.12 $$\eta f'''(\eta) + f''(\eta) + \frac{R}{2}(f'^2(\eta) - f''(\eta)f(\eta)) = K$$

1.2.13 $$\eta u''(\eta) + u'(\eta) + \frac{R}{2}(u(\eta)f'(\eta) - u'(\eta)f(\eta)) = d$$

1.2.14 $$\eta h''(\eta) + h'(\eta) = s^2 h(\eta) - 1 + \frac{R}{2}(f(\eta)h'(\eta) - h(\eta)f'(\eta))$$

where $K = \frac{-Ra^2A}{4V^2}$, $d = \frac{Ba^2}{4\nu V}$, $s^2 = \frac{i\omega a^2}{4\nu}$ and $R = \frac{Va}{\nu}$ is the crossflow Reynolds number. The boundary conditions given by equation 1.2.4 become

1.2..5 $$f(1) = 1 \quad f'(1) = 0 \quad f(0) = 0 \quad \lim_{\eta \to 0} \eta^{1/2} f''(\eta) = 0$$

1.2.16 $$u(1) = 0 \quad \lim_{\eta \to 0} \eta^{1/2} u'(\eta) = 0$$

1.2.17 $$h(1) = 0 \quad \lim_{\eta \to 0} \eta^{1/2} h'(\eta) = 0$$

The equation for pressure becomes

1.2.18 $$\frac{-p}{\rho} = -Az^2 - Bz + Cze^{i\omega t} + D + D_a e^{i\omega t} + V^2\left(\frac{f^2}{2\eta} - \frac{2f'}{R}\right)$$

The shear stress or skin friction at the wall is then given by

1.2.19 $$\tau_{rz} = \frac{-4\rho\nu z}{a^2} f''(1) + \frac{2\rho\nu}{a} Vu'(1) + \frac{Ca\rho}{2} h'(1)e^{i\omega t}$$

Equations 1.2.12 and 1.2.13 represent the similarity solutions to the problem of steady flow as studied by Terrill and Thomas [24]. Equation 1.2.14 represents the effects of suction and injection on unsteady flow.

Before proceeding we wish to comment on the solution of equation 1.2.13. It has been observed by Terrill and Thomas [24] that $u(\eta) = \frac{-B}{Aa} f'(\eta)$ is a particular solution of equation 1.2.13 satisfying the boundary conditions given by equation 1.2.16. This will be the only solution of equation 1.2.13 if the corresponding homogeneous problem has only the trivial solution. By using Sturm-Liouville theory Terrill and Thomas were able to show that if $R \leq 0$ and $f'(\eta) \geq 0$ on $(0,1)$ the homogeneous problem had only the trivial solution. Whether there are nontrivial solutions of the homogeneous problem in other cases was not examined by them. This work does not examine this problem further and following their lead we take $u(\eta) = \frac{-B}{Aa} f'(\eta)$ as the solution of equation 1.2.13. Thus the flow is described by the solutions of equation 1.2.12 and 1.2.14.

Section 1.3. Completeness of the Problem for the Steady Component of Velocity.

Since the equation for the unsteady component of velocity is coupled to the equation for the steady component of velocity, but not conversely, we begin our analysis by examining the solutions of equation 1.2.12. As discussed

previously various authors have examined the solutions of equation 1.2.12 and have found that for some values of R this equation has no solutions while for other values of R this equation has more than one solution. In attempting to repeat numerically their solutions of equation 1.2.12 in order to examine the numerical solutions of equation 1.2.14 two solutions of equation 1.2.12, not previously mentioned in the literature, were found. Thus it became important to examine how many solutions of equation 1.2.12 were possible. The following method for examining the solutions of equation 1.2.12 was motivated by the numerical technique used for obtaining solutions of this equation. This technique will be described further in Section 2.1.

By making the transformation

1.3.1 $$f(\eta) = \lambda g(\xi)$$

where

$$\eta = \xi/b$$

Equation 1.2.12 becomes

1.3.2 $$\xi g'''(\xi) + g''(\xi) + g'^2(\xi) - g(\xi)g''(\xi) = K_1$$

where

$$K_1 = \frac{K}{\lambda b^2} \quad \text{and} \quad \lambda = \frac{2}{R}$$

and boundary conditions 1.2.15 become

1.3.3 a) $g(0) = 0$ c) $g'(b) = 0$

b) $\lim_{\xi \to 0} \xi^{1/2} g''(\xi) = 0$ d) $g(b) = \frac{1}{\lambda} = R/2$

Since the transformation 1.3.1 is non-singular and from boundary conditions 1.3.3 it is seen that solutions of 1.2.12 can be examined by studying the zeroes of $g'(x)$ for the following initial value problem.

1.3.4a $\xi g'''(\xi) + g''(\xi) + g'^2(\xi) - g(\xi)g''(\xi) = K_1$

1.3.4b $g(0) = 0$ $g''(0) = \beta$

$g'(0) = \alpha$ $K_1 = \beta + \alpha^2$

where α and β are non-zero real constants.

Only solutions of 1.3.4 will be examined which satisfy the following:

a) $g(\xi)$ is analytic at zero

b) $g^V(\xi)$ is continuous for all $\xi \geq 0$.

By the assumptions on the flow any physically meaningful solution could be expected to satisfy these smoothness requirements. Thus the physical applicability of the solutions is not compromised by these requirements.

Theorem 1.3.1. Let $g(\xi)$ be any solution of 1.3.4 subject to a) and b) above, then $g'''(\xi)$ is decreasing for all $\xi \geq 0$.

Proof: Differentiating 1.3.4a twice gives

1.3.5 $$\xi g^{IV}(\xi) = g'''(\xi)(g(\xi) - 2) - g'(\xi)g''(\xi)$$

1.3.6 $$\xi g^{V}(\xi) = g^{IV}(\xi)(g(\xi) - 3) - g''(\xi)^2$$

and applying 1.3.4b gives

1.3.7a $$g'''(0) = -\frac{1}{2}\alpha\beta$$

1.3.7b $$g^{IV}(0) = -\frac{1}{3}\beta^2$$

Since $g^{IV}(0) < 0$ it is sufficient to show that $g^{IV}(\xi) \leq 0$ for all $\xi > 0$. Let $a > 0$ be any point such that $g^{IV}(a) = 0$, then from 1.3.6 $g^{V}(a) = \frac{-g''^2}{a} \leq 0$. Thus at any point where $g^{IV}(\xi)$ is zero its slope is zero or negative. Therefore $g^{IV}(\xi) \leq 0$ for all $\xi > 0$. Q.E.D.

The zeroes of $g'(\xi)$ will now be examined by examining all combinations of signs for α and β.

Theorem 1.3.2. If $\alpha < 0$ and $\beta < 0$ then $g'(\xi)$ has no zeroes.

Proof: In this case by 1.3.7a $g'''(0) = -\frac{1}{2}\alpha\beta < 0$, $g''(0) < 0$ and $g'(0) < 0$. Thus by Theorem 1.3.1 $g'''(\xi) < 0$ for all ξ. Thus $g''(\xi)$ and hence $g'(\xi)$ are less than zero for all ξ. Thus $g'(\xi)$ has no zeroes. Q.E.D.

Theorem 1.3.3. If $\alpha < 0$ and $\beta > 0$ then $g'(\xi)$ has two zeroes. See Figure 1.3.1 for a qualitative description of this solution.

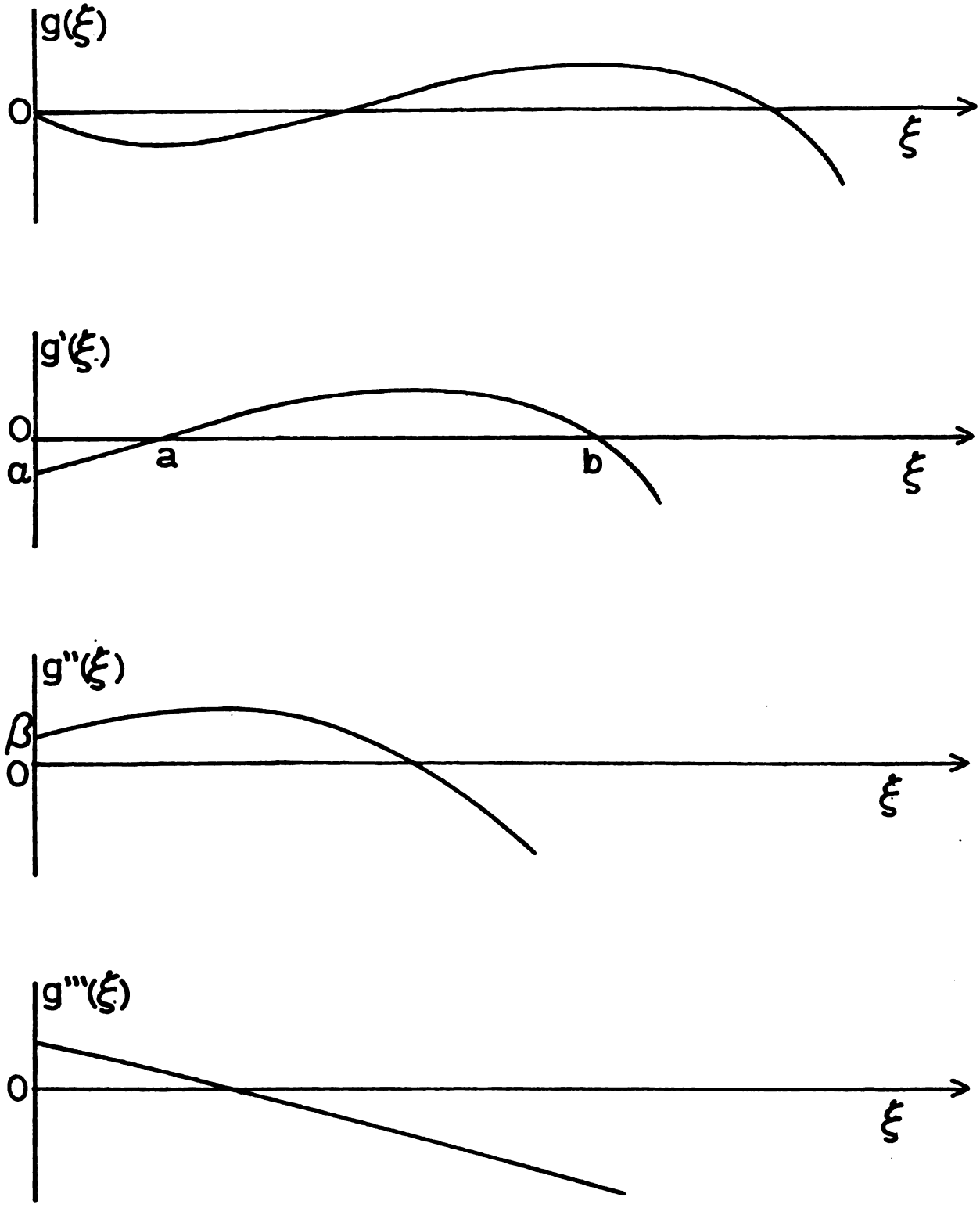

Figure 1.3.1.
The solution of equation 1.3.4. for $\alpha<0$ and $\beta>0$. The concavity of $g'''(\xi)$ is undetermined.

In this case $g'''(0) = -\frac{1}{2}\alpha\beta > 0$, $g''(0) > 0$, $g'(0) < 0$ and $K_1 = \beta + \alpha^2 > 0$. The proof of the theorem is contained in the following four lemmas.

Lemma 1.3.1. If $\alpha < 0$ and $\beta > 0$ there exists a point c such that $g'''(c) = 0$ and $g'''(\xi) > 0$ for all $0 \leq \xi < c$.

Proof: Suppose there is no such c. Then since $g'''(0) > 0$ $g'''(\xi) > 0$ for all ξ. Hence since $g''(0) > 0$, $g''(\xi) > 0$ for all ξ. Thus $g'(\xi)$ is increasing and concave up for all ξ and thus must cross the ξ-axis. After the point where $g'(\xi)$ crosses the ξ-axis $g(\xi)$ is increasing and concave up and must eventually exceed the value 3. But past the point where $g(\xi)$ exceeds the value 3, $g^{V}(\xi)$ must necessarily be negative as equation 1.3.6 shows. This makes $g'''(\xi)$ concave down and since by Theorem 1.3.1 $g'''(\xi)$ must be decreasing there must be a point c such that $g'''(c) = 0$ and $g'''(\xi) > 0$ for all $0 \leq \xi < c$. Q.E.D.

Lemma 1.3.2. There exists a point a such that $0 < a < c$ and $g'(a) = 0$.

Proof: At c since $g'''(c) = 0$ equation 1.3.5 gives $cg^{IV}(c) = -g'(c)g''(c)$. Since for $0 \leq \xi \leq c$ $g'''(\xi) \geq 0$ and since $g''(0) > 0$, $g''(c) > 0$. By Theorem 1.3.1 $g^{IV}(c) < 0$. Therefore $g'(c) > 0$. Thus since $g'(0) < 0$ there is a point $0 < a < c$ such that $g'(a) = 0$. Q.E.D.

At a $g(\xi)$ and its derivatives have the following properties:

$g(a) < 0 \qquad g'(a) = 0 \qquad g''(a) > 0 \qquad g'''(a) > 0$

By equation 1.3.3d this gives $R = 2g(a) < 0$. The solution $f(\eta)$ of 1.2.12 corresponding to this zero of $g'(x)$ will be denoted Section I solutions for injection.

Lemma 1.3.3. There exists a point $b > c$ such that $g'(b) = 0$.

Proof: Since for $\xi > c$ $g'''(\xi) < 0$ and by Theorem 1.3.1 $g''(\xi)$ will be decreasing and concave down and hence must eventually cross the ξ-axis. After $g''(\xi)$ cross the ξ-axis $g'(\xi)$ becomes decreasing and concave down. Hence there must be a point $b > c$ such that $g'(b) = 0$. Q.E.D.

At b equation 1.3.5 and Theorem 1.3.1 give $g'''(b)(g(b) - 2) = bg^{IV}(b) < 0$. Since at b $g'''(b) < 0$, $g(b) > 2$. Thus at b $g(\xi)$ and its derivatives have the following properties

$g(b) > 2 \qquad g'(b) = 0 \qquad g''(b) < 0 \qquad g'''(b) < 0$

By equation 1.3.3d this gives $R = 2g(a) > 4$. The solution $f(\eta)$ of 1.2.12 corresponding to this zero of $g'(\xi)$ will be denoted as Section V(i) solutions.

Lemma 1.3.4. $g'(\xi)$ has no further zeroes.

Proof: Since at b $g'''(b) < 0$ and by Theorem 1.3.1 $g'''(\xi) < 0$ for all $\xi > b$. Therefore since at b $g''(b) < 0$ $g''(\xi) < 0$ for all $\xi > b$. Therefore since $g'(b) = 0$ $g'(\xi)$ has no zeroes for $\xi > b$. Q.E.D.

Theorem 1.3.4. If $\alpha > 0$ and $\beta > 0$ then $g'(\xi)$ has one zero. See Figure 1.3.2 for a qualitative description of this solution.

In this case $g'''(0) < 0$, $g''(0) < 0$, $g'(0) > 0$ and $K_1 > 0$.

Proof: Since $g'''(0) < 0$ and by Theorem 1.3.1 $g''(\xi)$ is decreasing and concave down for all ξ. Therefore $g''(\xi)$ must eventually become negative and hence $g'(\xi)$ will be decreasing and concave down. Hence there must be a point a such that $g'(a) = 0$. That $g'(\xi)$ has no further zeroes follows from the same arguments as for Lemma 1.3.4. Q.E.D.

At point a equation 1.3.5 and Theorem 1.3.1 give $g'''(a)(g(a) - 2) = ag^{IV}(a) < 0$. Since at a $g'''(a) < 0$, $g(a) > 2$. Thus at $\xi = a$ $g(\xi)$ and its derivatives have the following properties.

$g(a) > 2$ $\quad$ $g'(a) = 0$ $\quad$ $g''(a) < 0$ $\quad$ $g'''(a) < 0$

By equation 1.3.3d this gives $R = 2g(a) > 4$. The solution $f(\eta)$ of 1.2.12 corresponding to this zero of $g'(x)$ will be denoted as Section V(ii) solutions.

Theorem 1.3.5. If $\alpha > 0$ and $\beta < 0$ then $g'(\xi)$ has either one zero or three zeroes. See Figures 1.3.3, 1.3.4, and 1.3.5 for a qualitative description of this case.

In this case $g'''(0) > 0$, $g''(0) < 0$, $g'(0) > 0$. K_1 may be positive or negative depending on the relative size of α and β.

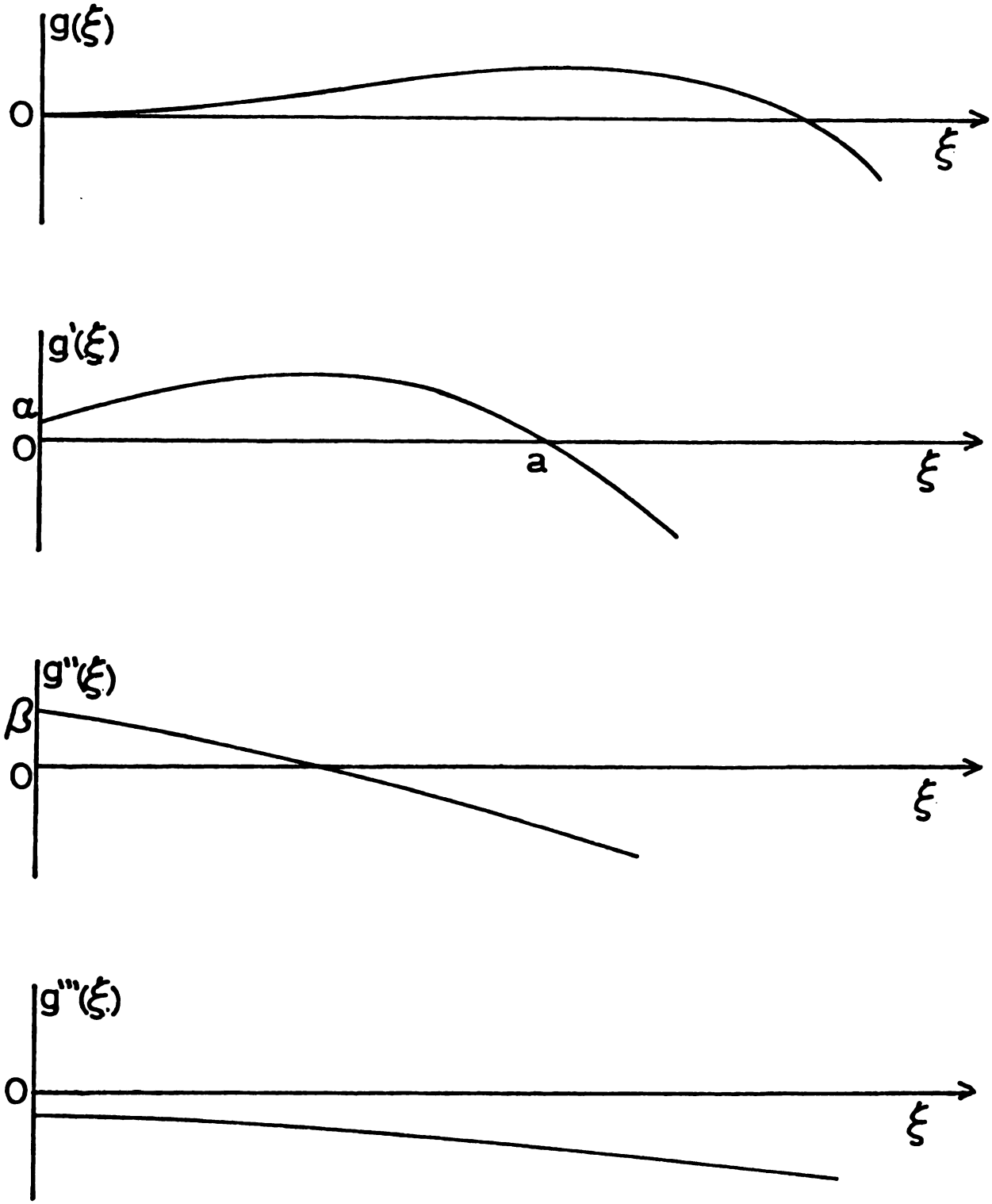

Figure 1.3.2.
The solution of equation 1.3.4. for $\alpha>0$ and $\beta>0$. The concavity of $g'''(\xi)$ is undetermined.

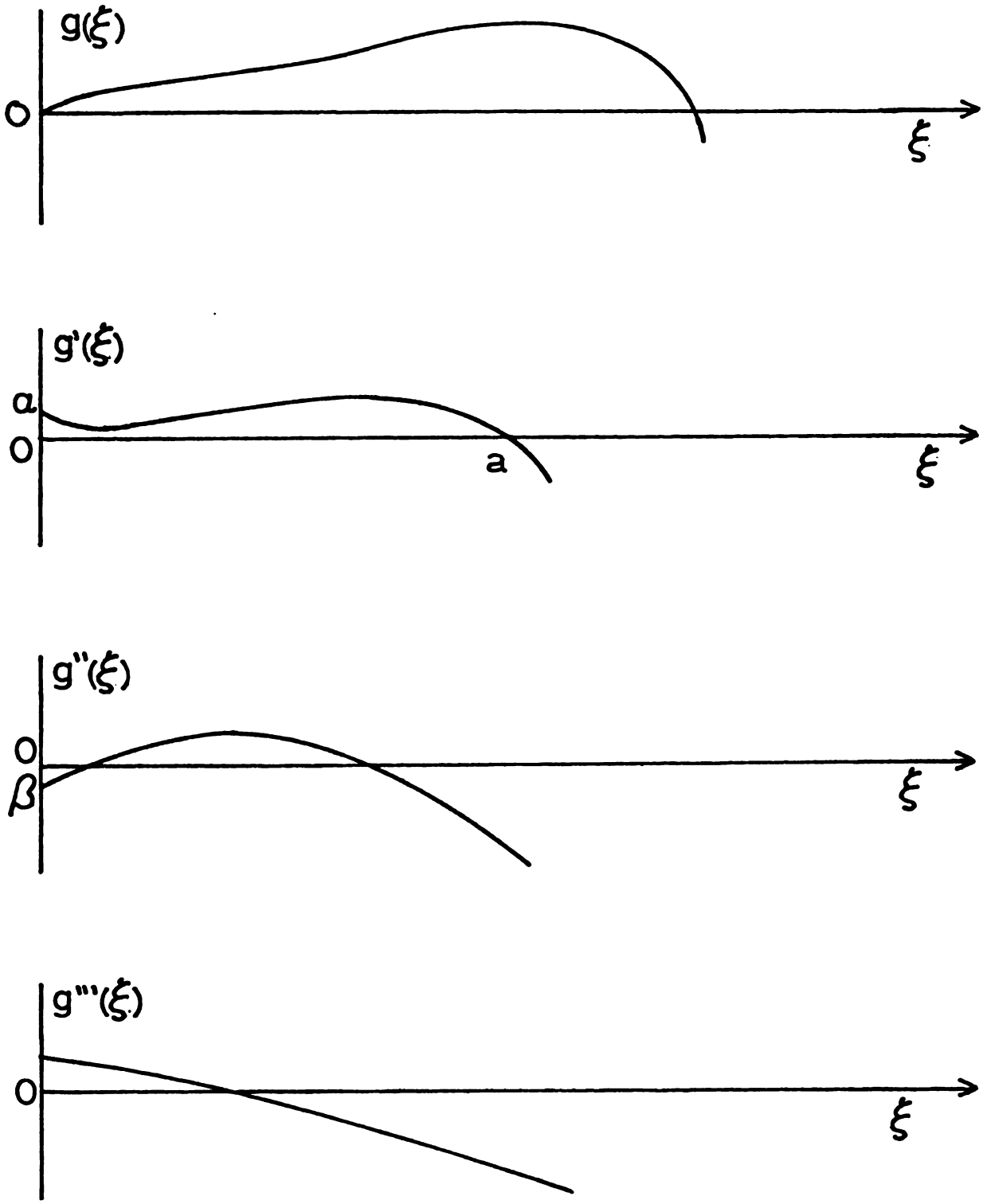

Figure 1.3.3.
The solution of equation 1.3.4. for $\alpha>0$ and $\beta<0$ if a is a Type I zero. The concavity of $g'''(\xi)$ is undetermined.

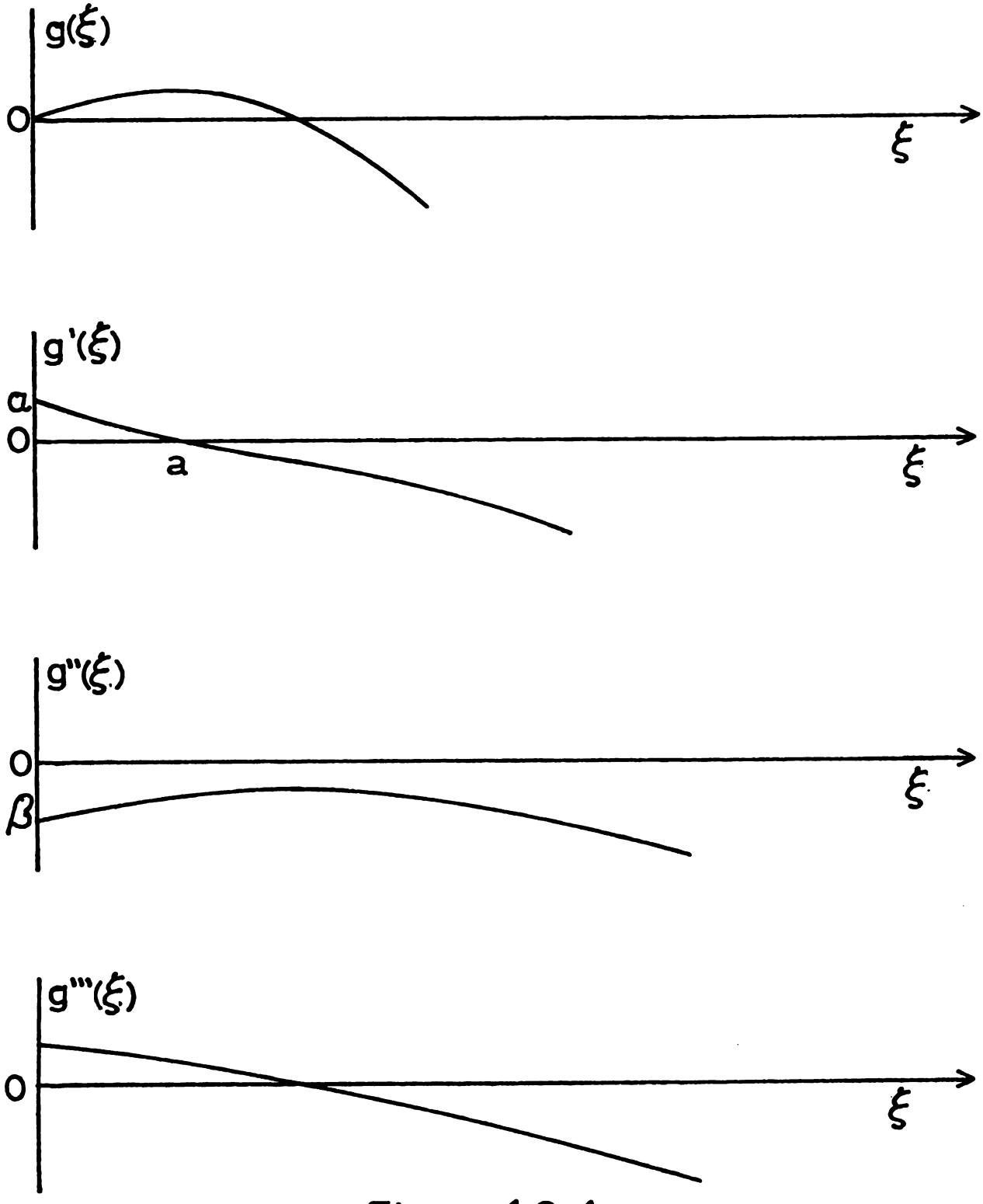

Figure 1.3.4.

The solution of equation 1.3.4. for $\alpha>0$ and $\beta<0$ if a is a Type II zero and there are no other zeroes. The concavity of $g'''(\xi)$ is undetermined.

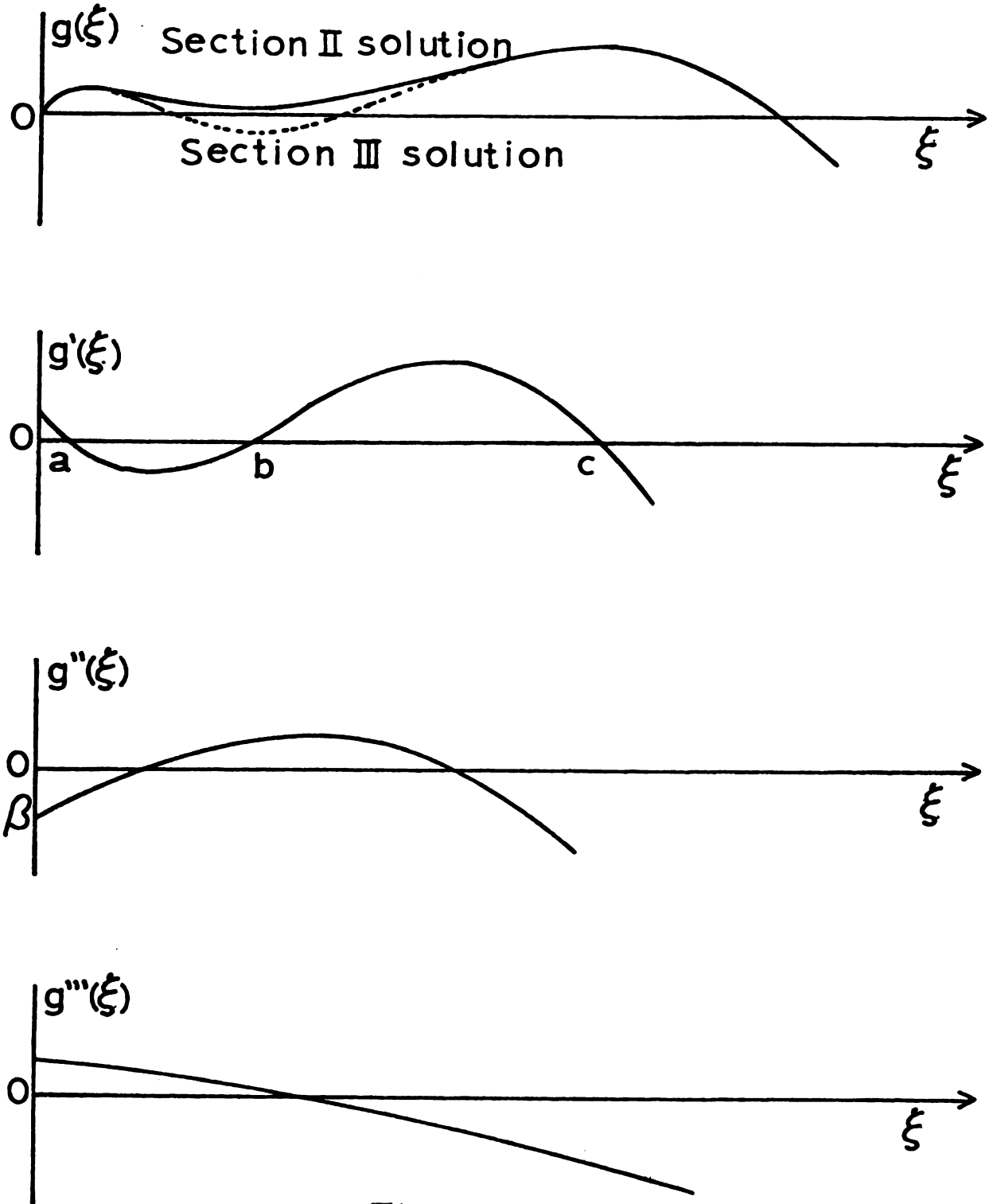

Figure 1.3.5.
The solution of equation 1.3.4. for $\alpha > 0$ and $\beta < 0$ if a is a Type II zero and there are other zeroes. The concavity of $g'''(\xi)$ is undetermined.

Again the proof of the theorem will be divided into several lemmas.

Lemma 1.3.5. If there exists a point c such that $g(\xi) > 2$ for all $\xi > c$ and $g(c) = 2$ then $g'(\xi)$ has a zero.

Proof: From equation 1.3.5 and Theorem 1.3.1 at c $-g''(c)g'(c) = cg^{IV}(c) < 0$. Therefore at c $g''(c)$ and $g'(c)$ must both have the same sign. Clearly if $g'(c)$ and $g''(c)$ are both negative there is a point $d < c$ such that $g'(d) = 0$. If $g''(c)$ and $g'(c)$ are both positive and if $g'''(c)$ is negative then by the same arguments as in the proof of Theorem 1.3.4 $g'(\xi)$ has a zero. If $g'(c)$, $g''(c)$ and $g'''(c)$ are all positive then $g'(\xi)$ has a zero by the same arguments as used in Lemma 1.3.1 and Lemma 1.3.2. Q.E.D.

Lemma 1.3.6. If $K_1 \neq 0$ and $g(\xi) < 2$ for all ξ then $g'(\xi)$ has a zero.

Proof: If there is no point d such that $g'(d) = 0$, then since $g(0) = 0$, $g'(0) > 0$, $g''(0) < 0$ $g(\xi)$ and its derivatives must have the following properties for large values of ξ. $g'(\xi) \to 0^+$, $g''(\xi) \to 0^-$ and $\xi g'''(\xi) \to 0^+$. The following argument establishes the latter limit. If $\xi g'''(\xi) = O(1)$ for large values of ξ then $g''(\xi) = O(\ln \xi)$. But this contradicts $g''(\xi) \to 0^-$. Therefore from equation 1.3.4a

$$\lim_{\xi \to \infty} \xi g'''(\xi) = \lim_{\xi \to \infty} (g''(\xi)(g(\xi) - 1) - g'^2(\xi) + K_1)$$

and hence $K_1 = 0$. But this contradicts the hypothesis of the lemma. Therefore $g'(\xi)$ must have a zero. Q.E.D.

Lemma 1.3.7. If $K_1 = 0$ and $g(\xi) < 2$ for all ξ then $g'(\xi)$ has a zero.

Proof: Suppose $g'(\xi) \neq 0$ for all ξ then since $g(0) = 0$, $g'(0) > 0$ and $g(\xi) \leq 2$ $g(\xi)$ must approach a constant C as ξ approaches infinity where $0 < C \leq 2$. Thus for large values of ξ

1.3.8 $$g(\xi) = C + \varphi(\zeta) \quad \text{when} \quad \zeta = \varepsilon\xi \quad \text{and} \quad \varepsilon << 1$$
and φ is small and $\lim_{\zeta \to \infty} \varphi(\zeta) = 0$.

Substituting 1.3.8 into 1.3.4a gives

1.3.9 $$\zeta\varphi''' + \varphi'' + \varphi'^2 - (C + \varphi)\varphi'' = 0.$$

Since φ is small linearizing the equation gives

1.3.10 $$\zeta\varphi''' + \varphi'' - C\varphi'' = 0$$

The solution of 1.3.10 is given by

$$\varphi = C_1 + C_2\zeta + C_3\zeta^{C+1}$$

Since φ is not identially zero and $\varphi(\infty) = 0$ $C_1 = C_2 = 0$ and $C_3 \neq 0$. Thus C must be such that $C + 1 < 0$ or $C < -1$. This contradicts $0 < C \leq 2$. Therefore $g'(\xi)$ has a zero. Q.E.D.

The above three lemmas establish that when $\alpha > 0$ and $\beta < 0$ $g'(\xi)$ has at least one zero. Let a be the first zero of $g'(\xi)$ then at a $g'''(a)$ may be positive or negative. If $g'''(a)$ is negative then a will be called a Type I zero and if $g'''(a)$ is positive a will be called a Type II zero.

Consider first the case that a is a Type I zero. In this case at a equation 1.3.5 and Theorem 1.3.1 give $g'''(a)(g(a) - 2) < 0$ and hence that $g(a) > 2$. It should be observed here that if a is a Type I zero then $g''(\xi)$ has two zeroes between 0 and a. This is established as follows. Since $g'''(a) < 0$ there is a point a_0, where $0 < a_0 < a$, such that $g'''(a_0) = 0$. From equation 1.3.5 and Theorem 1.3.1 at a_0 $-g'(a_0)g''(a_0) < 0$. Since a was assumed to be the first zero of $g'(\xi)$ and since $g'(0) > 0$ $g'(a_0) > 0$. Therefore $g''(a_0) > 0$. Therefore since $g''(0) < 0$ there is a point a_1, where $0 < a_1 < a_0$ such that $g''(a_1) = 0$ and $g'''(a_1) > 0$. Since $g''(a) < 0$ $g''(\xi)$ must have a second zero between a_0 and a. It should also be observed that $K_1 > 0$ for $g'(\xi)$ to have a Type I zero. As was shown above for $g'(\xi)$ to have a Type I zero there must be a point a_1 such that $g''(a_1) = 0$ and $g'''(a_1) > 0$. At a_1 equation 1.3.2 then gives $-g'^2(a_1) + K_1 = a_1 g'''(a_1) > 0$. This gives then $K_1 > g'^2(a_1) > 0$.

Thus for a Type I zero at a $g(\xi)$ and its derivatives have the following properties.

$g(a) > 2 \qquad g'(a) = 0 \qquad g''(a) < 0 \qquad g'''(a) < 0$

By equation 1.3.3d this gives $R = 2g(a) > 4$. The solutions of $f(\eta)$ of 1.2.12 corresponding to this zero of $g'(\xi)$ will be designated as a Section IV(ii) solutions.

Lemma 1.3.8. If the first zero of $g'(\xi)$ is a Type I zero then $g'(\xi)$ has no additional zeroes.

Proof: The same as for Lemma 1.3.4. Q.E.D.

Consider now that a is a Type II zero. In this case at a equation 1.3.5 and Theorem 1.3.1 give $g'''(a)(g(a) - 2) < 0$ and hence $g(a) < 2$. Since $g(0) = 0$ and $g'(0) > 0$ this gives $0 < g(a) < 2$. Thus for a Type II zero at a $g(\xi)$ and its derivatives have the following properties.

$0 < g(a) < 2 \qquad g'(a) = 0 \qquad g''(a) < 0 \qquad g'''(a) > 0$

From equation 1.3.3d this gives $0 < R < 4$. The solutions $f(\eta)$ of 1.2.12 corresponding to this zero of $g'(x)$ will be designated as Section I solutions for suction.

If $g'(\xi)$ has a Type II zero at a, $g'(\xi)$ may or may not have a second zero. The following lemma shows what conditions are necessary for $g'(\xi)$ to have a second zero.

Lemma 1.3.9. If $g'(\xi)$ has a Type II zero at a then $g'(\xi)$ will have a second zero if and only if there is a point $d > a$ such that $g''(d) = 0$.

Proof: The necessity is clear. Suppose there is a point d such that $g''(d) = 0$. Since at a $g(a) < 2$ and since $g'(\xi) \leq 0$ for all $a \leq \xi \leq d$. $g(\xi) < 2$ for all $a \leq \xi \leq d$. Therefore at d by equation 1.3.5 and Theorem 1.3.1 $g'''(d)(g(d) - 2) < 0$. Since $g(d) < 2$, $g'''(d) > 0$. Therefore for $\xi > d$, $g''(\xi)$ and $g'''(\xi)$ will both be positive. Therefore $g'(\xi)$ will be increasing and concave up. Since equation 1.3.5 and Theorem 1.3.1 show that in this case $g'''(\xi)$ cannot become negative before $g'(\xi)$ becomes positive, there is a point b such that $g'(b) = 0$. Q.E.D.

At b it was shown in the proof of the above lemma that $g(b) < 2$. Therefore if $g'(\xi)$ has a Type II zero at a and a second zero at b then $g(\xi)$ and its derivatives have the following properties at b.

$$g(b) < 2 \qquad g'(b) = 0 \qquad g''(b) > 0 \qquad g'''(b) > 0$$

From equation 1.3.3d this gives $R < 4$. The solution $f(\eta)$ of 1.2.12 corresponding to this zero of $g'(\xi)$ will be designated as a Section II solution if $R > 0$ and a Section III solution if $R < 0$. It should be observed here that again $K_1 > 0$. This follows by the same arguments as for a Type I zero since there is again a point a_1 such that $g''(a_1) = 0$ and $g'''(a_1) > 0$.

Lemma 1.3.10. If $g'(\xi)$ has a second zero at b then $g'(\xi)$ has a third zero at c where $c > b > 0$.

Proof: This follows from the same arguments as used in the proofs of Lemma 1.3.1 and Lemma 1.3.2. Q.E.D.

At c equation 1.3.5 and Theorem 1.3.1 give $g'''(c)(g(c) - 2) = cg^{IV}(c) < 0$. Since $g'''(c) < 0$, $g(c) > 2$. Thus at c $g(\xi)$ and its derivatives have the following properties.

$g(c) > 2$ $\quad$ $g'(c) = 0$ $\quad$ $g''(c) < 0$ $\quad$ $g'''(c) < 0$

By equation 1.3.3d this gives $R = 2g(c) > 4$. The solution $f(\eta)$ of 1.2.12 corresponding to this zero of $g'(\xi)$ will be designated as Section IV(i) solutions.

Lemma 1.3.11. $g'(\xi)$ has no further zeroes.

Proof: Same as for Lemma 1.3.4.

This completes the proof of Theorem 1.3.5. No results were obtained as to what conditions on α and β would determine whether $g'(\xi)$ would have one or three zeroes. However all the above possibilities were obtained numerically.

CHAPTER II

METHODS OF SOLUTION

Section 2.1. Numerical Solutions for the Steady Component of Velocity.

Numerical solutions of equation 1.2.12 subject to boundary conditions 1.2.15 were found by a scheme similar to that used by Terrill and Thomas[24]. As in Section 1.3 let

2.1.1 $$f(\eta) = \lambda g(\xi) \quad \text{where} \quad \eta = \xi/b$$

Then substituting equation 2.1.1 into equation 1.2.12 and boundary conditions 1.2.15 and setting $\lambda = \frac{2}{R}$ gives

2.1.2 $$\xi g'''(\xi) + g''(\xi) + g'^2(\xi) - g(\xi)g''(\xi) = K_1$$

where

2.1.3 $$K_1 = \frac{K}{\lambda b^2} = g'^2(0) + g''(0)$$

and

2.1.4 a) $g(0) = 0$ c) $g'(b) = 0$

b) $\lim_{\xi \to 0} \xi^{1/2} g''(\xi) = 0$ d) $g(b) = \frac{1}{\lambda} = \frac{R}{2}$

Now a solution of equation 1.2.12 subject to boundary conditions 1.2.15 can be found by choosing $g'(0)$ and $g''(0)$

and then numerically solving equation 2.1.2 until a point b is found such that $g'(b) = 0$. Then R and λ are found from equation 2.1.4d and K is found from equation 2.1.3. The inverse transformation then gives a solution of equation 1.2.12 subject to boundary conditions 1.2.15. Because of the presence of the term $\xi g'''(\xi)$ in equation 2.1.2 two different numerical techniques were used to solve for $g(\xi)$. In the interval $[0, \xi_t]$ where $0 < \xi_t < b$, $g(\xi)$, $g'(\xi)$ and $g''(\xi)$ were computed by the following Taylor series about zero:

$$2.1.5 \quad g(\xi) = \xi g'(0) + \frac{\xi^2}{2!} g''(0) + \cdots + \frac{\xi^6}{6!} g^{VI}(0)$$

$$2.1.6 \quad g'(\xi) = g'(0) + \xi g''(0) + \cdots + \frac{\xi^5}{5!} g^{VI}(0)$$

$$2.1.7 \quad g''(\xi) = g''(0) + \xi g'''(0) + \cdots + \frac{\xi^4}{4!} g^{VI}(0)$$

where

$$g'''(0) = -\frac{1}{2} g'(0) g''(0)$$

$$g^{IV}(0) = -\frac{1}{3} [g''(0)]^2$$

$$g^{V}(0) = \frac{1}{6} g'(0) [g''(0)]^2$$

$$g^{VI}(0) = -\frac{1}{30} [g'(0) g''(0)]^2 + \frac{1}{15} [g''(0)]^3$$

The error for each series is respectively $g^{VII}(\tau) \frac{\xi^7}{7!}$, $g^{VII}(\tau) \frac{\xi^6}{6!}$, and $g^{VII}(\tau) \frac{\xi^5}{5!}$ where $0 < \tau \leq \xi \leq \xi_t$.

On the interval $[0, \xi_t]$ $g^{VII}(\tau)$ was approximated by $g^{VII}(\tau) = g^{VII}(0) + \tau\, g^{VIII}(0)$ where

$$g^{VII}(0) = -\frac{7}{90}\, g'(0)\, [g''(0)]^3 - \frac{1}{60}\, [g'(0)]^3 [g''(0)]^2$$

$$g^{VIII}(0) = -\frac{1}{7}\left[\frac{13}{45}[g''(0)]^2 + \frac{1}{9}[g'(0)]^2[g''(0)]^3 + \frac{1}{15}[g'(0)]^4[g''(0)]^2\right]$$

The point ξ_t was then selected by requiring

$$\max_{0 \le \tau \le \xi_t} \left| g^{VII}(0) + \tau\, g^{VIII}(0) \right| \frac{\xi_t^5}{5!} \le 10^{-10}$$

The values $g(\xi_t)$, $g'(\xi_t)$, $g''(\xi_t)$ and ξ_t obtained were then used as the initial values for the numerical integration of equation 2.1.2 on $[\xi_t, b]$. The numerical integration was carried out using Gill's modification of the fourth order Runge-Kutta method [5]. The Runge-Kutta subroutine RKGS that was used can be found listed in reference [20]. This subroutine has the advantage of automatically adjusting the step size, h, to satisfy a user specified error bound at each step. The error bound, δ, at each step is computed from the following:

$$\delta = \frac{1}{15}\left(a_1 \left|g_1 - g_2\right| + a_2 \left|g_1' - g_2'\right| + a_3 \left|g_1'' - g_2''\right|\right)$$

where a_1, a_2, and a_3 are weights specified by the user and g_1 is the computed value of the function at an increment of $2h$ using a step size of $2h$ and g_2 is the computed value of the function at an increment of $2h$ using a step size h.

If δ exceeded the specified bound, the step size was automatically adjusted. It was found the error could be controlled quite well by setting $a_1 = 0.0$, $a_2 = 0.5$ and $a_3 = 0.5$. In computing numerical solutions for $h(\eta)$, $f'(\eta)$ and $f''(\eta)$ also were each weighted at 0.5 and all other weights were zero.

By this method accurate solutions of equation 1.2.12 could be obtained. The major difficulty with this method is selecting the value of $g'(0)$ and $g''(0)$ to obtain a particular type of solution for a particular value of R. It was found that the easiest way to do this was to select a fixed value of $g'(0)$ and only vary $g''(0)$. This turned out to be especially useful in obtaining all the possible solutions in the case where $g'(0) > 0$ and $g''(0) < 0$.

A major disadvantage of this method is that only solutions of equation 1.2.12 are obtained for which $f''(0)$ is finite even though the boundary condition $\lim_{\eta \to \infty} \sqrt{\eta}\, f''(\eta) = 0$ permits the possibility of solutions for which $f''(0)$ is not finite.

Section 2.2. Numerical Solutions for the Unsteady Component of Velocity.

Once $f(\eta)$ has been found from equation 1.2.12 equation 1.2.14 for $h(\eta)$ is a linear differential equation with variable coefficients. To find a solution of $h(\eta)$ of

1.2.14 satisfying the boundary conditions 1.2.17 two real constants C_1 and C_2 must be found such that

2.2.1a $$h_R\,(0,\ C_1,\ C_2) = C_1$$

2.2.1b $$h_i\,(0,\ C_1,\ C_2) = C_2$$

and

2.2.2a $$h_R\,(1,\ C_1,\ C_2) = 0$$

2.2.2b $$h_i\,(1,\ C_1,\ C_2) = 0$$

where h_R and h_i are the real and imaginary parts respectively of a solution of 1.2.14. Equations 2.2.2 are a system of two equations and two unknowns and since 1.2.14 is a linear differential equation, this is a linear system [7]. Thus Newton's method for solving two equations and two unknowns will be exact in one iteration. Therefore if C_1^0 and C_2^0 are initial guesses for C_1 and C_2 then the exact values of C_1 and C_2 are given by

2.2.3a $$C_1 = C_1^0 + \left(h_i(1)\ \frac{\partial h_R(1)}{\partial C_2} - h_R(1)\ \frac{\partial h_i(1)}{\partial C_2}\right)/A_0$$

2.2.3b $$C_2 = C_2^0 + \left(h_R(1)\ \frac{\partial h_i(1)}{\partial C_1} - h_i(1)\ \frac{\partial h_R(1)}{\partial C_1}\right)/A_0$$

2.2.3c $$\text{where}\quad A_0 = \frac{\partial h_R(1)}{\partial C_1}\ \frac{\partial h_i(1)}{\partial C_2} - \frac{\partial h_R(1)}{\partial C_2}\ \frac{\partial h_i(1)}{\partial C_1}$$

Here $h_R(1)$ and $h_i(1)$ are the real and imaginary parts respectively of the solution of 1.2.14 with initial

2.2.4 condition $h(0) = c_1^0 + i\,c_2^0$ and evaluated at one.

The $\frac{\partial h_R(1)}{\partial c_1}$ and the $\frac{\partial h_i(1)}{\partial c_1}$ are found as the real and imaginary parts respectively evaluated at one of the solutions of

$$2.2.5 \quad \eta w''(\eta) + w'(\eta) = S^2 w(\eta) + \frac{R}{2}\left(f(\eta)w'(\eta) - w(\eta)f'(\eta)\right)$$

with

$$2.2.6 \quad w(0) = 1.0$$

and $\frac{\partial h_R(1)}{\partial c_2}$ and $\frac{\partial h_i(1)}{\partial c_2}$ are found as the real and imaginary parts respectively evaluated at one of the solutions of 2.2.5 but with initial condition

$$2.2.7 \quad w(0) = i$$

Again because of the presence of the terms $\eta h''(\eta)$ and $\eta w''(\eta)$ in equations 1.2.14 and 2.2.5 respectively two different numerical techniques were used to solve these equations. As in the previous section on the interval $[\eta_t, 1]$ where $0 < \eta_t < 1$ equations 1.2.14 and 2.2.5 were integrated numerically using the Runge-Kutta method referred to in the previous section. On the interval $[0, \eta_t]$ $h(\eta)$ and $h'(\eta)$ were computed from the following Taylor series at zero.

$$2.2.8 \quad h(\eta) = h(0) + h'(0)\eta + \cdots + h^V(0)\,\frac{\eta^5}{5!}$$

2.2.9 $$h'(\eta) = h'(0) + h''(0)\eta + \cdots + h^{V}(0)\frac{\eta^4}{4!}$$

The error terms in 2.2.8 and 2.2.9 are given by $h^{VI}(\tau)\frac{\eta^6}{6!}$ and $h^{VI}(\tau)\frac{\eta^5}{5!}$ respectively where $0 \leq \tau \leq \eta \leq \eta_t$. On the interval $[0,\eta_t]$ $h^{VI}(\tau)$ was approximated by

2.2.10 $$h^{VI}(\tau) = h^{VI}(0) + \tau h^{VII}(0)$$

The point, η_t, at which the numerical integration was begun was determined by setting $\eta_t = \xi_t/b$. It was found by choosing η_t in this manner was sufficient to guarantee

$$\max_{0\leq\tau\leq\eta_t} |h_0^{VI}(0) + \tau h^{VII}(0)| \frac{\eta_t^5}{5!} \leq 10^{-8}$$

Exactly the same technique was used to compute $w(\eta)$ and $w'(\eta)$ on $[0,\eta_t]$ with the same bound on the corresponding error.

This technique had two advantages. First the exact value for $h(\eta)$ at zero was obtained after one integration across the interval $[0,1]$. Secondly this technique avoids the numerically difficult problem of having to integrate towards zero and apply the condition $\lim_{\eta\to 0} \sqrt{\eta}\, h'(\eta) = 0$.

However, this technique also had two disadvantages. First the evaluation of the partial derivatives required for 2.2.3 introduces extra numerical integration. Secondly a more serious disadvantage was that if the solution $f(\eta)$ of

1.2.12 had a boundary layer at one then numerical inaccuracies resulted from having to integrate into the boundary layer. This problem was the most severe for the Section IV (ii) and V (ii) solutions of 1.2.12 for large crossflow Reynolds numbers.

Section 2.3. Asymptotic Methods.

Solutions of equations 1.2.12 and 1.2.14 were also sought by using perturbation techniques. The crossflow Reynolds number was used as the perturbation parameter and asymptotic solutions were sought for both large and small values of this parameter. Since solutions of 1.2.14a depend on solutions of 1.2.12, but not conversely, equation 1.2.12 was examined first. An asymptotic solution of the form

$$2.3.1 \qquad f(\eta) = \nu_0(\epsilon) f_0(\eta) + \nu_1(\epsilon) f_1(\eta) + \cdots$$

was assumed where ϵ is the perturbation parameter. Equation 2.3.1 was then substituted into equations 1.2.12 and boundary conditions 1.2.15. By examining the limits as ϵ goes to zero the gauge functions $\nu_0(\epsilon), \nu_1(\epsilon), \cdots$ were determined. Then equating the terms of the same order resulted in a sequence of boundary value problems for $f_0(\eta), f_1(\eta), \cdots,$. The sequence of differential equations was then solved and the boundary conditions applied. If the sequence of functions were able to satisfy all their respective boundary conditions, then the problem of finding an

asymptotic series for $f(\eta)$ was completed. If, however, these functions were unable to satisfy all the boundary conditions, the technique of matched asymptotic expansions was used to find an asymptotic solution. In this case equation 2.3.1 with appropriate fewer boundary conditions was taken as the solution in the outer region. In the inner region equation 1.2.12 was rescaled in terms of a new inner variable and a second asymptotic expansion valid in the inner region was found. The two asymptotic series were then matched in an intermediate region. This technique is discussed in detail in references [12] and [27]. Using the results obtained for $f(\eta)$ asymptotic solutions were obtained for $h(\eta)$ by using the same techniques.

The asymptotic results were then compared with the results obtained from numerical integration.

CHAPTER III

THE STEADY COMPONENT OF VELOCITY

Section 3.1. Numerical Results

Numerical solutions were obtained for each of the possible types of zeroes of $g'(\xi)$ discussed in Section 1.3 by the method discussed in Section 2.1. Figure 2.1.1 summarizes these results by plotting $-f''(1)$ which, as equation 1.2.19 shows, is proportional to the skin friction at the wall versus the Reynolds number. This format for discussing the results for the steady component of velocity was originally used by Terrill and Thomas [24]. Two solutions were found for $-\infty < R < 2.3$ and $9.1 < R < 20.6$. For $2.3 < R < 9.1$ no solutions were found and for $20.6 < R < \infty$ four solutions were found. Section I, Section II, Section III, Section IV(ii) and Section V(ii) solutions have been found and discussed previously by Terrill and Thomas [24] and others [3, 8, 16, 30, 33]. However the complete set of Section IV(i) and Section V(i) solutions have not appeared previously in the literature. Also the graph of $-f''(1)$ versus R is not as simple for R between 9.2 and 20.6 as has been previously reported by Terrill and Thomas [24]. As mentioned in Section 1.1 the reason for no similarity solutions for $2.3 < R < 9.1$ has been studied

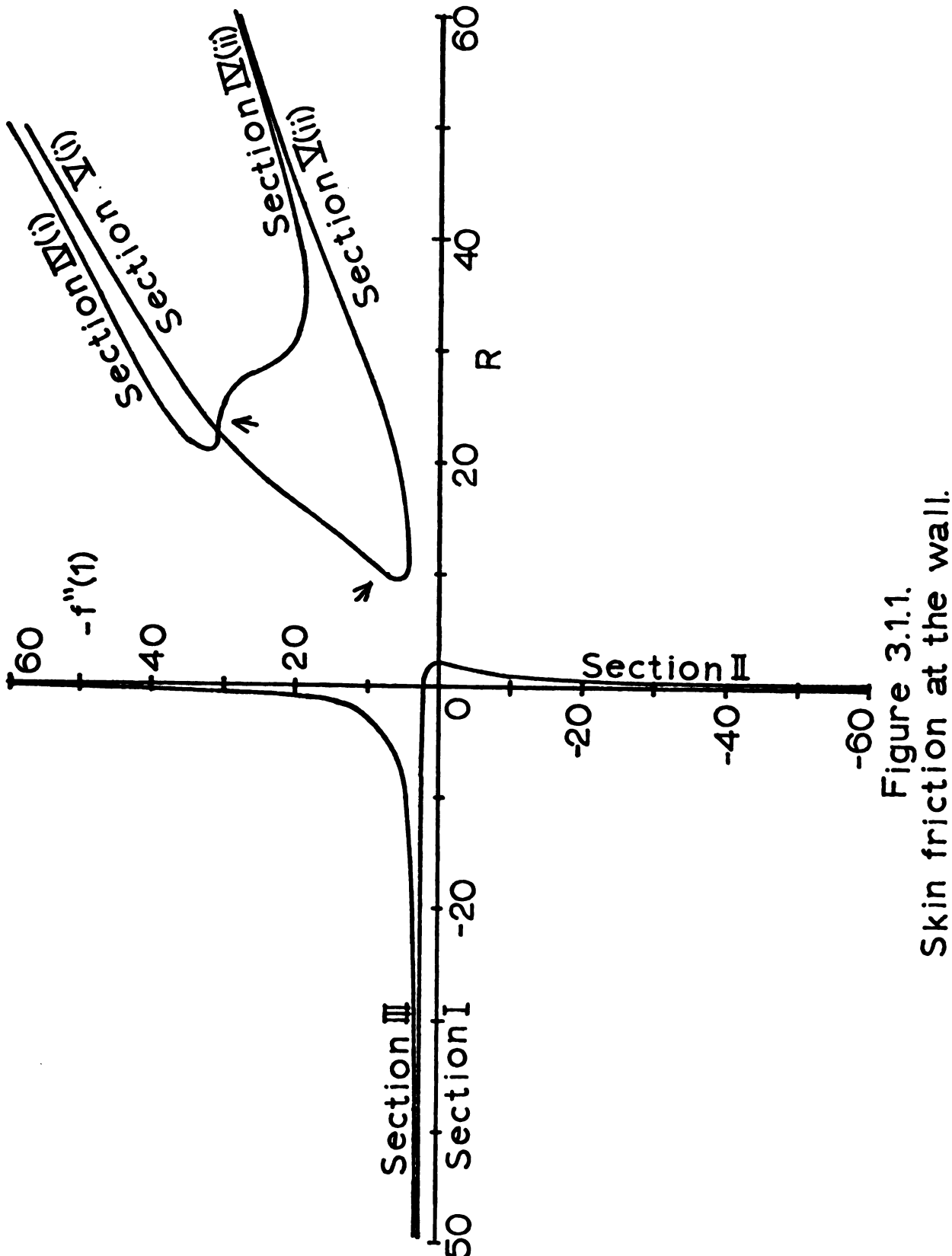

Figure 3.1.1.
Skin friction at the wall.

by Weissberg [29]. By studying the inlet flow he was able to show that for approximately these values of cross-flow Reynolds number similarity flow is not developed. Also it should be noted that the discussion of the zeroes of $g'(\xi)$ in Section 1.3 indicated there would be no solutions for $R = 4$.

The characteristics of each type of solution will be briefly discussed here.

1) Section I solutions $(-\infty < R < 2.3)$. In Figure 3.1.2 the axial velocity profiles of several Section I solutions are graphed to indicate their characteristics. Section I solutions exhibit no reverse flow and all velocity profiles are concave down except those for R near 2.3 which have an inflection point. These solutions have an inflection point because the value of K in equation 1.2.12 changes sign at $R = 1.2$. From $K = \frac{-Ra^2A}{4v^2}$ and equation 1.2.18 it is seen this change in sign corresponds to a change in sign of the linear component of the pressure gradient.

2) Section II solutions $(0 < R < 2.3)$. Two of the axial velocity profiles for these solutions are shown in Figure 3.1.3. These flows for small suction have three characteristics of interest. First they exhibit a region of reverse flow near the wall of the tube. The graph for $R = 2.29$ does not indicate this clearly since as R approaches 2.3 the width of the region of reverse flow near the wall approaches zero. Second as $R \to 0^+$ the velocity at the center

of the tube becomes infinite. Third as $R \to 2.3$ the Section I and Section II solutions approach the same velocity profile.

3) Section III solutions $(-\infty < R < 0)$. Graphs of the axial velocity profiles of these solutions are shown in Figures 3.1.3 and 3.1.4. There are four observations to be made about these solutions. First they exhibit a region of reverse flow near the center of the tube. Second as $R \to 0^-$ the velocity at the center of the tube becomes infinite. Third the velocity profiles for small injection are similar of those of Section II except the direction of the flow is reversed. Fourth for large values of the Reynolds number, that is for large injection, the Section III solutions approach the same velocity profile as large injection Section I solutions except for a boundary layer at the center of the tube.

Mathematically the reason for the discontinuity for $R = 0$ in the Section II and Section III solutions can be explained relatively easily. In section 3.1 it was shown that Section II and Section III solutions were obtained for the second zero, if any, of a so called Type II zero. If b is this zero then as $g(b) \to 0^+$, and hence $R \to 0^+$, gives a Section II solution with reverse flow near the wall while as $g(b) \to 0^-$, and hence $R \to 0^-$, yields a Section III solution with reverse flow near the center of the tube. Since $g''(b)$ is not zero and since these two limits give such

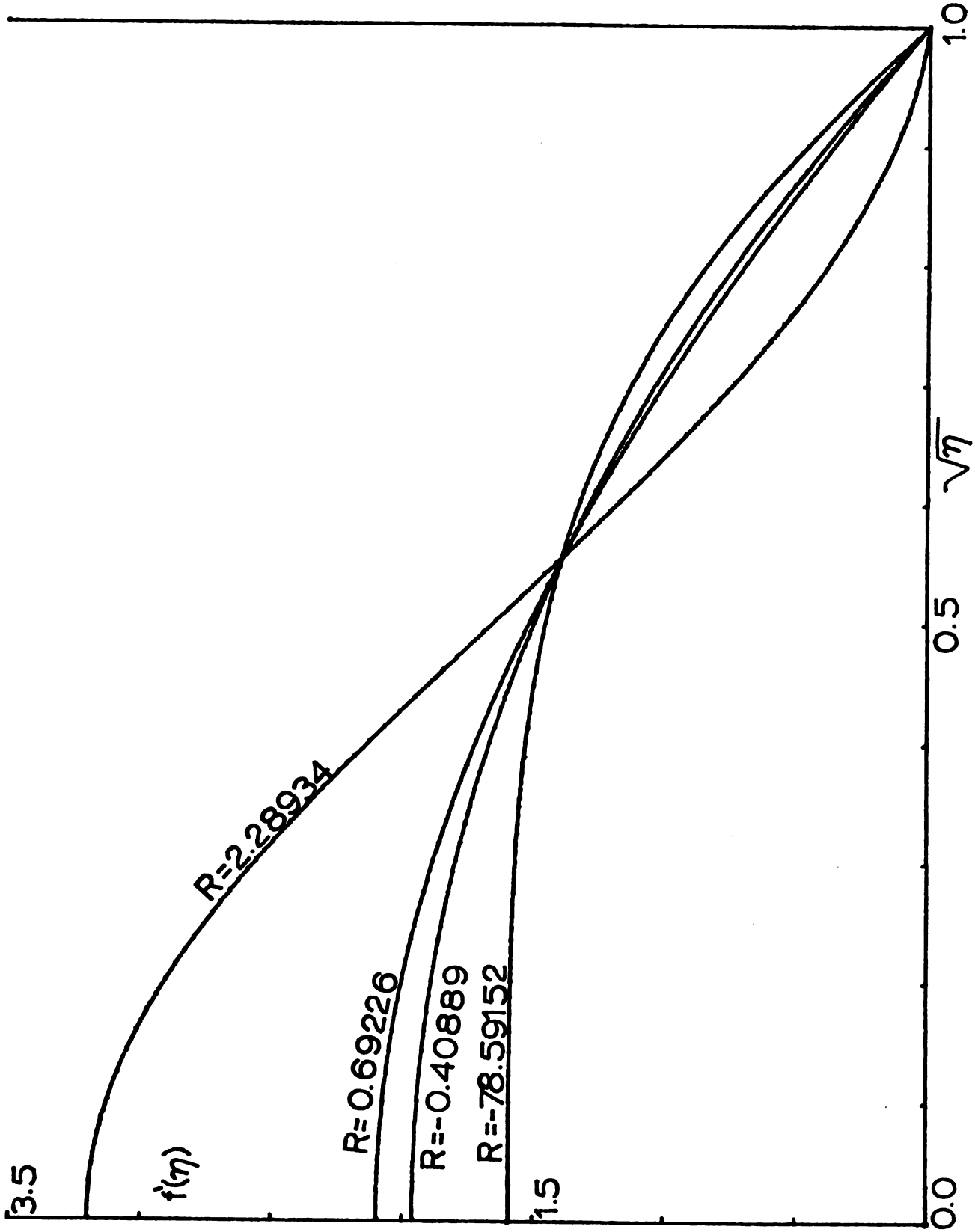

Figure 3.1.2.

Axial velocity profiles for Section I solutions.

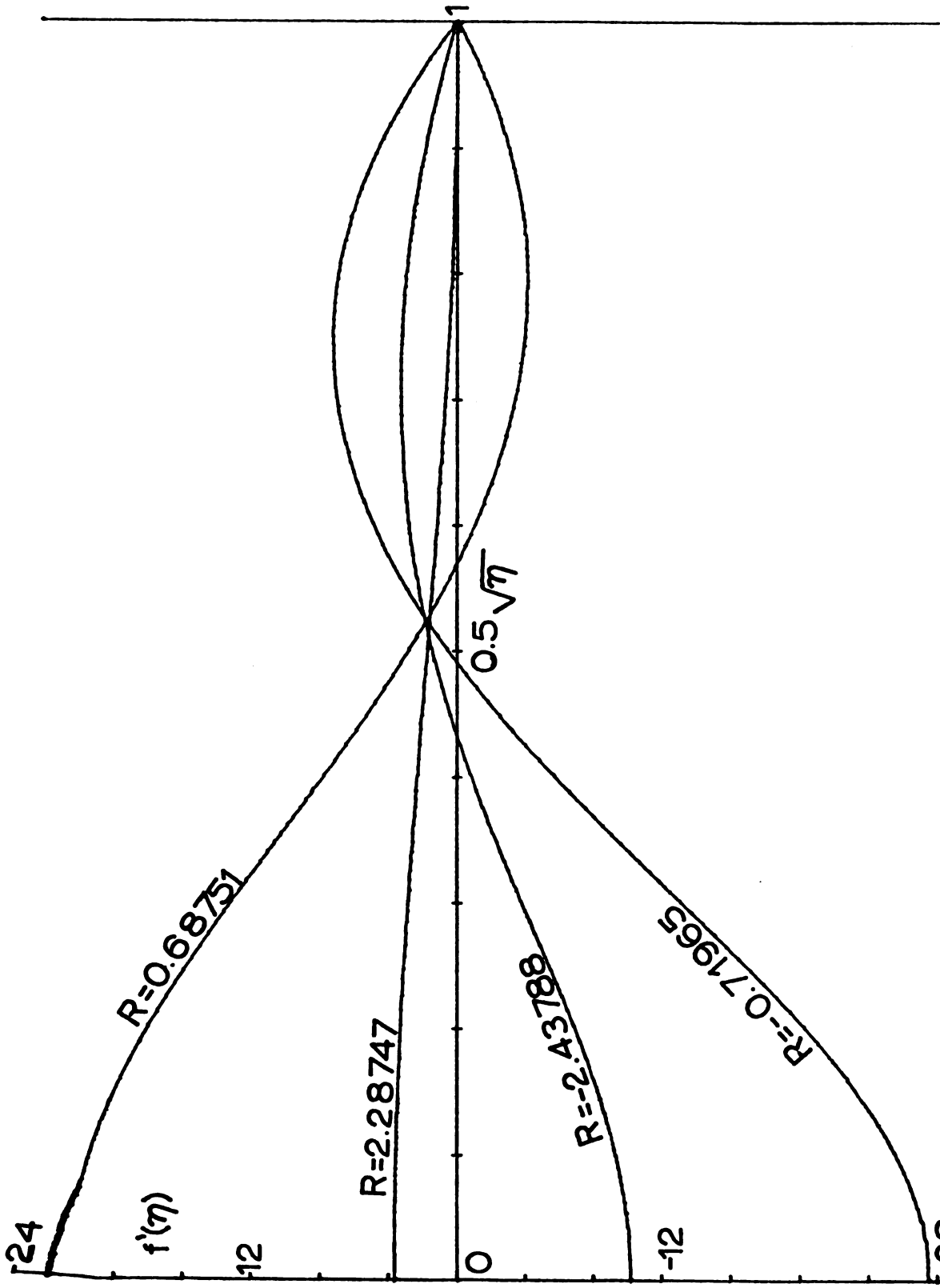

Figure 3.1.3.

Axial velocity profiles for Section II and Section III solutions for small R.


Ax

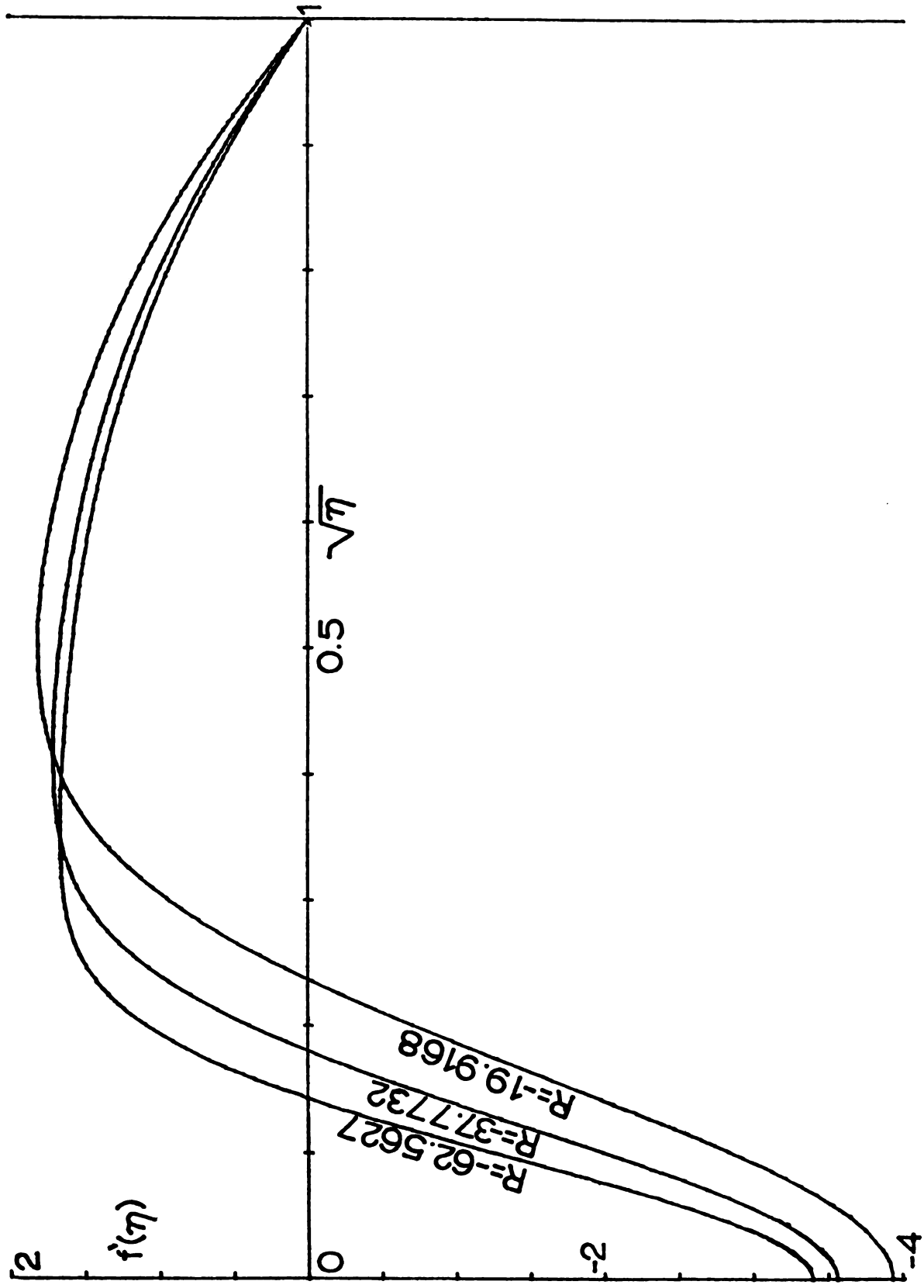

Figure 3.14.

Axial velocity profiles for Section III solutions.

different velocity profiles a singularity at $R = 0$ is to be expected.

4) Section IV(i) solutions $(20.6 < R < \infty)$. Graphs of the axial velocity profiles of the Section IV(i) solutions are found in Figure 3.1.5. Two features of these solutions are of interest. First there are two Section IV(i) solutions for $20.6 < R < 23.7$. Second these solutions have forward flow at the center and wall of the tube but have an intermediate region of reverse flow.

5) Section IV(ii) solutions $(23.7 < R < \infty)$. Graphs of the velocity profiles of these solutions are found in Figure 3.1.6. These solutions have three interesting properties. First there is no region of reverse flow. Second as $R \to 23.7$ the Section IV(ii) and Section IV(i) solutions approach the same velocity profile. Third the velocity at the center of the tube for these solutions has a maximum at $R = 23.7$ and a minimum at $R = 28.4$.

6) Section V(i) solutions $(10.1 < R < \infty)$. The graphs of the axial velocity profiles for these solutions are given in Figure 3.1.7. Two features of these solutions will be noted here. First these solutions have a region of reverse flow near the center of the tube. Second as $R \to \infty$ the Section V(i) and Section IV(i) solutions appear to approach the same velocity profile except at zero where the Section IV(i) solution has a boundary layer while the Section V(i) solution does not.

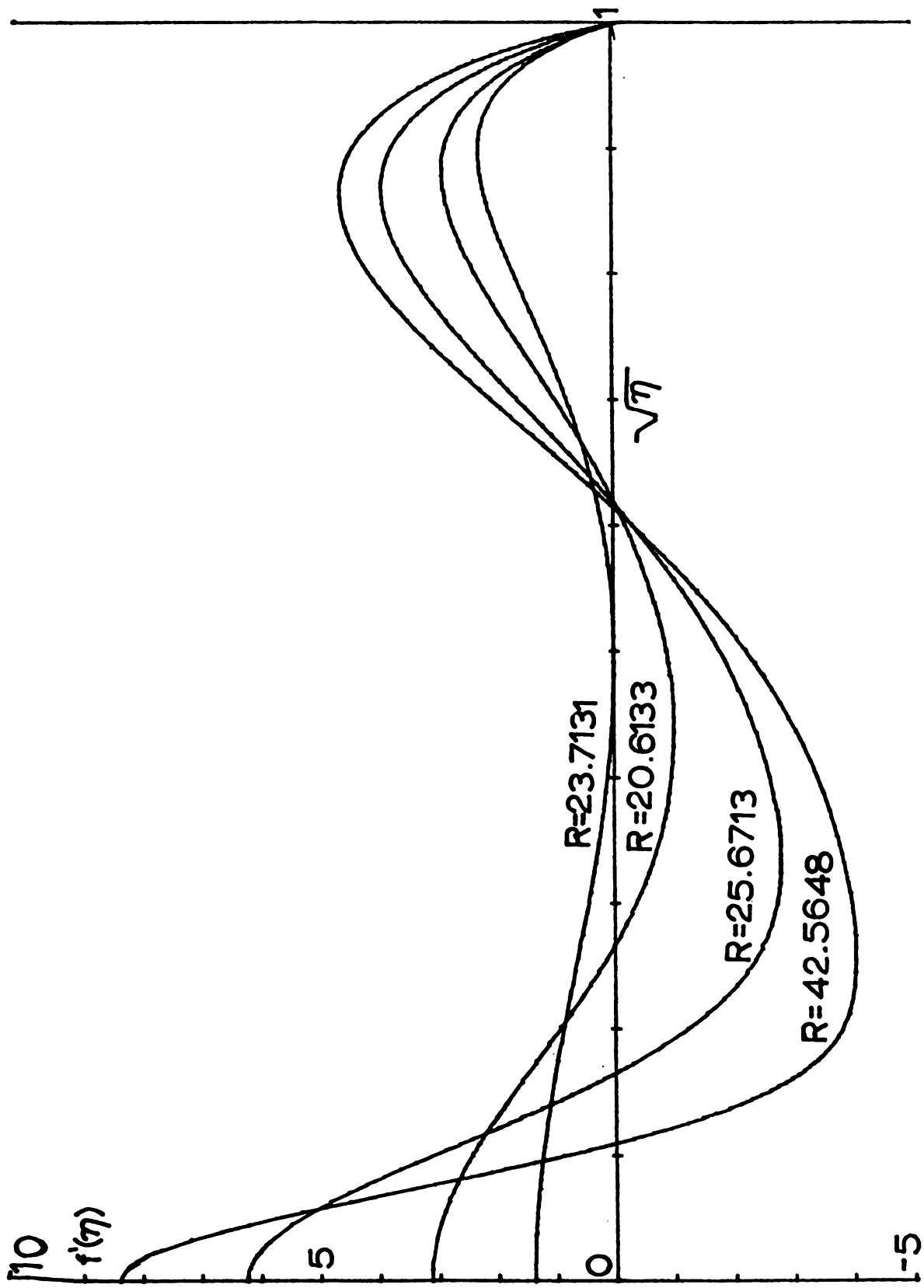

Figure 3.1.5.

Axial Velocity profiles for Section IV(i) solutions.

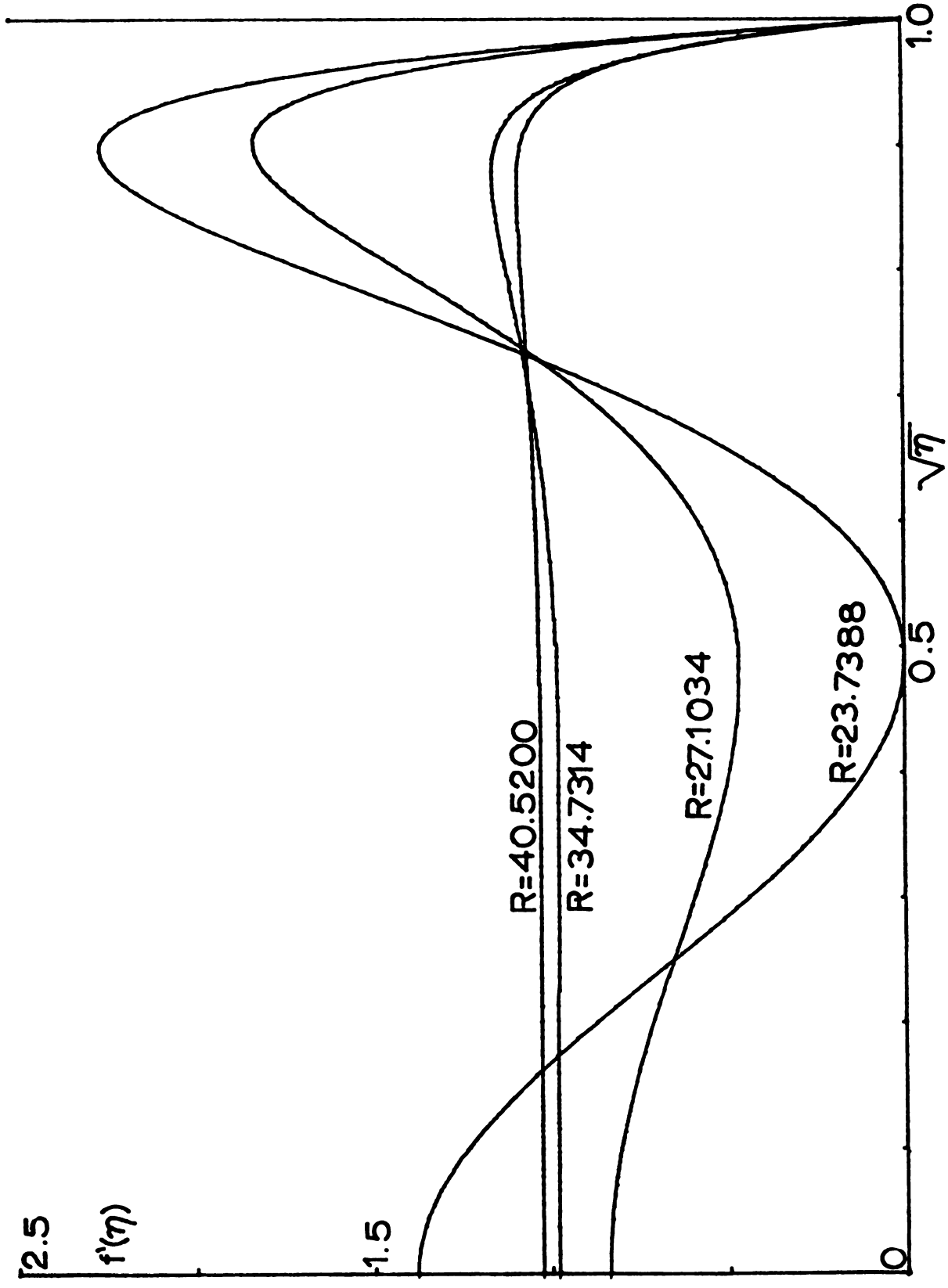

Figure 3.1.6

Axial velocity profiles for Section IV(ii) solutions.

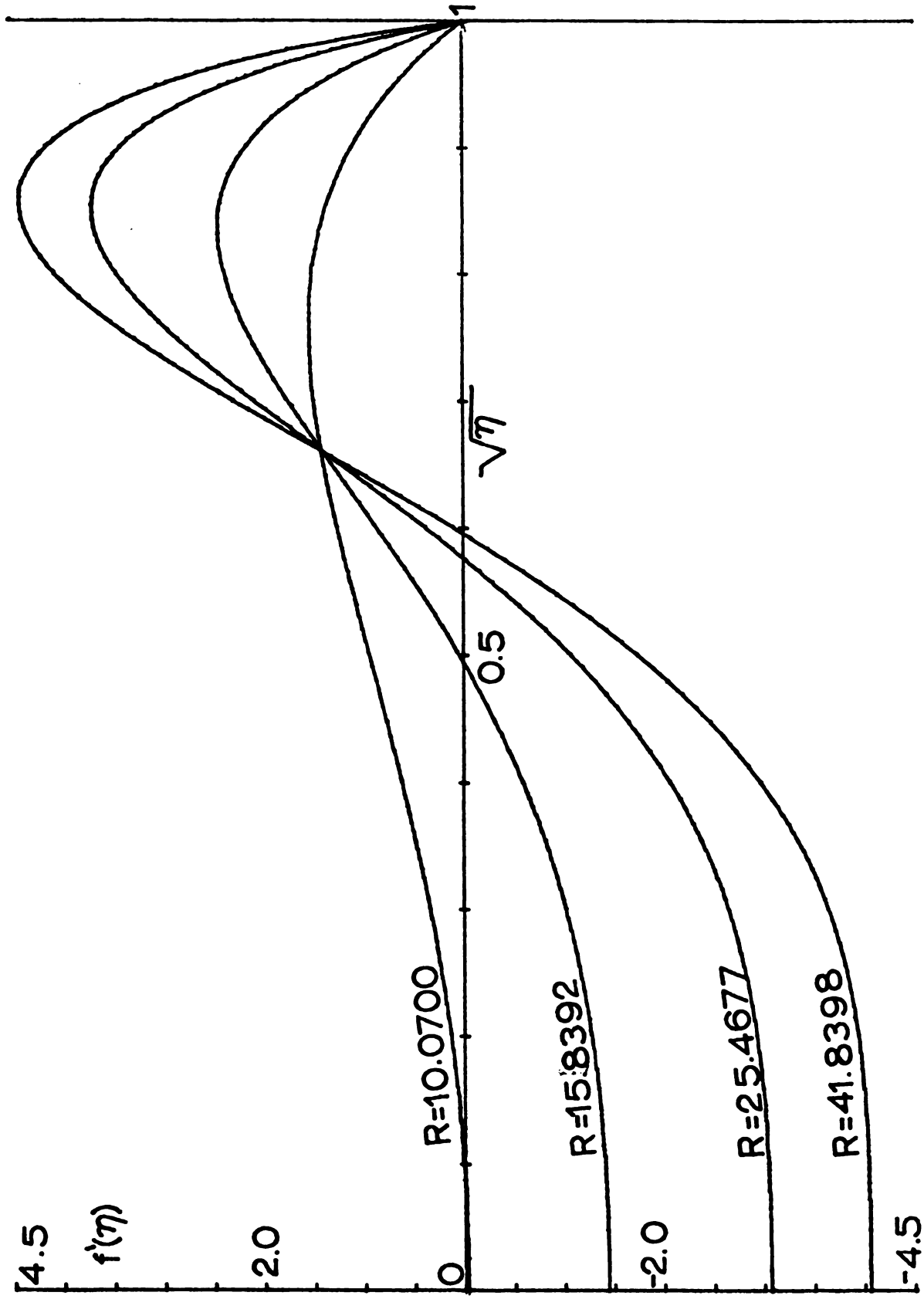

Figure 3.1.7.

Axial velocity profiles for Section V(i) solutions.

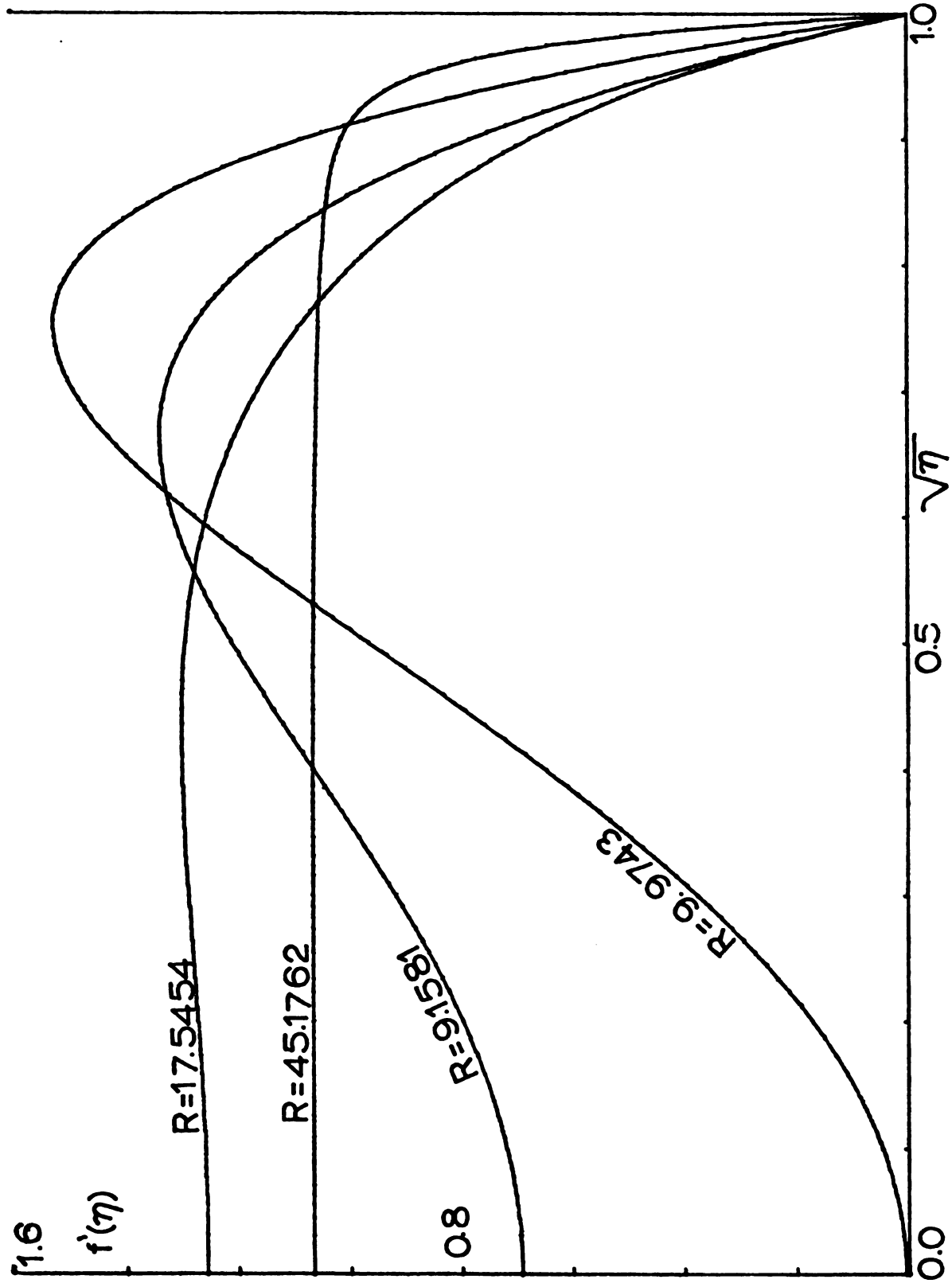

Figure 3.1.8.

Axial velocity profiles for Section V(ii) solutions.

7) Section V(ii) solutions $(9.2 < R < \infty)$. Graphs of the axial velocity profiles of these solutions are found in Figure 3.1.8. Five features of these solutions will be pointed out here. First for these solutions there is no region of reverse flow. Second for $9.1 < R < 10.0$ there are two Section V(ii) solutions. Third the axial velocity at the center of the tube for these solutions has a minimum at $R = 10.0$ and a maximum at $R = 14.5$. Fourth as $R \to \infty$ the Section V(ii) and Section IV(ii) solutions approach the same axial velocity profile. Fifth as $R \to 10.0$ the Section V(ii) and Section V(i) solutions approach the same axial velocity profile.

Section 3.2. Asymptotic Solutions for Large Injection.

Asymptotic solutions for large injection corresponding to Section I and Section III solutions were first studied by Yuan and Finkelstein [33] and Terrill and Thomas [24] respectively. Since these solutions will be required for the study of the unsteady component of velocity their results will be rederived and reexamined here. In equation 1.2.12 setting $\epsilon = -2/R$, where $\epsilon \ll 1$, we obtain the following formulation for the problem of large injection.

$$3.2.1 \qquad \epsilon(\eta f'''(\eta) + f''(\eta)) - f'^2(\eta) + f(\eta)f''(\eta) = -\beta^2$$

with boundary conditions

$$3.2.2 \qquad f(0) = 0 \qquad\qquad f(1) = 1$$

$$\lim_{\eta \to 0} \eta^{1/2} f''(\eta) = 0 \qquad\qquad f'(1) = 0$$

where

3.2.3 $$-\beta^2 = K\epsilon$$

The justification of 3.2.3 is contained in the results of Section 1.3.

An asymptotic series will now be sought which is valid in the region where the inertial forces are much larger than the viscous forces. Let

3.2.4 $$f(\eta) = f_0(\eta)\gamma_0(\epsilon) + f_1(\eta)\gamma_1(\epsilon) + \cdots$$

3.2.5 $$\beta = \beta_0 c_0(\epsilon) + \beta_1 c_1(\epsilon) + \cdots$$

Substituting 3.2.4 and 3.2.5 into equation 3.2.1 and collecting terms gives

3.2.6 $$\begin{aligned} &\epsilon\gamma_0(\eta f_0''' + f_0'') + \epsilon\gamma_1(\eta f_1''' + f_1'') + \gamma_0^2(f_0 f_0'' - f_0'^2) \\ &+ \gamma_0\gamma_1(-2f_0'f_1' + f_0 f_1'' + f_1 f_0'') + \gamma_1^2(-f_1'^2 + f_1 f_1'') + \cdots \\ &= -c_0^2\beta_0^2 - 2\beta_0\beta_1 c_0 c_1 - \beta_1^2 c_1^2 + \cdots \end{aligned}$$

Because $f(1) = 1$ and since in the region where the viscous forces are small the inertial forces must balance the pressure gradient we set, without loss of generality, $\gamma_0 = C_0 = 1$. Thus in this region the leading term satisfies

3.2.7 $$f_0'^2 - f_0 f_0'' = \beta_0^2$$

Physically since for injection we expect the vorticity generated at the wall would be carried toward the center of the tube, any accumulation of vorticity would occur at the

center of the tube. Thus any viscous layer would be expected to occur there and hence the asymptotic expansion 3.2.4 would be expected to be valid in a region away from the center of the tube.

Mathematically this can be established by the following arguments. Suppose that near the center of the tube the viscous forces are much smaller than the inertial forces but that at the wall there is a boundary layer. Then f_0 would be a solution of the following boundary value problem.

3.2.8 $$f_0'^2 - f_0 f_0'' = \beta_0^2$$

$$f_0(0) = 0 \qquad \lim_{\eta \to 0} \sqrt{\eta}\, f_0''(\eta) = 0 \qquad f_0(1) = 1$$

Since the solution of this equation represents inviscid flow near the center of the tube it would not be expected to satisfy the non-slip condition at the wall. Thus the condition $f_0'(1) = 0$ is dropped.

The possible solutions of equation 3.2.8 are

3.2.9a $$f_0(\eta) = \bar{K}\beta_0 \sinh \eta/\bar{K} \qquad \text{where} \quad \bar{K}\beta_0 \sinh \frac{1}{\bar{K}} = 1$$

3.2.9b $$f_0(\eta) = (-1)^m L\beta_0 \sin \eta/L \qquad \text{where} \quad (-1)^m L\beta_0 \sin \frac{1}{L} = 1$$

3.2.9c $$f_0(\eta) = \beta_0 \eta \qquad \text{where} \quad \beta_0 = 1$$

L and K are constants of integration. In the assumed boundary layer near the wall let $F(\lambda) = f(\eta)$ where

$\eta = 1 - \delta(\epsilon)\lambda$ and $\delta(\epsilon)$ is the width of the boundary layer. Substituting $F(\lambda)$ in equation 3.2.1 gives

$$3.2.10 \quad \epsilon((\lambda - \frac{1}{\delta(\epsilon)})F'''(\lambda) + F''(\lambda)) + F'^2(\lambda) - F(\lambda)F''(\lambda) = \delta^2\beta^2$$

$$F(0) = 1 \qquad F'(0) = 0$$

Since in the boundary layer the viscous and inertial forces are assumed to be of the same magnitude, we set $\delta(\epsilon) = \epsilon$. Since the outer solutions given by equation 3.2.9 expanded in inner variables give $f \sim 1 - \epsilon\lambda$, $F(\lambda)$ in the boundary layer must have the following expansion.

$$3.2.11 \qquad F(\lambda) = F_0(\lambda) + \epsilon F_1(\lambda) + \cdots$$

Substituting equation 3.2.11 into equation 3.2.10 and collecting terms gives

$$3.2.12 \quad \epsilon(\lambda F_0''' + F_0'') + \epsilon^2(\lambda F_1''' + F_1'') - F_0''' - \epsilon F_1'' - F_0'^2 + F_0F_0''$$

$$+ \epsilon(-2F_1'F_0' + F_0F_1'' + F_1F_0'') + \epsilon^2(-F_1'^2 + F_1F_1'') + \cdots$$

$$= -\epsilon^2\beta_0^2c_0^2 - 2\beta_0\beta_1\epsilon^2c_0c_1 - \epsilon^2\beta_1^2c_1^2 - \cdots$$

This gives the following problem for F_0.

$$3.2.13 \qquad -F_0''' - F_0'^2 + F_0F_0'' = 0$$

$$F_0(0) = 1 \quad F_0'(0) = 0 \quad F_0(\infty) = 1$$

The latter boundary condition comes from matching the inner and outer solution. It is clear that $F_0 = 1$ is a solution of 3.2.13, but it is not clear this is the only solution of

3.2.13. The following argument will however establish this. Assume $F_0'''(\lambda)$ is continuous for $\lambda \geq 0$.

Lemma 3.2.1. If $F_0(\lambda)$ is any solution of 3.2.13 such that there is a point a such that $F_0''(a) \leq 0$ then $F_0''(\lambda) \leq 0$ for all $\lambda \geq a$.

Proof: Suppose there is a point $b > a$ such that $F_0''(b) = 0$, then at b, $F_0'''(b) = -F_0'^2(b) \leq 0$. Thus at every point $b > a$ where $F_0''(b)$ is zero its slope is zero or negative. Thus since $F_0''(a) \leq 0$, $F_0''(\lambda) \leq 0$ for all $\lambda \geq a$. Q.E.D.

Theorem 3.2.1. The only solution of 3.2.13 is $F_0(\lambda) \equiv 1$.

Proof: Showing that $F_0(\lambda) \equiv 1$ is the only solution of 3.2.13 is equivalent to showing that for the following problem that if $b_0 \neq 0$ then $F_0(\infty) \neq 1$.

3.2.14 $$F_0'''(\lambda) = -F_0'^2(\lambda) + F_0(\lambda)F_0''(\lambda)$$

$$F_0(0) = 1 \qquad F_0'(0) = 0 \qquad F_0''(0) = b_0$$

The proof of the theorem is now broken down into two cases.

Case i) $b_0 < 0$.

If $b_0 < 0$, then $F_0''(0) < 0$ and thus $F_0''(\lambda) \leq 0$ for all λ by Lemma 3.2.1. Thus $F_0(\lambda)$ is decreasing and concave down for all λ. Hence $F_0(\infty) \neq 1$.

Case ii) $b_0 > 0$.

In this case $F_0''(0) > 0$ and thus $F_0'(\lambda)$ starts out at zero and is increasing. But if $F_0(\infty)$ is to equal 1, $F_0'(\lambda)$ cannot be positive for all λ. Thus there must be a point b such that $F_0''(b) < 0$ and $F_0'(b) = 0$. Then by the same argument as in case i) $F_0(\lambda)$ is decreasing and concave down for all $\lambda \geq b$. Thus $F_0(\infty) \neq 1$. Q.E.D.

A similar result that will be useful in a later section will be stated here as a corollary.

Corollary 3.2.1. The only solution of the following problem is $F_0 \equiv 1$.

3.2.15 $$F_0'''(\lambda) = F_0'^2(\lambda) - F_0(\lambda)F_0''(\lambda)$$

$$F_0(0) = 1 \qquad F_0'(0) = 0 \qquad F_0(\infty) = 1$$

Proof: This result follows easily if the direction of the inequalities in the proofs of Theorems 3.2.1 and Lemma 3.2.1 are reversed. Q.E.D.

Thus Theorem 3.2.1 establishes the solution of 3.2.3 is $F_0 \equiv 1$. From 3.2.12 and the boundary conditions for $F(\lambda)$ the following problem for F_1 would be obtained.

3.2.16 $$\lambda F_0''' + F_0'' - F_1''' - 2F_1'F_0' + F_0F_1'' + F_1F_0'' = 0$$

$$F_0(0) = 0 \qquad F_0'(0) = 0$$

The solution of 3.2.16 is

$$F_1 = B(e^{\lambda} - 1 - \lambda) \quad \text{where } B \text{ is a constant.}$$

However because of the term e^{λ} this solution will not be able to match any outer solution. A similar analysis would show there could be no boundary layer or shock layer between the center and wall of the tube. Therefore if there is a viscous layer it must occur at the center of the tube. Thus the leading term of the outer expansion satisfies the following boundary value problem.

3.2.17 $$f_0'^2 - f_0 f_0'' = \beta_0^2$$

$$f_0(0) = 0 \quad f_0(1) = 1 \quad f_0'(1) = 0 \quad \lim \sqrt{\eta}\ f_0''(\eta) = 0$$

This case is unusual in that even though the order of the equation was reduced all the boundary conditions can still be satisfied. The solution of equation 3.2.17 is $f_0 = \cos \beta_0 (\eta - 1)$ where $\beta_0 = (2k + 1)\pi/2$ and k is an integer.

Since the most general first order solution includes the zeroth order viscous effects we set, without loss of generality, $\gamma_1 = c_1 = \epsilon$. This gives the following first order problem.

3.2.18 $$\eta f_0''' + f_0'' - 2f_0' f_1' + f_0 f_1'' + f_1 f_0'' = -2\beta_0\beta_1$$

$$f_1(1) = 0 \quad f_1'(1) = 0$$

The solution of equation 3.2.18 is given by

$$3.2.19 \quad f_1(\eta) = \sin \beta_0(\eta-1)\left[-\beta_0 + \frac{\beta_0^3}{2}\int_1^\eta \frac{s^2 ds}{\cos \beta_0(s-1)}\right]$$

$$+ \left[\frac{1}{\beta_0}\cos \beta_0(\eta-1) + \eta \sin \beta_0(\eta-1)\right]\left[\frac{3\beta_0}{2} - \frac{\beta_0^3}{2}\int_1^\eta \frac{sds}{\cos \beta_0(s-1)}\right]$$

$$- 3/2 + \frac{\beta_1}{\beta_0}\cos \beta_0(\eta-1)$$

The integrals in equation 3.2.19 require that $\cos \beta_0(\eta-1)$ must not be zero for $0 \leq \eta \leq 1$. Using $\beta_0 = \pi/2(2k+1)$ this requires that $\sin \pi/2(2k+1)\eta$ must not be zero on this interval. Thus we must have $k = 0$. The same conclusion can be obtained from the theoretical results of Section 3.1 by observing that f''' and hence f_0''' cannot change sign in the interval $[0,1]$. Therefore

$$3.2.20 \qquad f_0 = \sin \frac{\pi\eta}{2} \quad \text{and} \quad \beta_0 = \frac{\pi}{2}$$

The theoretical results of Section 1.3 showed two and only two solutions were possible for injection. The numerical results of Section 3.1 showed that both solutions could be obtained for large injection. As Figure 3.1.2 shows the Section I solutions exhibit no reverse flow and the velocity profiles vary smoothly from the wall to the center of the tube. From the theoretical results of Section 1.3 we have that f, f', f'', f''' and f^{IV} do not change signs in the interval $[0,1]$ for Section I injection solutions. Thus for large injection Section I solutions no viscous layer is expected at the center of the tube. However, as Figure 3.2.4 shows, the Section III solutions exhibit a region of reverse flow as well as a rapid

change in the axial velocity profile near the center of the tube. Therefore for large injection Section III solutions a viscous layer is expected near the center of the tube. Thus for Section I solutions it is expected that the viscous forces are much smaller than the inertial forces throughout the tube. This would require then that equation 3.2.4 be valid for all η and thus that $f_1(0) = 0$ and $\lim_{\eta \to \infty} \sqrt{\eta}\ f_1''(\eta) = 0$. From equation 3.2.19 this then gives

$$\beta_1 = \frac{\pi}{2} + \frac{\pi^3}{16} \int_0^1 \frac{s^2 ds}{\cos \frac{\pi}{2}(s-1)} - \frac{3}{2} . \tag{3.2.21}$$

The regular perturbation expansion thus obtained is asymptotic to the Section I solutions and is the one first obtained by Yuan and Finkelstein [33].

Since for the Section III solutions a viscous layer near the center of the tube would be expected, equation 3.2.4 would be valid only as an outer expansion in the region near the wall. In the inner region let $F(\lambda) = f(\eta)$ where $\lambda = \eta/\delta(\epsilon)$ and $\delta(\epsilon)$ is the width of the inner region. Substituting this into equation 3.2.1 gives

$$\epsilon(\lambda F'''(\lambda) + F''(\lambda)) - F'^2(\lambda) + F(\lambda)F''(\lambda) = -\delta^2\beta^2 \tag{3.2.22}$$

$$F(0) = 0 \qquad \lim_{\lambda \to \infty} \sqrt{\lambda}\ F''(\lambda) = 0$$

Expanding the outer solution given by equations 3.2.20 and 3.2.19 into the inner region gives

3.2.23 $$f \sim \frac{\pi\lambda}{2}\,\delta(\epsilon) + O(\delta(\epsilon))$$

Therefore in the inner region F has the expansion

3.2.24 $$F = F_0(\lambda)\delta(\epsilon) + F_1(\lambda)\nu_1(\epsilon) + \cdots$$

Substituting equation 3.2.24 into equation 3.2.22 and boundary conditions and collecting terms gives

3.2.25 $$\epsilon\delta(\epsilon)(\lambda F_0''' + F_0'') + \epsilon\nu_1(\lambda F_1''' + F_1'') + \delta^2(F_0F_0'' - F_0'^2)$$
$$+ \nu_1\delta(-2F_0'F_1' + F_0F_1'' + F_1F_0'') + \nu_1^2(-F_1'^2 + F_1F_1'')$$
$$= -\delta^2\beta_0^2 - 2\beta_0\beta_1\epsilon\delta^2 - \beta_1^2\epsilon^2\delta^2 - \cdots$$

Since in the boundary layer the viscous and inertial forces will be of the same magnitude, we need to set $\delta(\epsilon) = \epsilon$. Therefore the leading term of the inner solution satisfies the following problem.

3.2.26 $$\lambda F_0''' + F_0'' - F_0'^2 + F_0F_0'' = -\beta_0^2$$

with boundary conditions

$$F_0(0) = 0 \qquad \lim_{\lambda\to 0} \sqrt{\lambda}\; F_0''(\lambda) = 0 \qquad F_0'(\infty) = \frac{\pi}{2}$$

The latter condition results from matching the leading terms of the inner and outer solutions and, as was previously determined, $\beta_0 = \frac{\pi}{2}$. The solution of 3.2.26 was found by Terrill and Thomas [24] and is given by

3.2.27 $$F_0 = \frac{\pi\lambda}{2} - 3 + 3e^{\frac{-\pi\lambda}{2}}$$

Now matching the leading term of the inner solution with the two term outer solution gives for this case,

$$\beta_1 = \frac{3}{2} + \frac{\pi}{2} + \frac{\pi^3}{16} \int_0^1 \frac{s^2 ds}{\cos \frac{\pi}{2}(s-1)}$$

The solution thus obtained is asymptotic to the Section III solutions and is the asymptotic expansion for Section III solutions first obtained by Terrill and Thomas [24].

Section 3.3. Asymptotic Solutions for Small Injection and Suction.

Asymptotic solutions in the case of small injection and suction (small crossflow Reynolds number), were first studied by Yuan and Finkelstein [33] for the Section I solutions and by Terrill and Thomas [24] for the Section II and Section III solutions. Their results will be re-derived and discussed here. Letting $\epsilon = -R/2$, where $|\epsilon| << 1$, the small injection and suction problem is formulated as follows.

3.3.1 $$\eta f'''(\eta) + f''(\eta) - \epsilon(f'^2(\eta) - f(\eta)f''(\eta)) = K$$

$$f(1) = 1 \qquad f(0) = 0$$

$$f'(1) = 0 \qquad \lim_{\eta \to 0} \eta^{1/2} f''(\eta) = 0$$

The theoretical results of Section 1.3 show that K is negative for all Section II and Section III solutions and for all Section I injection solutions. However for section

I suction solutions there are no theoretical results on the sign of K. Our numerical results do show that for $0 \leq R \leq 1.2$ K is negative while for $1.2 < R < 2.3$ K is positive. Thus in contrast to the previous section no sign will be assigned to K in the following analysis.

Asymptotic series of the following form will now be sought for $f(\eta)$ and K. Let

3.3.2 $$f(\eta) = \gamma_0(\varepsilon)f_0(\eta) + \gamma_1(\varepsilon)f_1(\eta) + \cdots$$

3.3.3 $$K = \beta_0 C_0(\varepsilon) + \beta_1 C_1(\varepsilon) + \cdots$$

Substituting equations 3.3.2 and 3.3.3 into equation 3.3.1 and collecting terms gives

3.3.4 $$\gamma_0(\eta f_0''' + f_0'') + \gamma_1(\eta f_1''' + f_1'') + \varepsilon\gamma_0^2(-f_0'^2 + f_0 f_0'') + \varepsilon\gamma_0\gamma_1(-2f_0'f_1' + f_0 f_1'' + f_1 f_0'') + \varepsilon\gamma_1^2(-f_1'^2 + f_1 f_1'') + \cdots = \beta_0 C_0(\varepsilon) + \beta_1 C_1(\varepsilon) + \cdots$$

As equation 3.3.4 shows there are two possibilities for the leading term of the asymptotic expansion. Either the viscous terms are much larger than the inertial terms in which case we set, without loss of generality, $\gamma_0 = C_0 = 1$ or the viscous and inertial terms are of the same magnitude in which case we set, again without loss of generality, $\gamma_0 = C_0 = \frac{1}{\varepsilon}$.

The first case with $\gamma_0 = C_0 = 1$ leads to an expansion for $f(\eta)$ and K in powers of ϵ of the following form.

3.3.5 $$f = f_0 + \epsilon f_1 + \cdots$$

3.3.6 $$K = \beta_0 + \epsilon \beta_1 + \cdots$$

where f_0 and f_1 and β_0 and β_1 are determined by the following two problems respectively.

3.3.7 $$f_0''' + f_0'' = \beta_0$$

$$f_0(1) = 1 \qquad f_0(0) = 0$$

$$f_0'(1) = 0 \qquad \lim_{\eta \to \infty} \sqrt{\eta}\, f_0''(\eta) = 0$$

3.3.8 $$\eta f_1''' + f_1'' - f_0'^2 + f_0 f_0'' = \beta_1$$

$$f_1(1) = 0 \qquad f_1(0) = 0$$

$$f_1'(1) = 0 \qquad \lim_{\eta \to \infty} \sqrt{\eta}\, f_1''(\eta) = 0$$

Solving 3.3.7 and 3.3.8 gives

3.3.9 $$f_0 = 2\eta - \eta^2$$

3.3.10 $$f_1 = \frac{\eta^4}{18} - \frac{\eta^3}{3} + \frac{\eta^2}{2} - \frac{2}{9}\eta$$

The calculation of further terms is straight forward. This is the solution first obtained by Yuan and Finkelstein [33] and corresponds to the Section I small injection and suction solutions.

The second case with $\gamma_0 = C_0 = \frac{1}{\epsilon}$ leads to the following problems for the leading term.

3.3.11 $$\eta f_0''' + f_0'' - f_0'^2 + f_0 f_0'' = \beta_0$$

$$f_0(1) = 0 \qquad f_0(0) = 0$$

$$f_0'(1) = 0 \qquad \lim_{\eta \to 0} \sqrt{\eta}\ f_0''(\eta) = 0$$

Terrill and Thomas [24] were able to find an approximate solution of 3.3.11 by essentially computing the Taylor series near zero and near one and matching the two series at an intermediate point. The approximate solution they found is given by the following. In the interval $[0, \eta^*]$ where $\eta^* = 0.262$

3.3.12 $$f_0 = \beta\eta + 3e^{-\beta\eta} - 3$$

where $\beta = 4.196$ and $\beta_0 = -\beta^2$.

and in the interval $(\eta^*, 1]$,

3.3.13 $$f_0 = 8.81(\eta + \eta \ln \eta - \eta^2) + 1.577(1 + \eta \ln \eta - \eta) - 0.435(1 - \eta)^5 - 0.082(1 - \eta)^6 - 0.071(1 - \eta)^7 - 0.082(1 - \eta)^8 + O[(1 - \eta)^9]$$

The solution they thus obtained was asymptotic to the Section II and Section III solutions for small suction and injection respectively.

Section 3.4. Asymptotic Solutions for Large Suction.

The problem of asymptotic solutions for large suction have been examined by Terrill and Thomas [24] with supplementary results by Terrill in [23]. The solutions obtained in these papers are asymptotic to the Section IV(ii) and Section V(ii) solutions. In this section the asymptotic expansions they obtained will be rederived and reexamined in the light of the theoretical results previously obtained. Letting $0 < \epsilon = 2/R \ll 1$ the problem for large suction will be formulated as follows.

3.4.1 $$\epsilon(\eta f'''(\eta) + f''(\eta)) + f'^2(\eta) - f''(\eta)f(\eta) = \beta^2$$

$$f(1) = 1 \qquad f(0) = 0$$

$$f'(1) = 0 \qquad \lim_{\eta \to 0} \eta^{1/2} f''(\eta) = 0$$

where $\beta^2 = \epsilon K$. That K is necessarily positive follows from the theoretical results of Section 1.3. An asymptotic expansion will now be sought which is valid in the region where the inertial forces are much larger than the viscous forces. Let

3.4.2 $$f(\eta) = f_0(\eta)\gamma_0(\epsilon) + f_1(\eta)\gamma_1(\epsilon) + \cdots$$

3.4.3 $$\beta = \beta_0 C_0(\epsilon) + \beta_1 C_1(\epsilon) + \cdots$$

Substituting 3.4.2 and 3.4.3 into equation 3.4.1 and collecting terms gives

3.4.4 $$\varepsilon\gamma_0(\eta f_0''' + f_0'') + \varepsilon\gamma_1(\eta f_1''' + f_1'') + \gamma_0^2(f_0'^2 - f_0 f_0'')$$
$$+ \gamma_1\gamma_0(2f_0'f_1' - f_0 f_1'' - f_1 f_0'') + \gamma_1^2(f_1'^2 - f_1 f_1'') + \cdots$$
$$= C_0^2\beta_0^2 + 2\beta_0\beta_1 C_0 C_1 + \beta_1^2 C_1^2 + \cdots$$

The leading term of the expansion, f_0, will satisfy the following differential equation.

3.4.5 $$f_0'^2 - f_0 f_0'' = \beta_0^2$$

The region of validity of expansion 3.4.2 will now be discussed.

We first consider the possibility that $f(\eta)$ has a regular perturbation expansion as was found for the case of large injection. Then f_0 would have to satisfy the following boundary conditions:

3.4.6 $$f_0(0) = 0 \qquad f_0(1) = 1$$
$$\lim_{\eta\to 0} \sqrt{\eta}\, f_0''(\eta) = 0 \qquad f_0'(1) = 0$$

As was shown in Section 3.2 the solution of 3.4.5 subject to 3.4.6 would be

3.4.7 $$f_0 = \sin\frac{\pi\eta}{2}$$

However 3.4.7 gives $f_0'''(0) = \frac{-\pi^2}{4}$ which contradicts theoretical results of Section 1.3 which showed $f'''(0) > 0$ for all suction solutions. Thus unlike the case of large

injection there can be no regular perturbation solution for large suction.

A second possibility is that expansion 3.4.2 is valid near the wall but that there is a viscous layer near the center of the tube. By the same analysis as was used in deriving equation 3.2.26 for the leading term in the viscous layer for large injection Section III solutions, it can be shown that the leading term, $F_0(\lambda)$, in the viscous layer in this case would have to be a solution of the following problem.

$$3.4.8 \qquad \lambda F_0'''(\lambda) + F_0''(\lambda) + F_0'^2(\lambda) - F_0(\lambda)F_0''(\lambda) = \frac{\pi^2}{4}$$

$$F_0(0) = 0 \qquad \lim_{\lambda \to 0} \sqrt{\lambda}\ F_0''(\lambda) = 0 \qquad F_0'(\infty) = \frac{\pi}{2}$$

But equation 3.4.8 is the same as equation 1.3.2 so the results that held for $g(\xi)$ in Section 1.3 will hold for $F_0(\lambda)$. Since as $\lambda \to \infty$, $F_0(\lambda) \to \frac{\pi\lambda}{2} + C$ where C is a constant, $F_0(\lambda)$ must eventually exceed three. Then by equation 1.3.6 $F_0^V(\lambda)$ will be negative. This and Theorem 1.3.1 would require $F_0'''(\lambda)$ to be decreasing and concave down and thus $F_0'''(\lambda)$ must go negative. This then makes $F_0''(\lambda)$ decreasing and concave down and hence it too must go negative. Then $F_0'(\lambda)$ is decreasing and concave down and hence $F_0'(\lambda) \to -\infty$. Thus problem 3.4.8 has no solution. Thus if there is a region where the inertial forces are larger than the viscous forces it must be at the center of

the tube. Physically this is to be expected since the fluid being withdrawn from the tube has the effect of confining the vorticity in the region near the wall. A further discussion of this confinement of vorticity at the wall due to suction is to be found in Batchelor [1].

Therefore since $f(1) = 1$, without loss of generality, we set $\gamma_0 = C_0 = 1$. This gives the following problem for the leading term of the outer expansion.

3.4.9 $$f_0'^2 - f_0 f_0'' = \beta_0^2$$

$$f_0(0) = 0 \qquad f_0(1) = 1 \qquad \lim_{\eta \to 0} \sqrt{\eta}\ f_0''(\eta) = 0$$

The possible solutions of 3.4.9 are

3.4.10 $$f_0(\eta) = \bar{K}\beta_0 \sinh \eta/\bar{K} \quad \text{where} \quad \bar{K}\beta_0 \sinh \frac{1}{\bar{K}} = 1$$

3.4.11 $$f_0(\eta) = (-1)^m L\beta_0 \sin \eta/L \quad \text{where} \quad (-1)^m L\beta_0 \sin \frac{1}{L} = 1$$

3.4.12 $$f_0(\eta) = \eta$$

K and L are constants of integration and m is an integer. In the inner region let $F(\lambda) = f(\eta)$ where $\eta = 1 - \delta(\epsilon)\lambda$ and $\delta(\epsilon)$ is the width of the boundary layer. Substituting this into equation 3.4.1 gives

3.4.13 $$\epsilon((\lambda - \frac{1}{\delta(\epsilon)})F'''(\lambda) + F''(\lambda)) + F'^2(\lambda) - F(\lambda)F''(\lambda) = \delta^2(\epsilon)\beta^2$$

$$F(0) = 1 \qquad F'(0) = 0$$

Si

ar

Si

3.

gi

in

3.

Su

3.

The

3.4

The

out

of

Pro

3.4

be

Since in the boundary layer the viscous and inertial terms are to be of the same magnitude it is seen that $\delta(\epsilon) = \epsilon$. Since the three possible outer solutions, given by equation 3.4.10, 3.4.11, and 3.4.12, when expanded in inner variables give $f \sim 1 - \epsilon\lambda$, $F(\lambda)$ must have the following expansion in the boundary layer.

3.4.14 $$F(\lambda) = F_0(\lambda) + \epsilon F_1(\lambda) + \cdots$$

Substituting 3.4.14 into 3.4.13 and collecting terms gives

3.4.15 $$\epsilon(\lambda F_0''' + F_0'') + \epsilon^2(\lambda F_1''' + F_1'') - F_0''' - \epsilon F_1''' + F_0'^2 - F_0F_0''$$
$$+ \epsilon(2F_1'F_0' - F_0F_1'' - F_1F_0'') + \epsilon^2(F_1'^2 - F_1F_1'') + \cdots$$
$$= \epsilon^2\beta_0^2 + 2\beta_0\beta_1C_1\epsilon^2 + \beta_1^2\epsilon^2C_1^2 + \cdots$$

Therefore the leading term in the inner region satisfies

3.4.16 $$-F_0''' + F_0'^2 - F_0F_0'' = 0$$

$$F_0(0) = 1 \qquad F_0'(0) = 0 \qquad F_0(\infty) = 1$$

The last boundary condition comes from matching with the outer solution. By Corollary 3.2.1 the unique solution of 3.4.16 is $F_0 \equiv 1$.

Before examining the first order inner solution the problem of which of the outer solutions, given by equations 3.4.10, 3.4.11, and 3.4.12, is the appropriate one should be resolved. The resolution lies in examining $f'''(0)$.

Differentiating equation 3.4.1 once and evaluating it at $\eta = 0$ gives

3.4.17 $$f'''(0) = -\frac{1}{2\varepsilon} f'(0)f''(0)$$

Since in a region where the viscous terms are much smaller than the inertial terms it has been shown that the leading term in the expansion for $f'(0)$ is finite and non-zero, the leading term of the expansion for $f''(0)$ and hence $f'''(0)$, must be zero for otherwise, as equation 3.4.17 shows, the viscous terms at the center of the tube would no longer be small relative to the inertial terms. This then requires $f_0'''(0) = 0$. Since only equation 3.4.12 satisfies this requirement, $f_0 = \eta$ is the correct outer solution.

Returning now to the first order inner solution it is seen that it satisfies the following problem.

3.4.18 $$\lambda F_0''' + F_0'' - F_1''' + 2F_1'F_0' - F_0F_1'' - F_1F_0'' = 0$$

$$F_1(0) = 0 \qquad F_1'(0) = 0$$

The solution of 3.4.18 is given by

3.4.19 $$F_1(\lambda) = C_1(\lambda - 1 + e^{-\lambda})$$

where C_1 is a constant of integration. Matching the two term inner expansion with the leading term of the outer expansion gives, if exponentially small terms are ignored in matching, $C_1 = -1$ and $\gamma_1 = \varepsilon$. This gives from equation

3.4

fol

3.4

So

f

pe

ex

3.

3.

3

T

a

a

a

e

T

i

s

3

3.4.4 that the first order outer solution satisfies the following problem.

$$3.4.20 \qquad \eta f_0''' + f_0'' + 2f_0'f_1' - f_0f_1'' - f_1f_0'' = 2\beta_0\beta_1$$

$$f_1(0) = 0 \qquad \lim_{\eta\to 0} \sqrt{\eta}\, f_1''(\eta) = 0$$

Solving and matching with the two term inner solution gives $f_1 = \eta$ and $\beta_1 = 1$. Continuing as above and ignoring experimentally small terms in matching gives the following expansions for the outer solution, inner solution and β.

$$3.4.21 \qquad f(\eta) = \eta + \epsilon\eta + 3\epsilon^2\eta + O(\epsilon^3)$$

$$3.4.22 \qquad F(\lambda) = 1 - \epsilon(\lambda - 1 + e^{-\lambda}) - \epsilon^2((2\lambda + 3)e^{-\lambda} + \lambda - 3) + O(\epsilon^3)$$

$$3.4.23 \qquad \beta = 1 + \epsilon + 3\epsilon^2 + O(\epsilon^3)$$

These expansions were first obtained by Terrill and Thomas [24] and were found to be asymptotic to both the Section IV(ii) and Section V(ii) solutions. As was first observed by Terrill and Thomas [24] this leads to the conclusion that the difference between these two solutions is exponentially small. Terrill [23] was able to find inner and outer solutions which included these exponentially small terms. His results are given as follows.

For the outer solution

$$3.4.24 \qquad f = \epsilon\xi + \epsilon\bar{\delta}(\epsilon)g_1(\xi) + O(\epsilon\bar{\delta}^2(\epsilon))$$

where

3.4.25 $$\xi = \beta\eta/\epsilon$$

3.4.26 $$\beta = 1 + \epsilon + 3\epsilon^2 + 18\epsilon^3 + \frac{591}{4}\epsilon^4 + O(\epsilon^5)$$

3.4.27 $$\bar{\delta}(\epsilon) = \pm \frac{1}{(2\epsilon)^{3/2}} \exp(-\frac{1}{2} - \frac{1}{2\epsilon})\{1 - \frac{9\epsilon}{2} - \frac{51}{8}\epsilon^2 - \frac{617}{16}\epsilon^3 + O(\epsilon^4)\}$$

3.4.28 $$g_1(\xi) = \xi - \xi^2 + \frac{\xi^3}{6}$$

The plus sign on $\bar{\delta}(\epsilon)$ corresponds to the Section V(ii) solution and the minus sign corresponds to the Section IV(ii) solutions.

For the inner solution

3.4.29 $$F(\lambda) = 1 + \epsilon(1 - \lambda - e^{-\lambda}) + \epsilon^2(3 - \lambda - (2\lambda + 3)e^{-\lambda}) + O(\epsilon^2) + \frac{\bar{\delta}(\epsilon)}{\epsilon}\{-\frac{1}{3}(\lambda - 1 + e^{-\lambda}) + \epsilon(\frac{\lambda^2}{2} - \frac{\lambda}{6} + 2 + e^{-\lambda}(\frac{-\lambda^2}{6} - \frac{5\lambda}{3} - 2)) + O(\epsilon^2)\} + O(\frac{\bar{\delta}^2}{\epsilon^2})$$

No asymptotic or approximate solutions for the Section IV(i) or Section V(i) solutions were obtained. It appears that in these solutions viscous and inertial effects are everywhere important. However since it was known from the theoretical results of Section 1.3 that a Section V(i) solution corresponded to the second zero of a Section I injection solution, the asymptotic Section I injection solution was examined to see if asymptotic solutions could be obtained for Section V(i) solution. However no results were obtained.

CHAPTER IV

THE UNSTEADY COMPONENT OF VELOCITY

Section 4.1. Numerical Results.

Numerical solutions of equation 1.2.14 for $h(\eta)$, the unsteady component of velocity, were found for various values of the crossflow Reynolds number and for various values of the non-dimensionalized parameter α, where $\alpha = \frac{a}{2}\sqrt{\frac{\omega}{\nu}}$, by the technique discussed in Section 2.2. The solutions for $h(\eta)$ are classified according to the same scheme as the corresponding steady solutions. For example, if $f(\eta)$ in equation 1.2.14 was a Section I solution, then the solution of 1.2.14 for $h(\eta)$ would also be designated as a Section I solution. The numerical results will be presented and examined in terms of the following properties: a) The non-dimensionalized maximum skin friction at the wall. From equation 1.2.19 we see that this is given by $|h'(1)|$. b) The phase lag of the skin friction at the wall relative to the pulsatile pressure gradient. This is given by $\theta = \tan^{-1}\left(\frac{-h_i'(1)}{h_R'(1)}\right)$ where $0 \leq \theta \leq \pi$ and h_R and h_i are the the real and imaginary parts respectively of $h(\eta)$. c) The non-dimensionalized axial velocity profile. As equation 1.2.11b shows, this is given by the real part of $h(\eta)e^{i\omega t}$.

Section I Solutions

a) Maximum skin friction at the wall.

Case i) α small. (See Figure 4.1.1)

There is a rapid decrease in skin friction with increased injection. Increased suction results in a large and rapid increase in skin friction until $R = 1.2$. For $1.2 \leq R < 2.3$ there is a marked decrease in skin friction.

Case ii) α large. (See Figure 4.2.2)

For a fixed amount of suction or injection increasing α results in a decrease of skin friction. However for α large and fixed, injection further decreases skin friction. For suction as α increases the maximum near $R = 1.2$ is suppressed and for α sufficiently large the maximum occurs at $R = 2.3$.

b) Phase lag of the skin friction from the pulsatile pressure gradient.

Case i) α small. (See Figure 4.1.3)

For all values of injection the phase lag is small. Increasing injection further reduces the phase lag. However as suction is increased there is a large and rapid increase in the phase lag until $R = 1.2$ where it attains a maximum. A further increase in suction causes a decrease in the phase lag.

Case ii) α large. (See Figure 4.1.4)

For a fixed amount of injection increasing α increases the phase lag but for a fixed α increasing injection decreases the phase lag. For suction as α increases the maximum phase lag near $R = 1.2$, is suppressed and for α sufficiently large the maximum occurs at $R = 2.3$.

c) Axial velocity profiles.

Case i) α small. (See Figures 4.1.5 - 4.1.6)

For injection the velocity profiles are parabolic with the maximum velocity occurring at the center of the tube and virtually in phase with the pressure gradient. Increasing injection decreases the magnitude of the maximum velocity and tends to flatten the velocity profile.

For suction the velocity profiles are also parabolic with the maximum occurring at the center of the tube. Increasing suction up to $R = 1.2$ increases the magnitude of the velocity at its maximum, but for $1.2 \leq R \leq 2.3$ the maximum velocity magnitude is decreased. For increased suction there is also a phase shift in the velocity profile relative to the pressure gradient with the maximum phase shift occurring near $R = 1.2$.

Case ii) α large. (See Figures 4.1.7 - 4.1.8)

For a fixed amount of injection increasing α results in a phase shift of the velocity profile relative to the

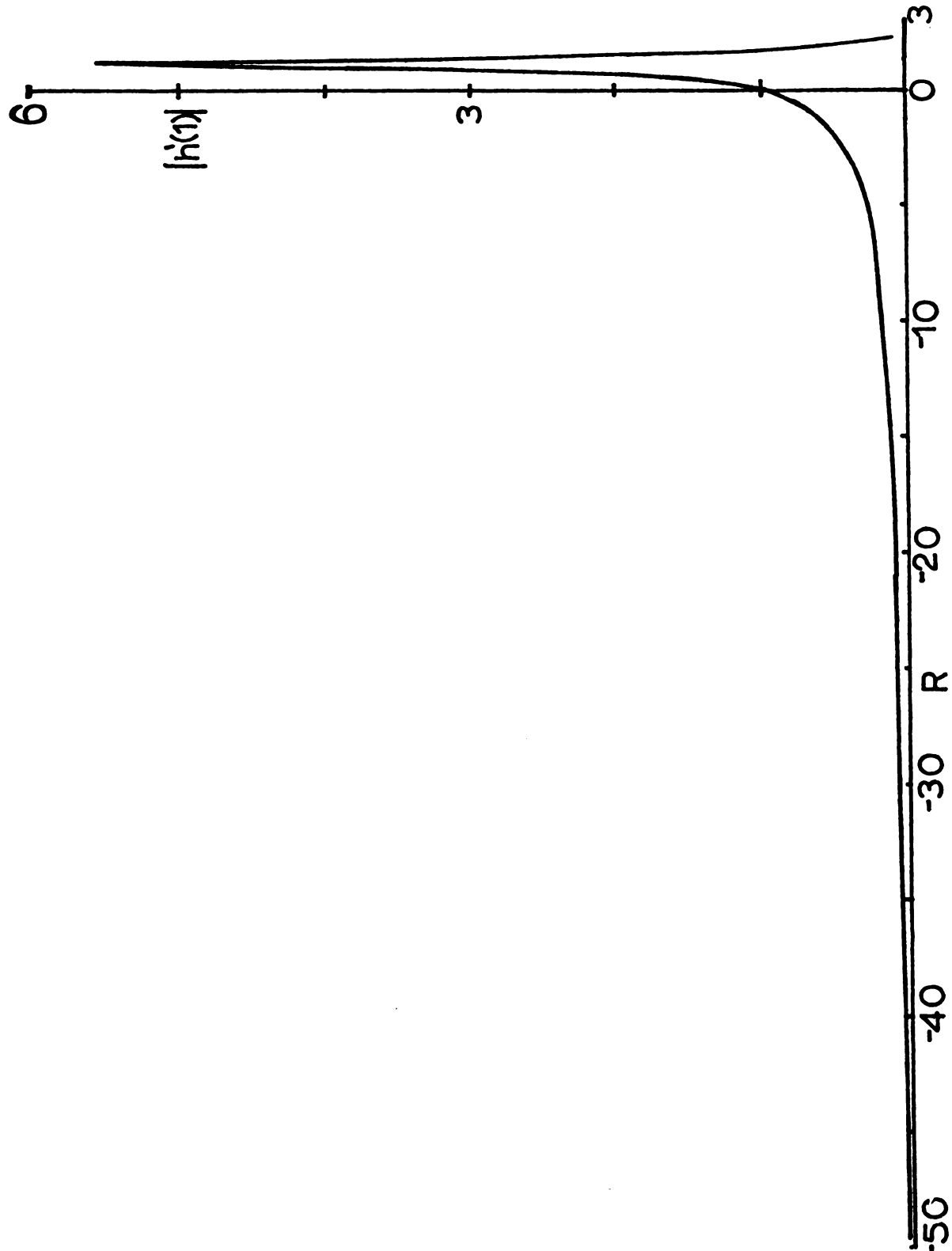

Figure 4.1.1. Maximum skin friction at the wall for $a^2=0.2$ for Section I solutions.

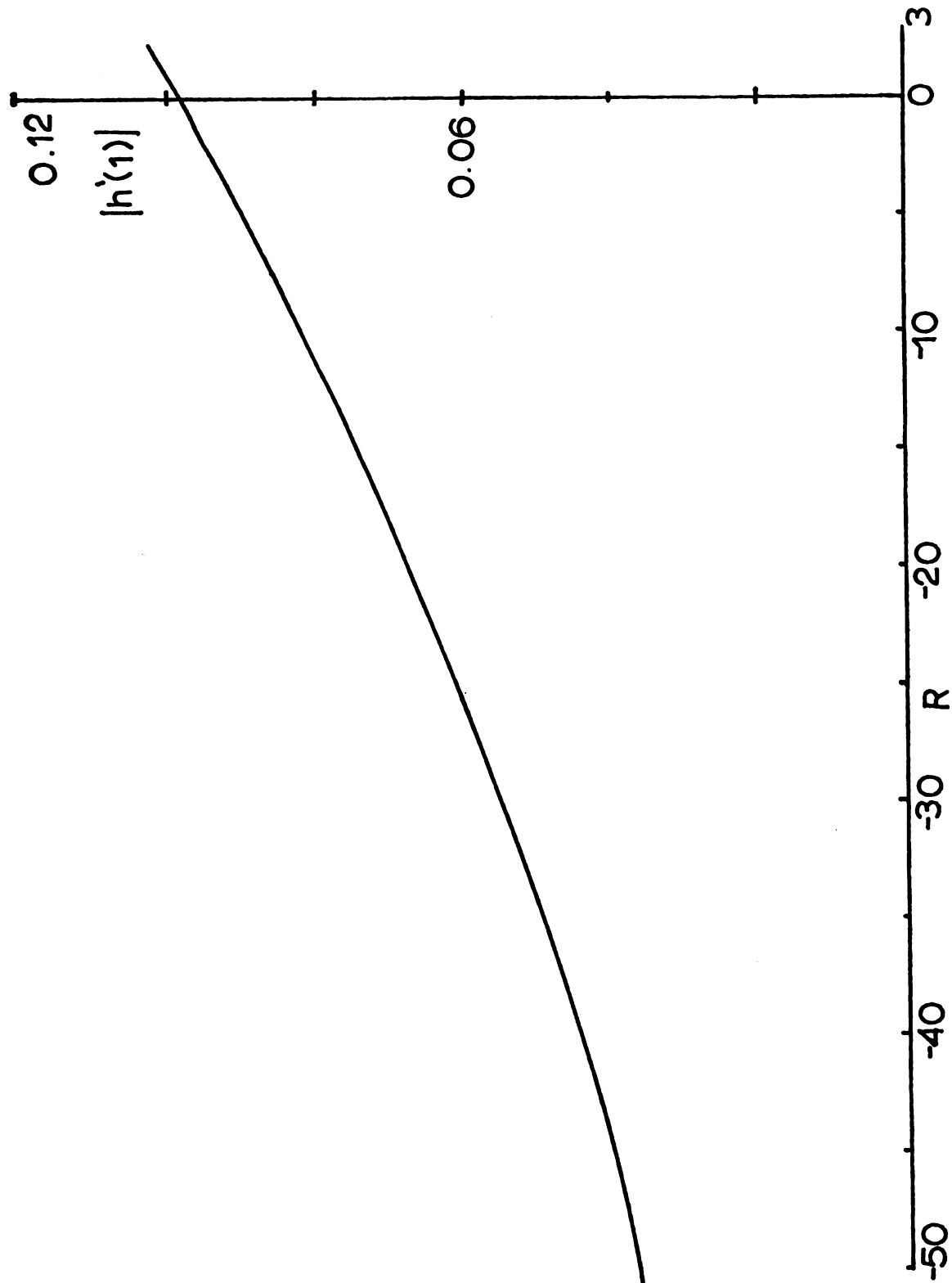

Figure 4.1.2. Maximum skin friction at the wall for α^2=100.0 for SectionI solutions.

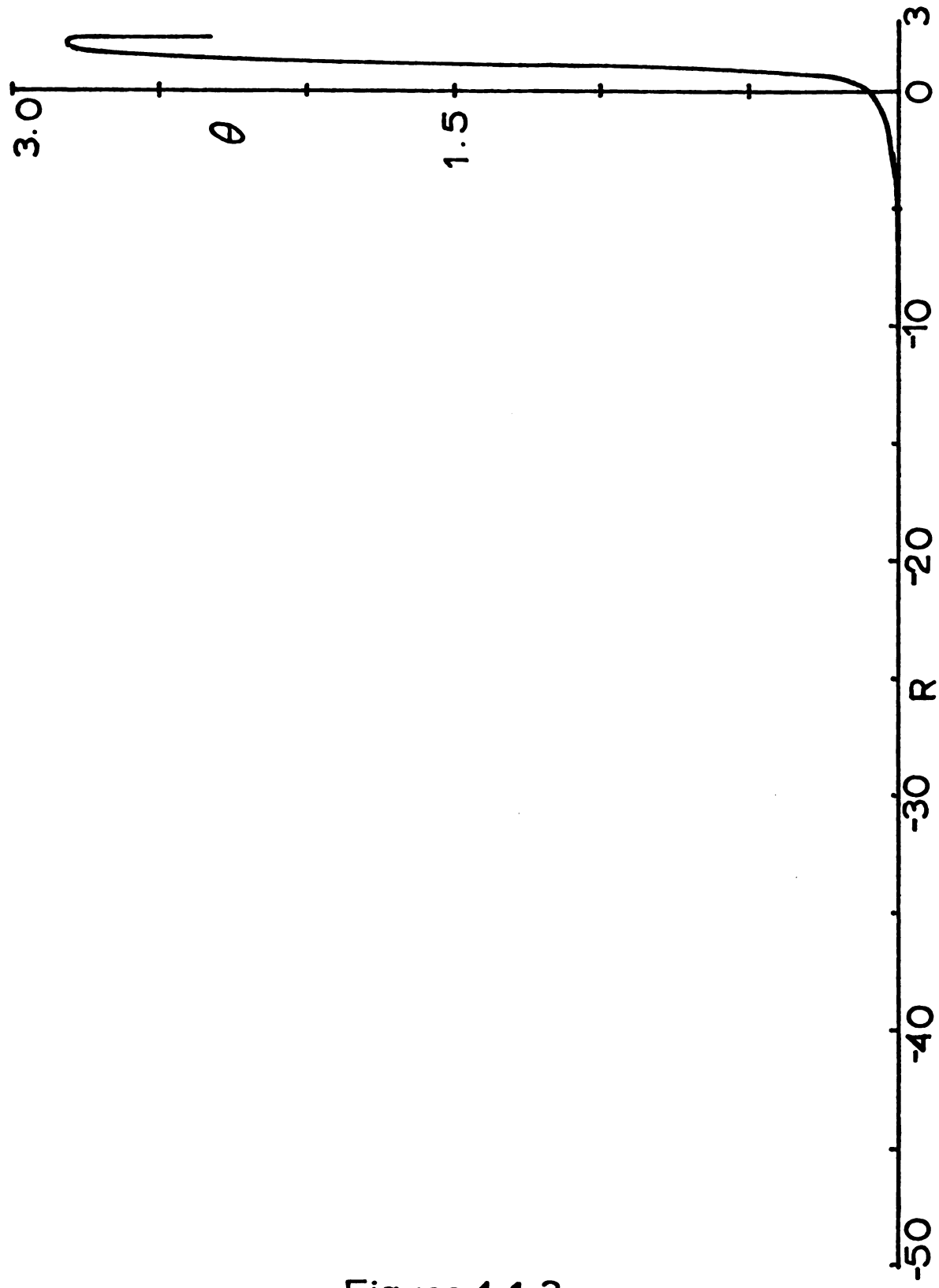

Figure 4.1.3.
Phase lag for α^2=0.2 for Section I solutions.

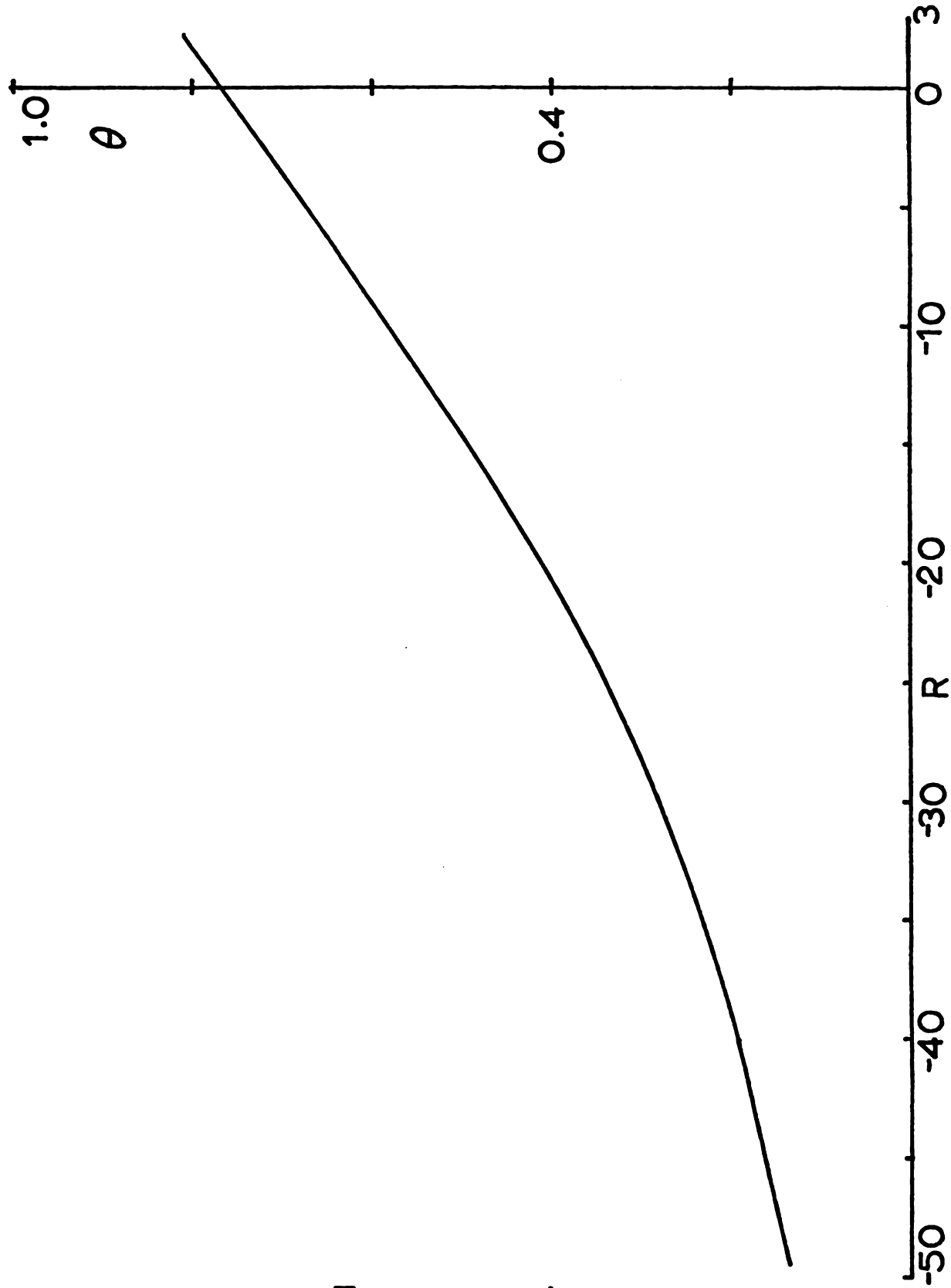

Figure 4.1.4.
Phase lag for α^2=100.0 for Section I solutions.

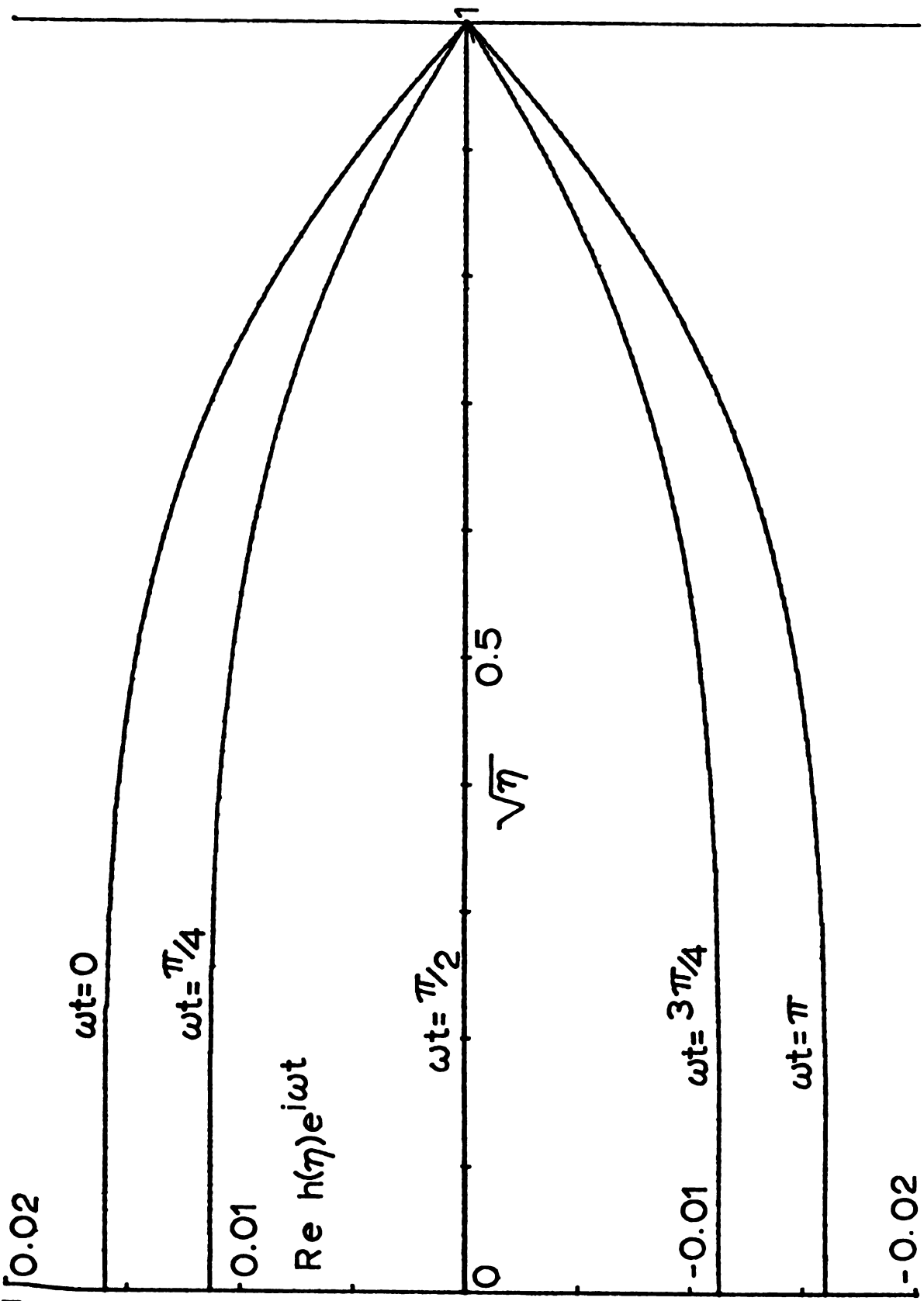

Figure 4.1.5. Axial velocity profile for a Section I solution with R=-78.59152 and α^2=0.2.

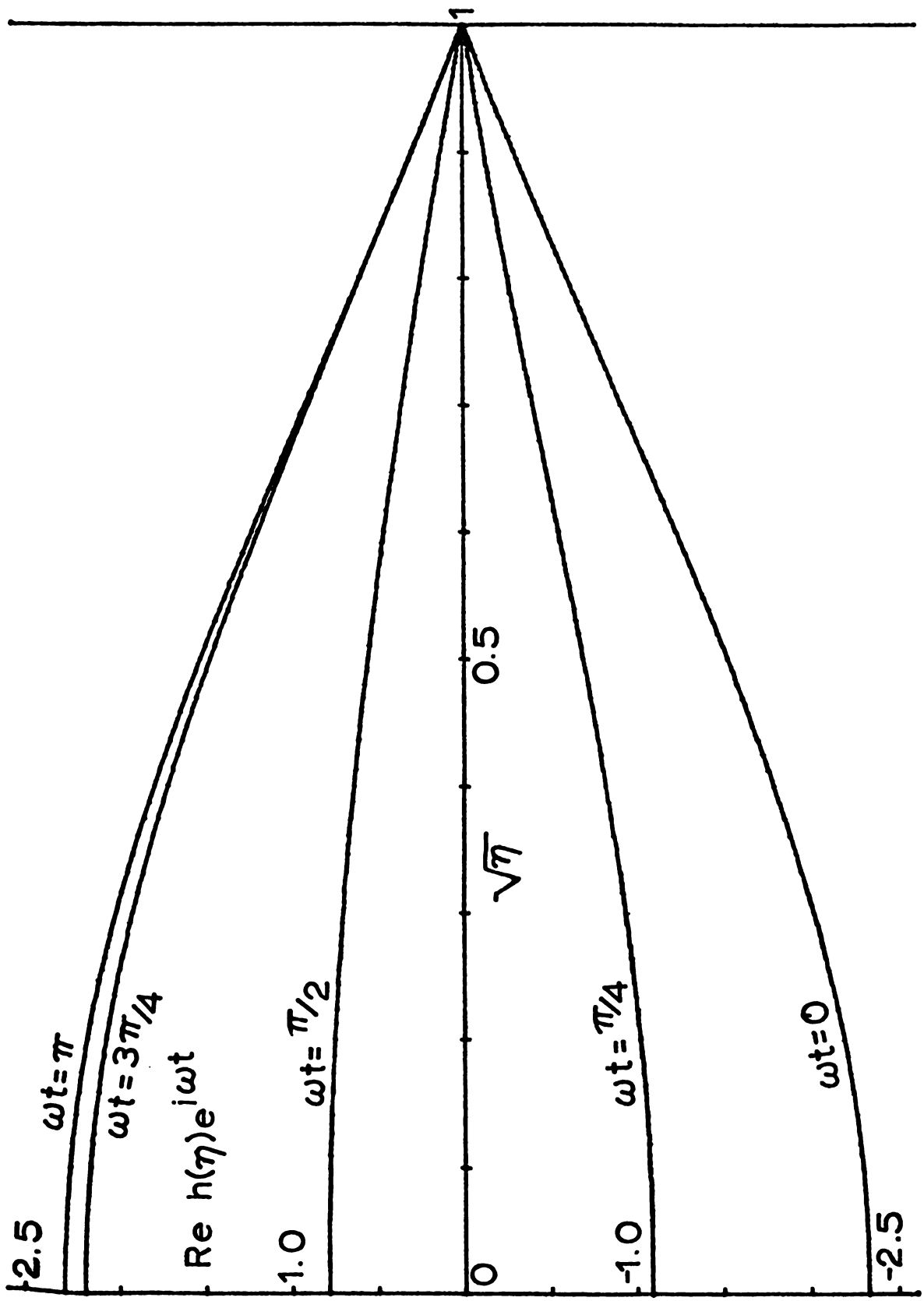

Figure 4.1.6. Axial velocity profile for a Section I solution with $R=1.63266$ and $\alpha^2=0.2$.

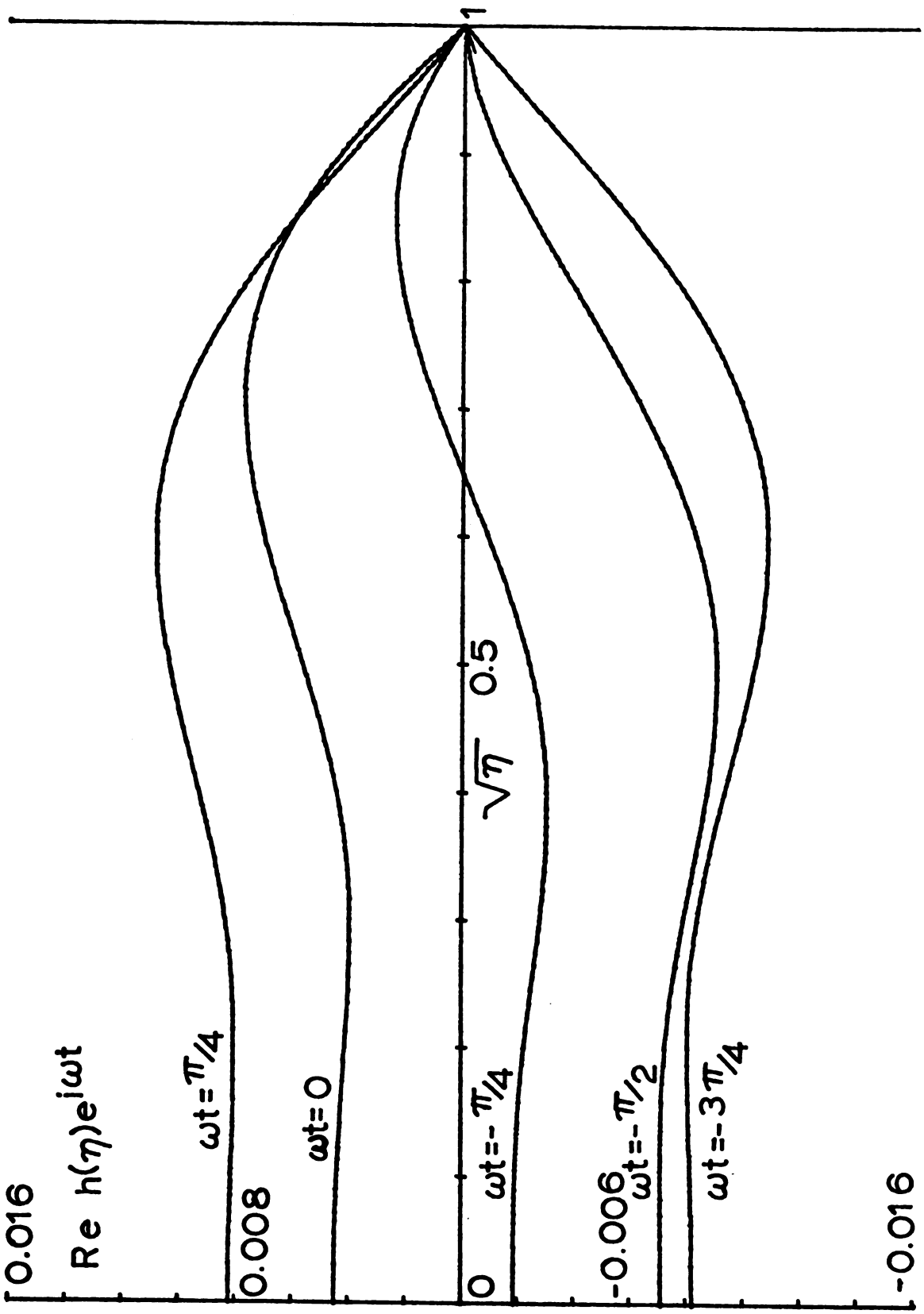

Figure 4.1.7. Axial velocity profile for a Section I solution with R=-78.59152 and α^2=100.0.

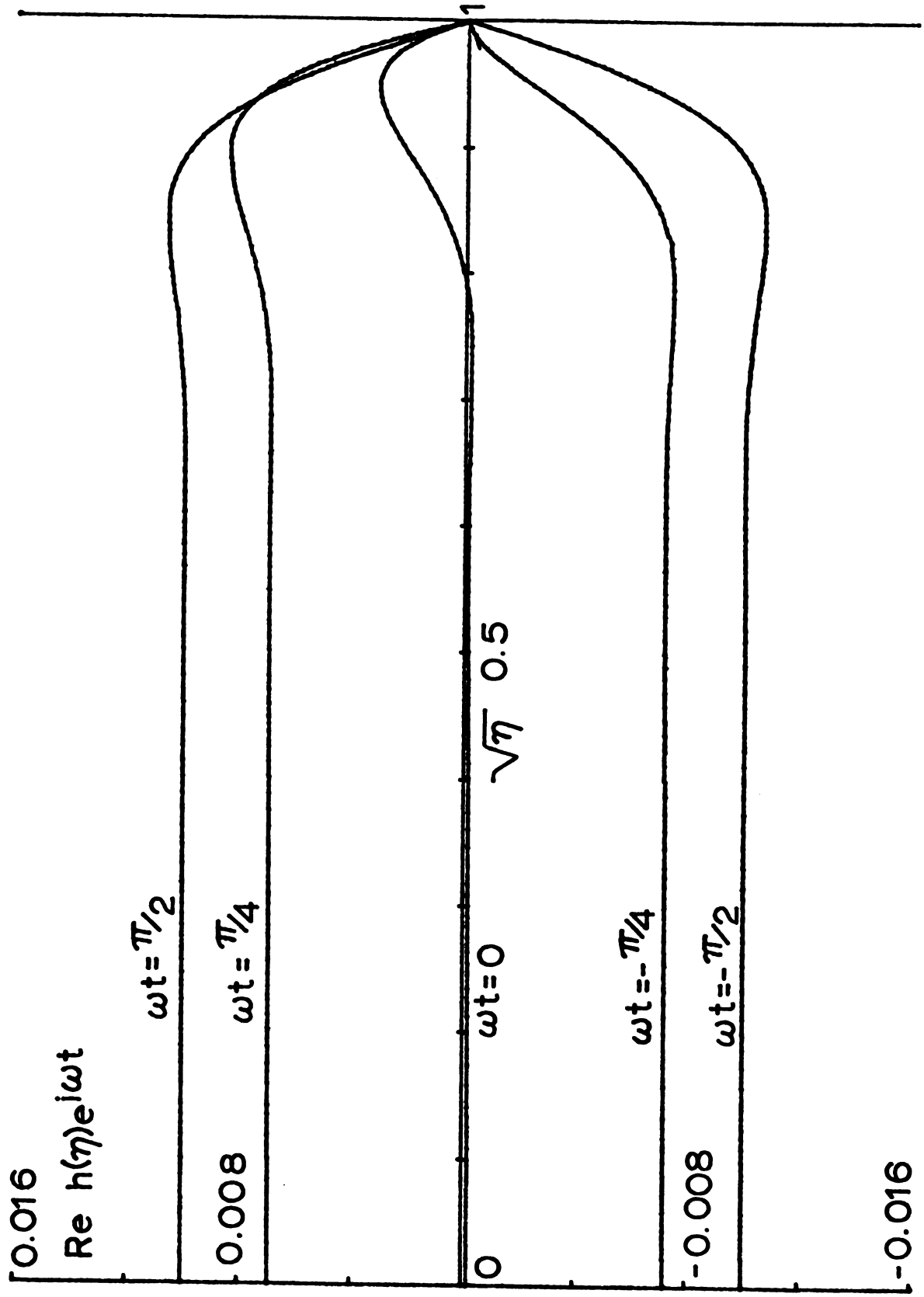

Figure 4.1.8. Axial velocity profile for a Section I solution with R=1.63266 and α^2=100.0.

pressure gradient, in shifting the maximum velocity toward the wall, and in a decrease in the magnitude of the veloctiy. For α large, increasing injection shifts the maximum velocity back toward the center of the tube.

For a fixed amount of suction increasing α causes the maximum magnitude of the velocity to be shifted towards the wall but the size of the maximum to be decreased. For α sufficiently large the maximum magnitude of the velocity and the maximum phase shift for suction occur at $R = 2.3$.

Section II and Section III Solutions

Unlike the steady state Section II and Section III solutions, the unsteady state solutions remain finite as the crossflow Reynolds number approaches zero.

a) Maximum skin friction at the wall.

Case i) α small. (See Figure 4.1.9)

For this case the maximum skin friction occurs near $R = 0$. An increase of suction or injection results in a marked decrease in skin friction.

Case ii) α large. (See Figure 4.1.10)

As α is increased for a fixed amount of injection or suction the magnitude of skin friction decreases. However as α is increased the maximum value of skin friction near $R = 0$

is suppressed and shifted toward larger values of suction until eventually the maximum occurs at $R = 2.3$. Thus for large values of α increased suction results in increased skin friction while increased injection results in decreased skin friction.

b) Phase lag of the skin friction from the pulsatile pressure gradient.

Case i) α small. (See Figure 4.1.11)

For injection the phase lag is small and is further reduced by increased injection. For suction, however, the phase lag increases rapidly as suction increases and attains a maximum at $R = 2.3$.

Case ii) α large. (See Figure 4.1.12)

Increasing α results in increased phase lag for both suction and injection. However for fixed α increased injection still decreases the phase lag while increased suction increases the phase lag.

c) Axial velocity profiles.

Case i) α small. (See Figures 4.1.13 - 4.1.14)

For both suction and injection the flow is divided into two regions which are π radians out of phase and separated by a point of velocity reversal. Increasing suction moves the stagnation point toward the wall while increased

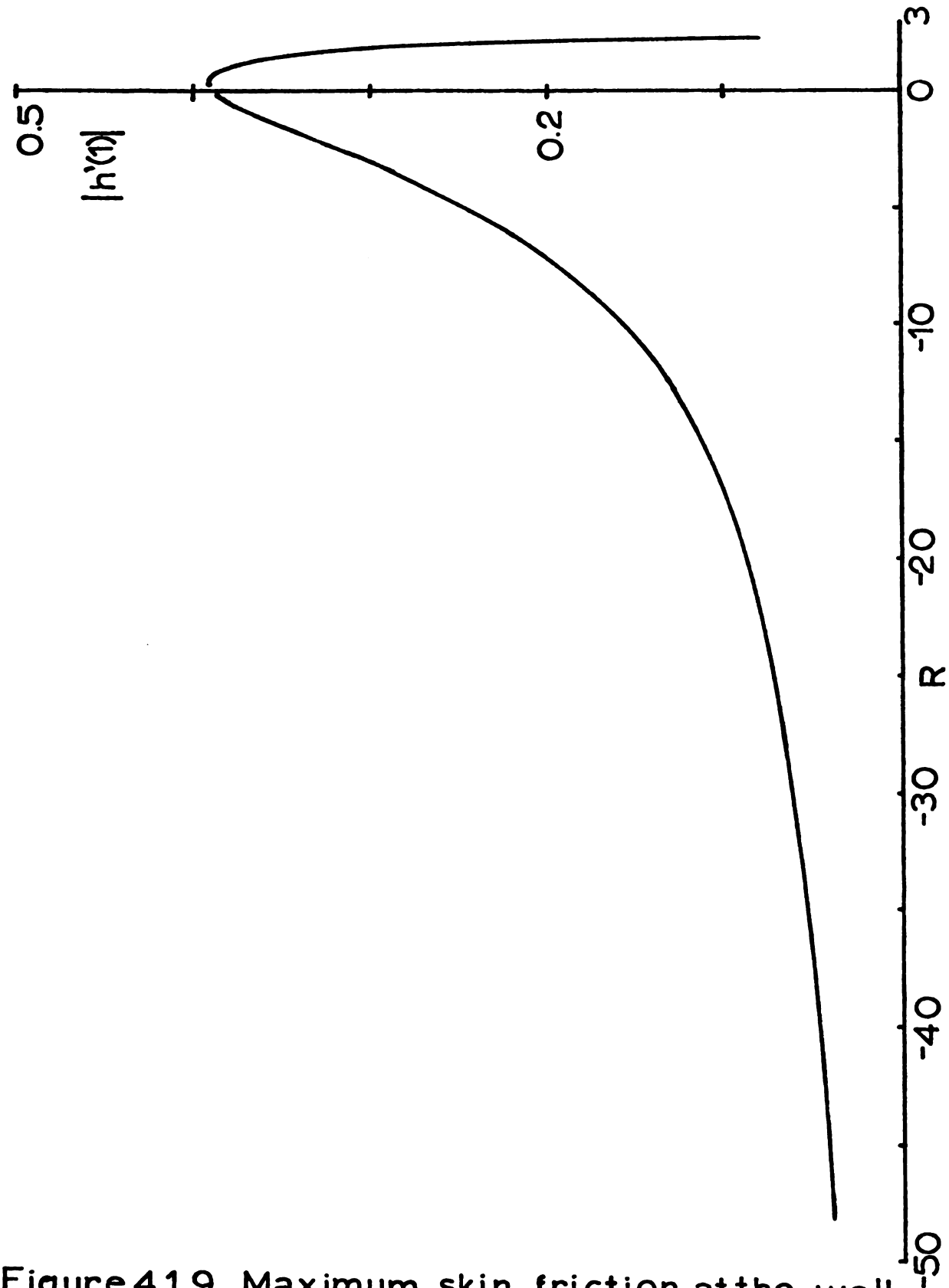

Figure 4.1.9. Maximum skin friction at the wall for Section II and Section III solutions with $\alpha^2=0.2$.

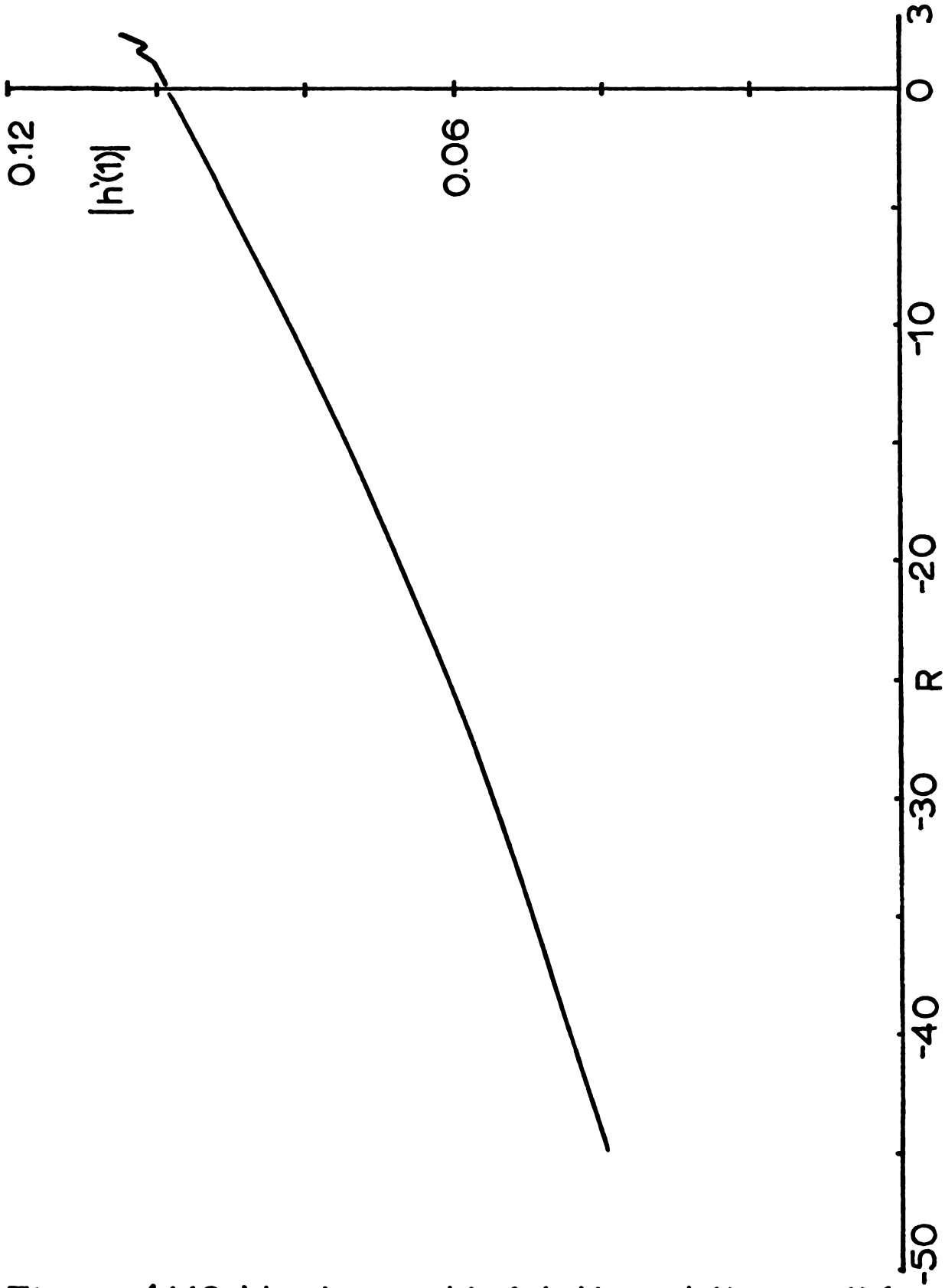

Figure 4.1.10. Maximum skin friction at the wall for Section II and Section III solutions with α^2=100.0.

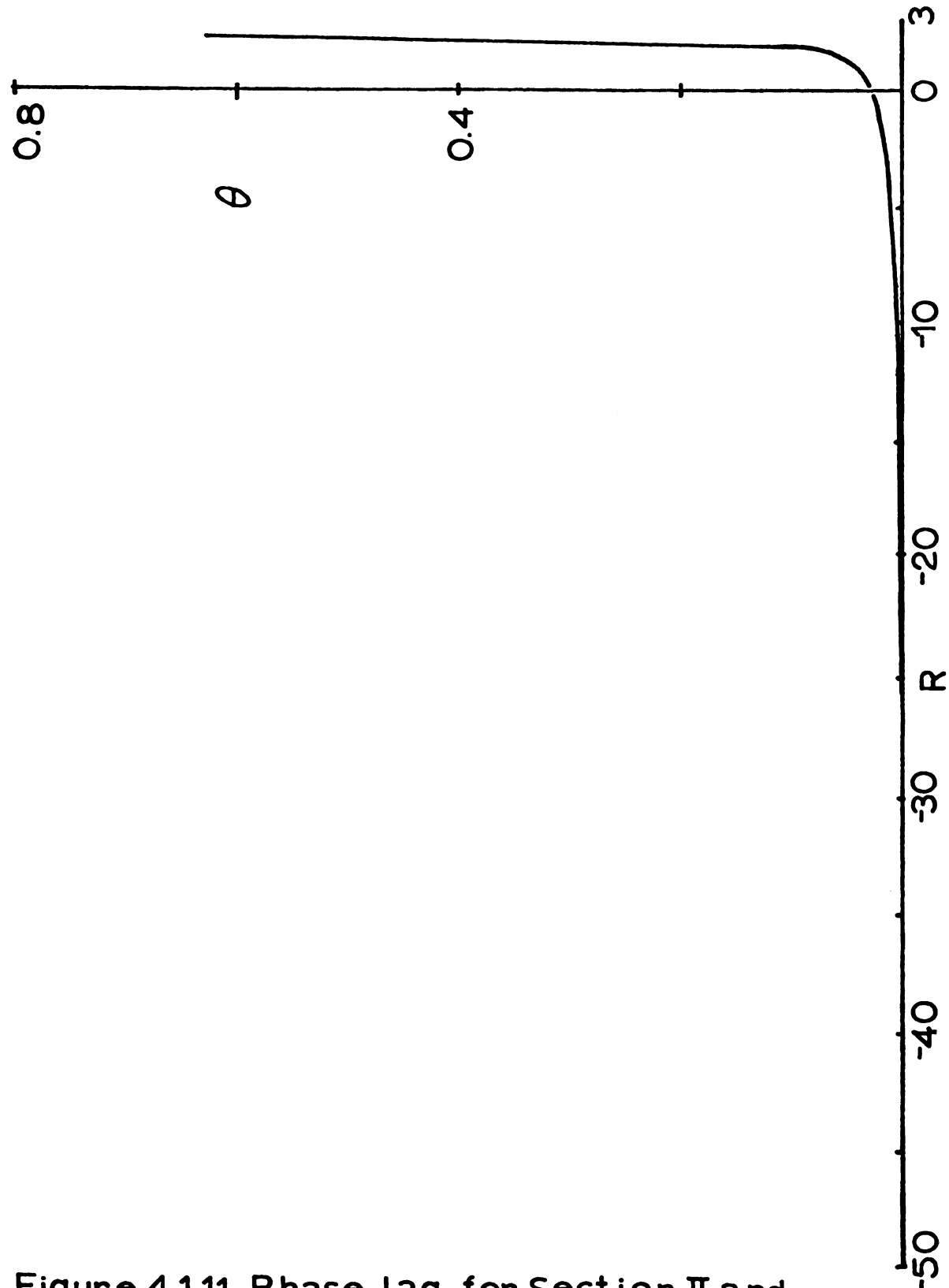

Figure 4.1.11. Phase lag for Section II and Section III solutions with $\alpha^2=0.2$.

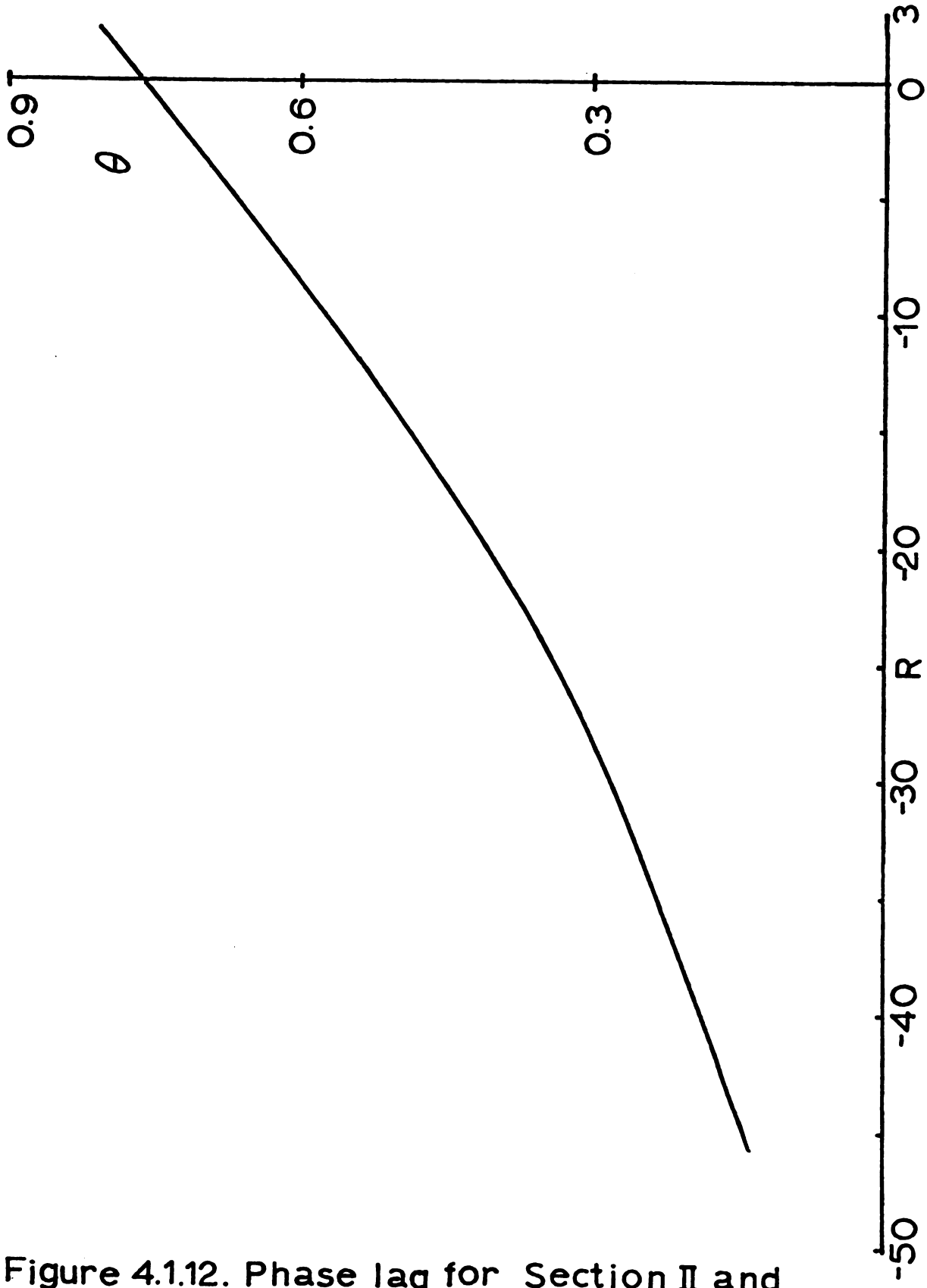

Figure 4.1.12. Phase lag for Section II and Section III solutions with α^2=100.0.

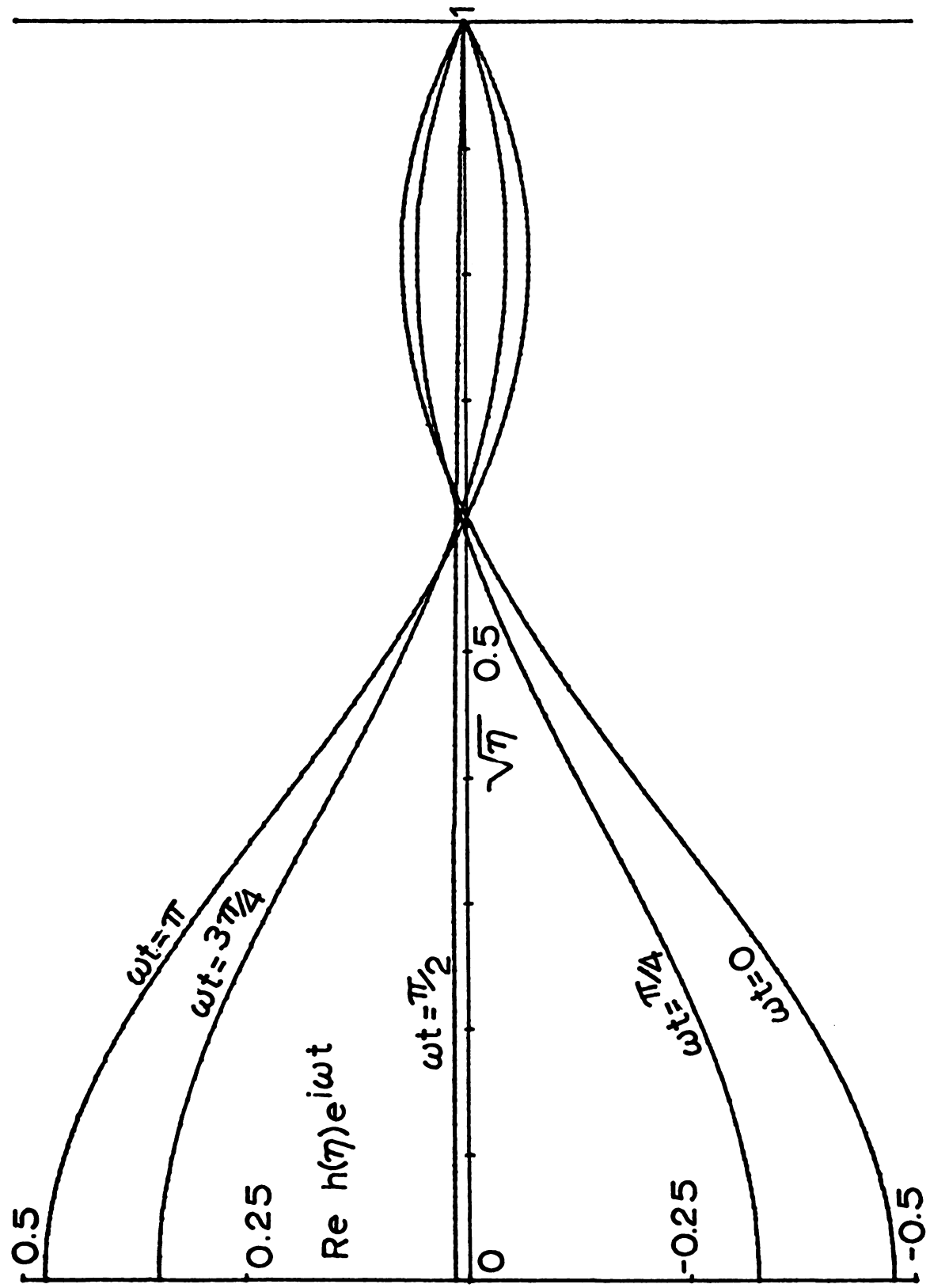

Figure 4.1.13. Axial velocity profile for a Section II solution with R=1.11343 and α^2=0.2.

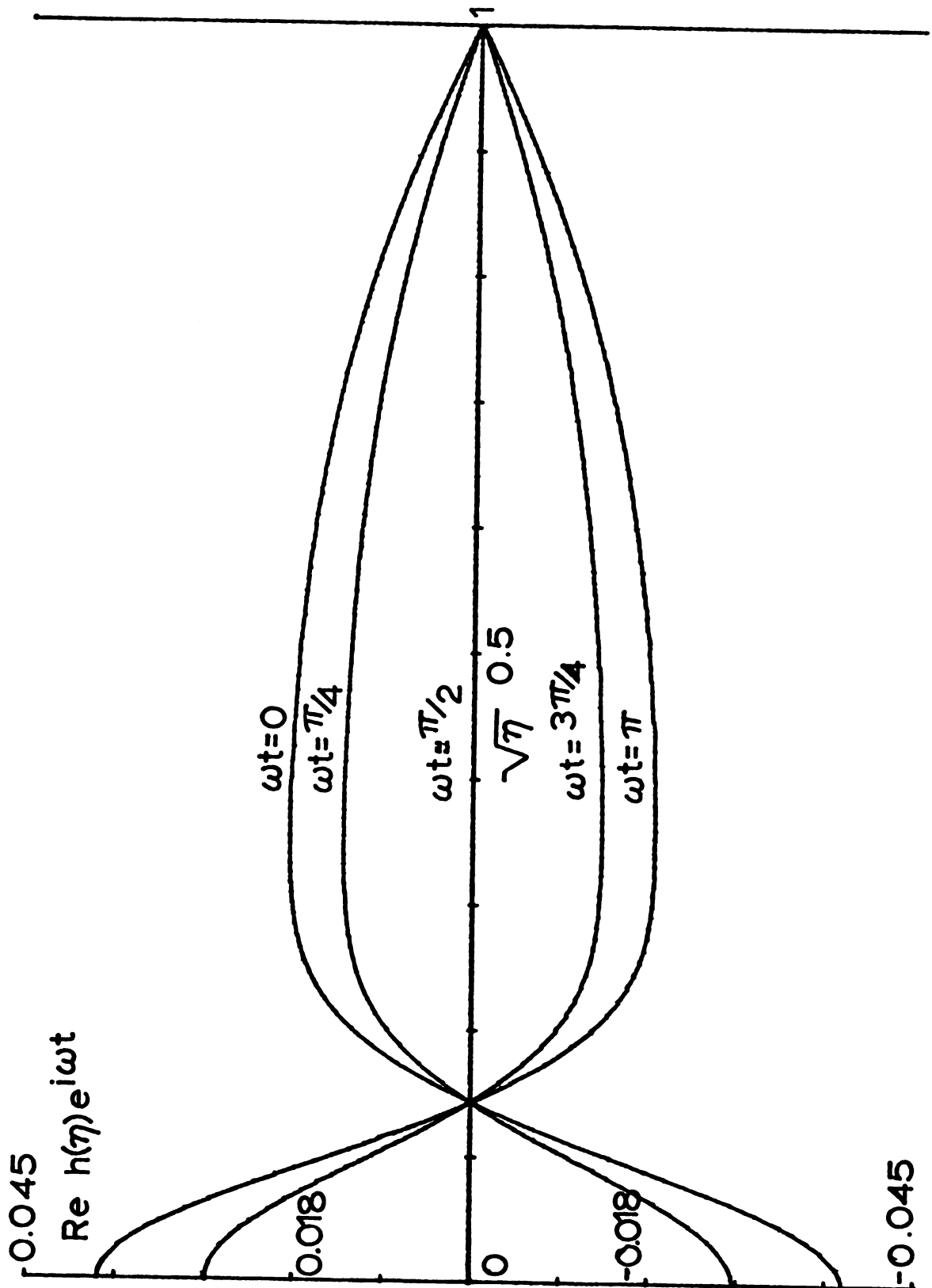

Figure 4.1.14. Axial velocity profile for a Section III solution with $R=-62.5627$ and $\alpha^2=0.2$.

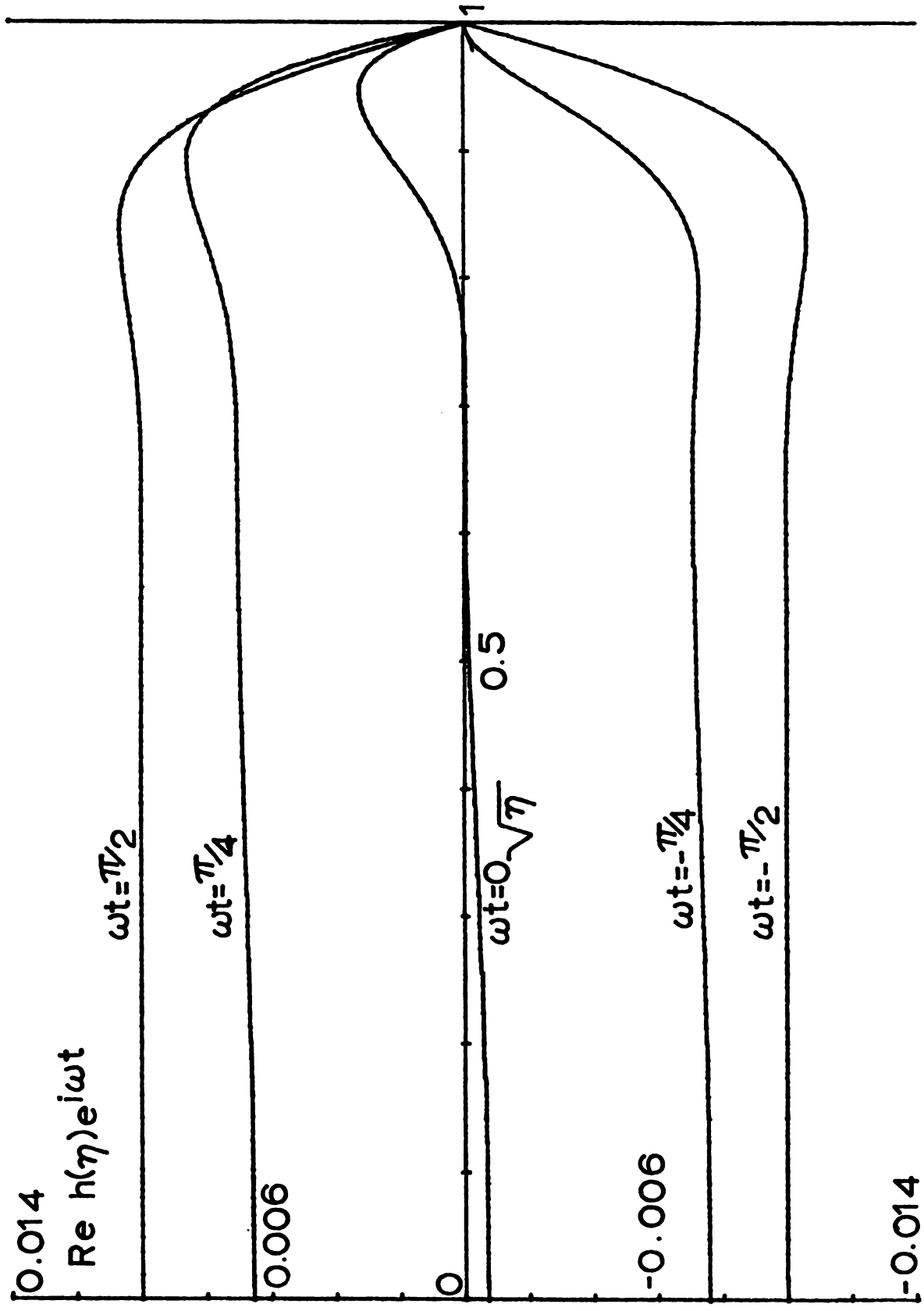

Figure 4.1.15. Axial velocity profile for a Section II solution with R=1.11343 and α^2=100.0.

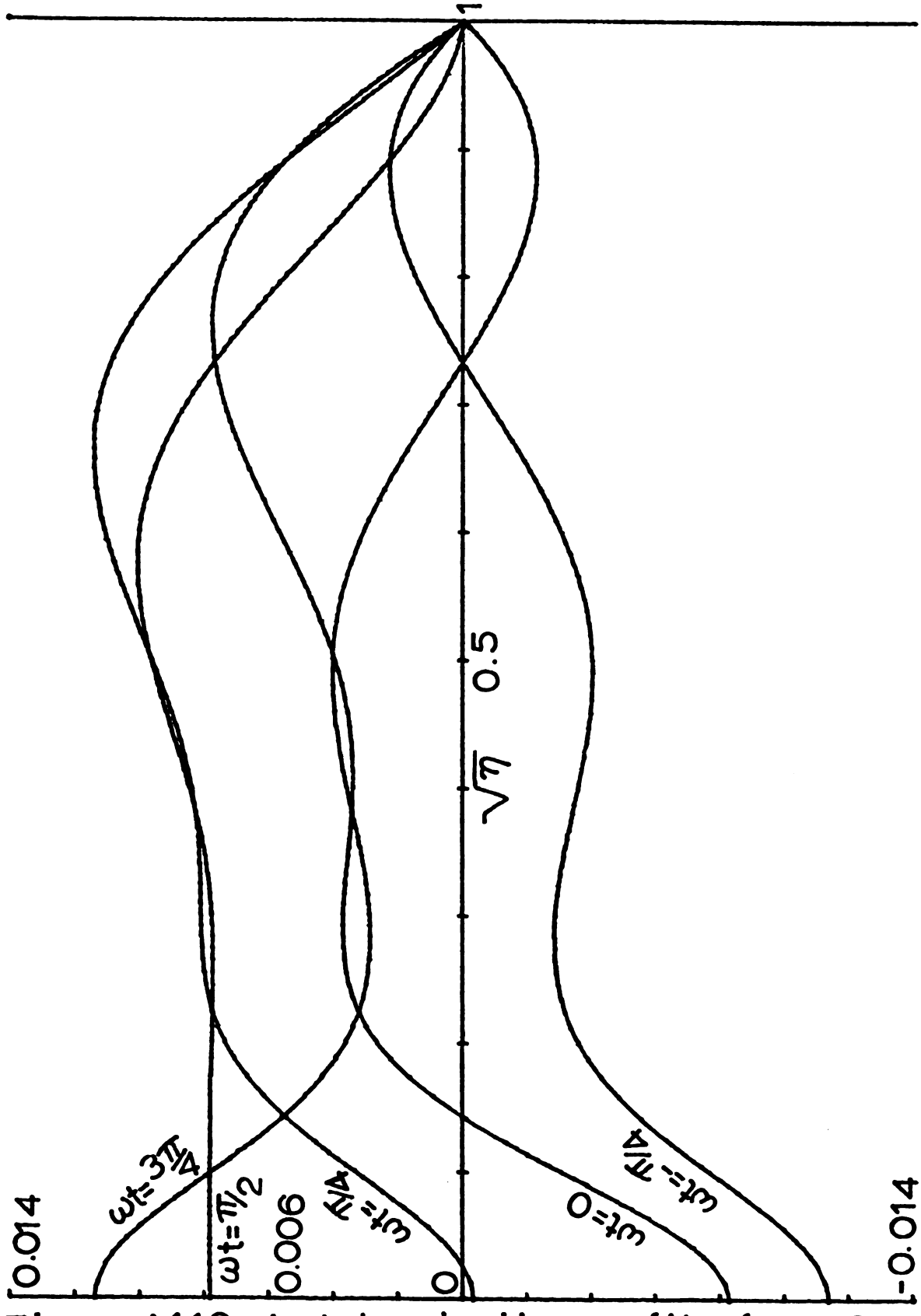

Figure 4.1.16. Axial velocity profile for a Section III solution with R=-62.5627 and α^2=100.0.

injection moves it toward the center of the tube. In this case the flow is either in phase with the pressure gradient of π radians out of phase. As suction is decreased or injection increased the magnitude of the maximum velocity, which occurs near the center of the tube, is decreased.

Case ii) α large. (See Figures 4.1.5 - 4.1.6)

For a fixed value of suction or injection increasing α results in shifting the maximum velocity toward the wall, in a phase shift of the velocity profile relative to the pressure gradient, in the flow no longer separating into two regions, and in a decrease of the magnitude of the maximum velocity. For α large and fixed, increased injection results in shifting the maximum velocity back toward the center of the tube.

Section IV(i) Solutions

a) Maximum skin friction at the wall.

Case i) α small. (See Figure 4.1.17)

In this case the maximum skin friction occurs at $R = 23.7$. As suction is first decreased to $R = 20.6$ and then increased the skin friction decreases markedly.

Case ii) α large. (See Figure 4.1.18)

For a fixed value of suction the skin friction decreases as α increases. For α large and fixed, as suction

is first decreased to $R = 20.6$ and then increased the skin friction decreases.

b) Phase lag of the skin friction from the pulsatile pressure gradient.

Case i) α small. (See Figure 4.1.19)

For this case the phase lag is virtually π radians for all values of suction, but increases slightly as suction is first decreased to $R = 20.6$ and then increased.

Case ii) α large. (See Figure 4.1.21)

For a fixed amount of suction increasing α decreases the phase lag. However for α sufficiently large the minimum phase lag no longer occurs at $R = 23.7$.

c) Axial velocity profiles.

Case i) α small. (See Figure 4.1.22)

The flow in this case separates into three regions separated by two points of velocity reversal. As suction first decreases from 23.7 to 20.6 and then increases the magnitude of the velocity of the flow is decreased while the maximum velocity is shifted from the wall toward the center of the tube.

Case ii) α large. (See Figure 4.1.23)

As α is increased for a fixed amount of suction there results a decrease in the magnitude of the velocity,

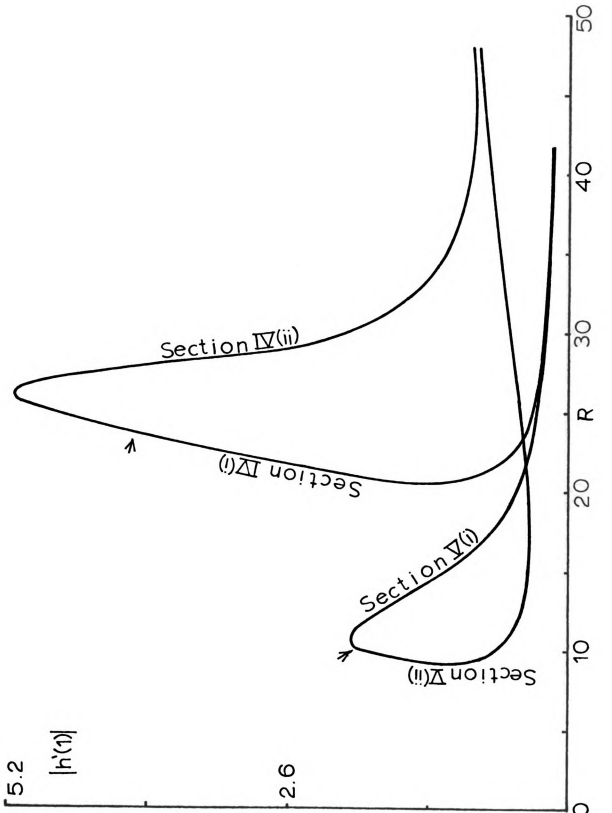

Figure 4.1.17. Maximum skin friction at the wall for Section IV and V solutions with $\alpha^2=0.2$.

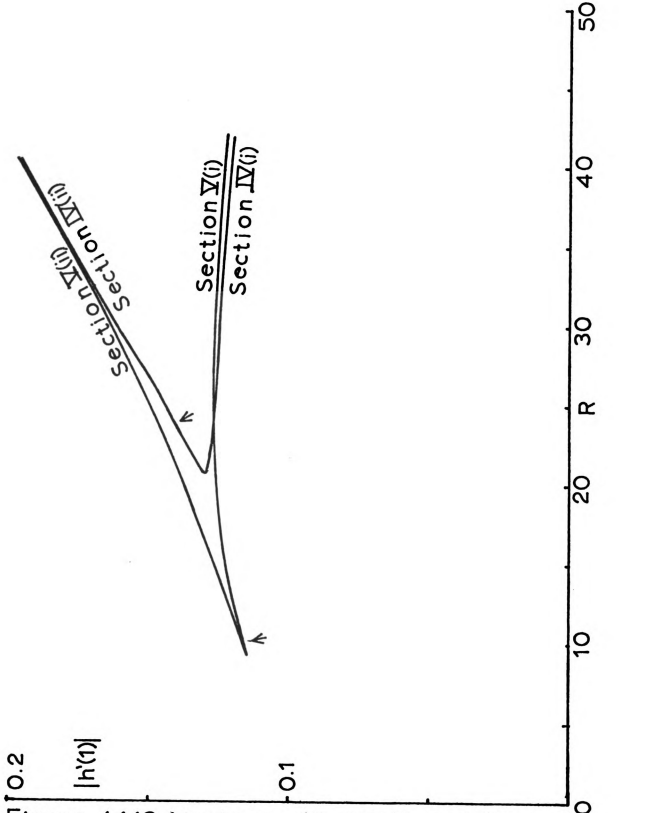

Figure 4.1.18. Maximum skin friction at the wall for Section IV and V solutions with α^2=100.0.

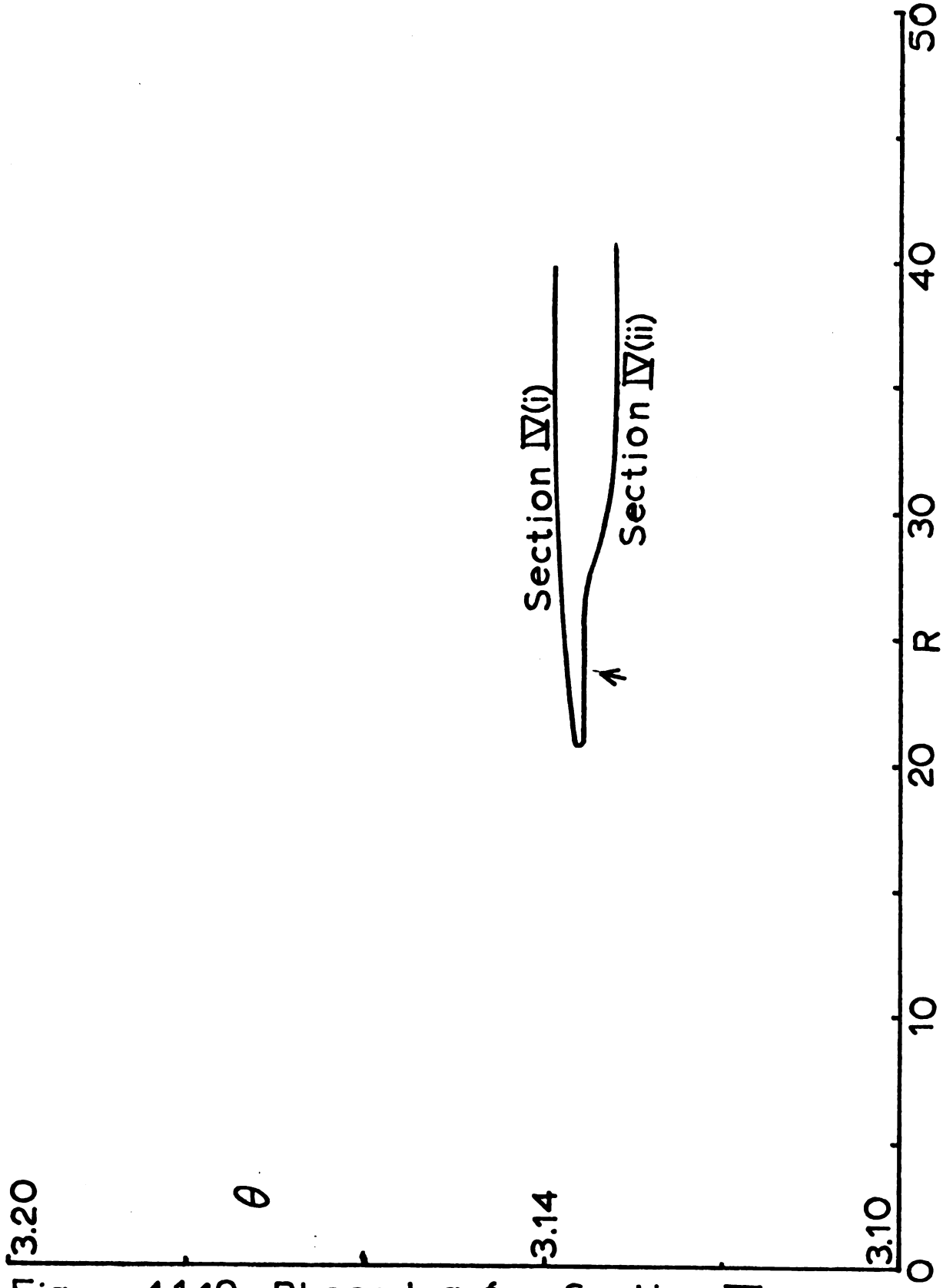

Figure 4.1.19. Phase lag for Section IV solutions with $\alpha^2=0.2$.

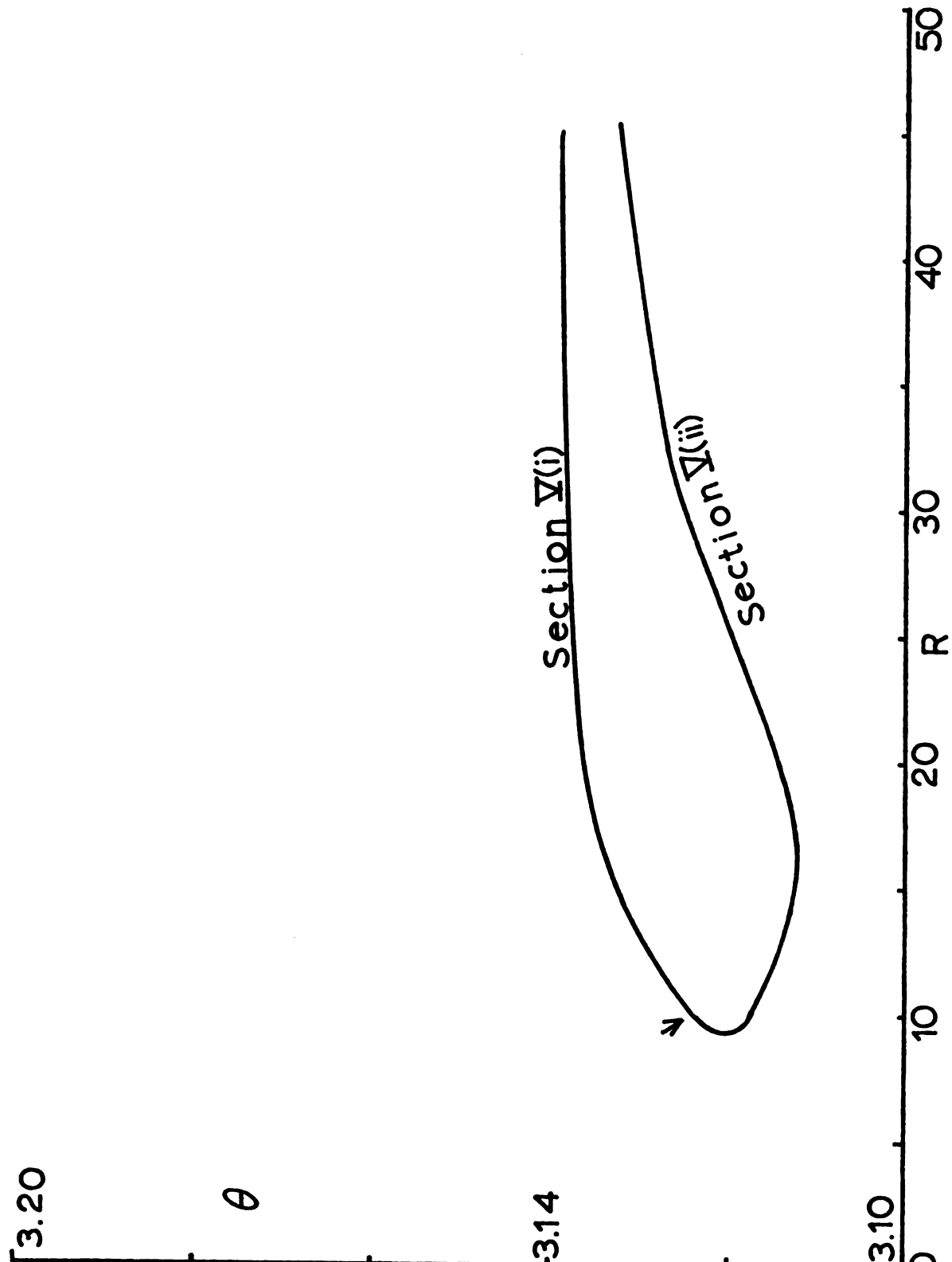

Figure 4.1.20. Phase lag for Section V solutions with $a^2=0.2$.

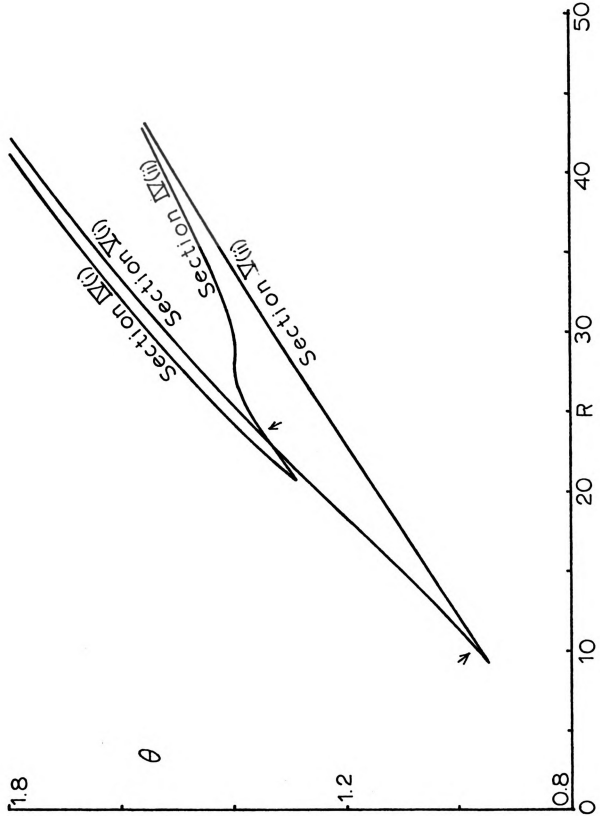

Figure 4.1.21. Phase lag for Section IV and Section V solutions with α^2=100.0.

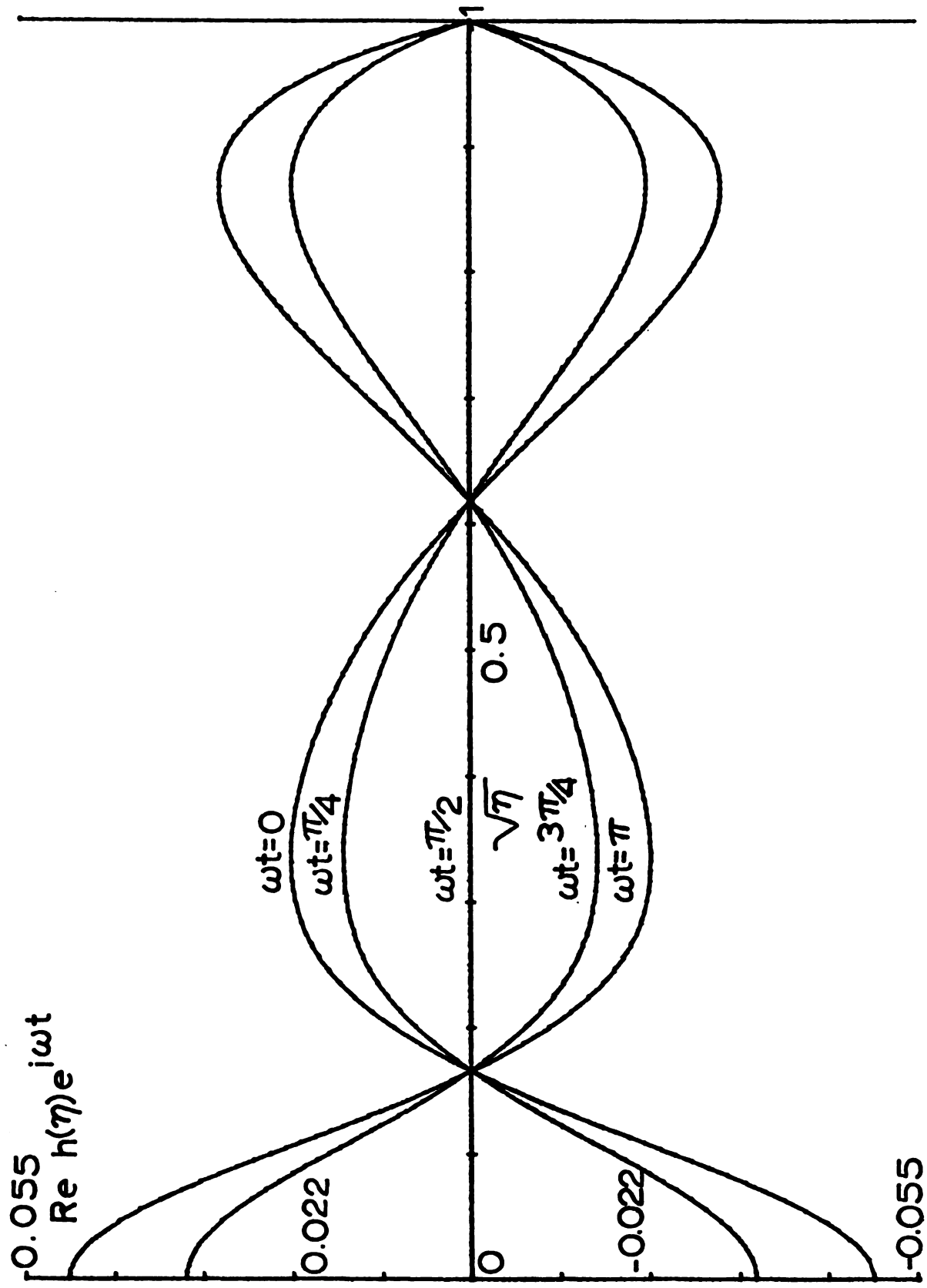

Figure 4.1.22. Axial velocity profile for a Section IV(i) solution with R=25.6713 and α^2=0.2.

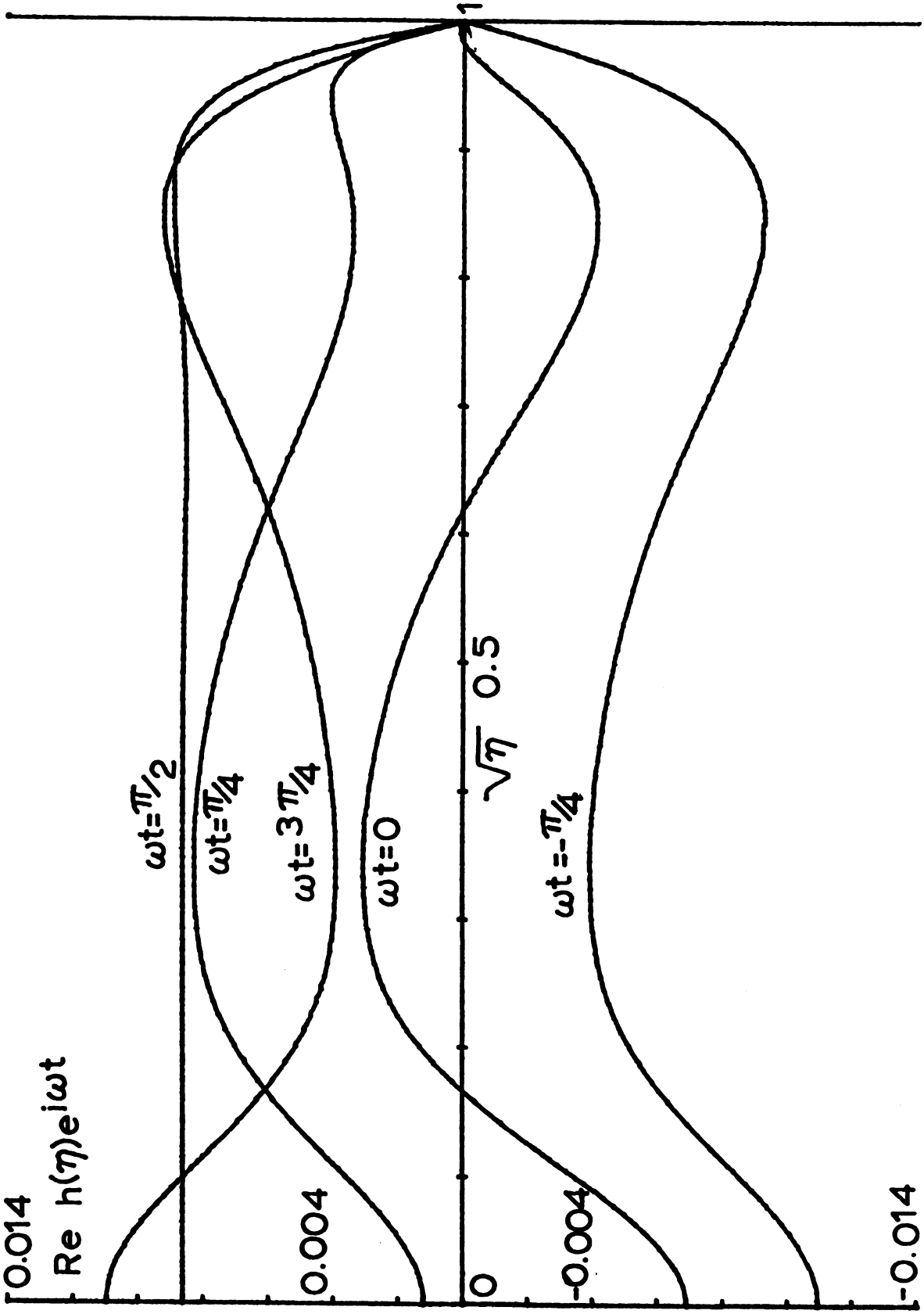

Figure 4.1.23. Axial velocity profile for a Section IV(i) solution with R=25.6713 and α^2=100.0.

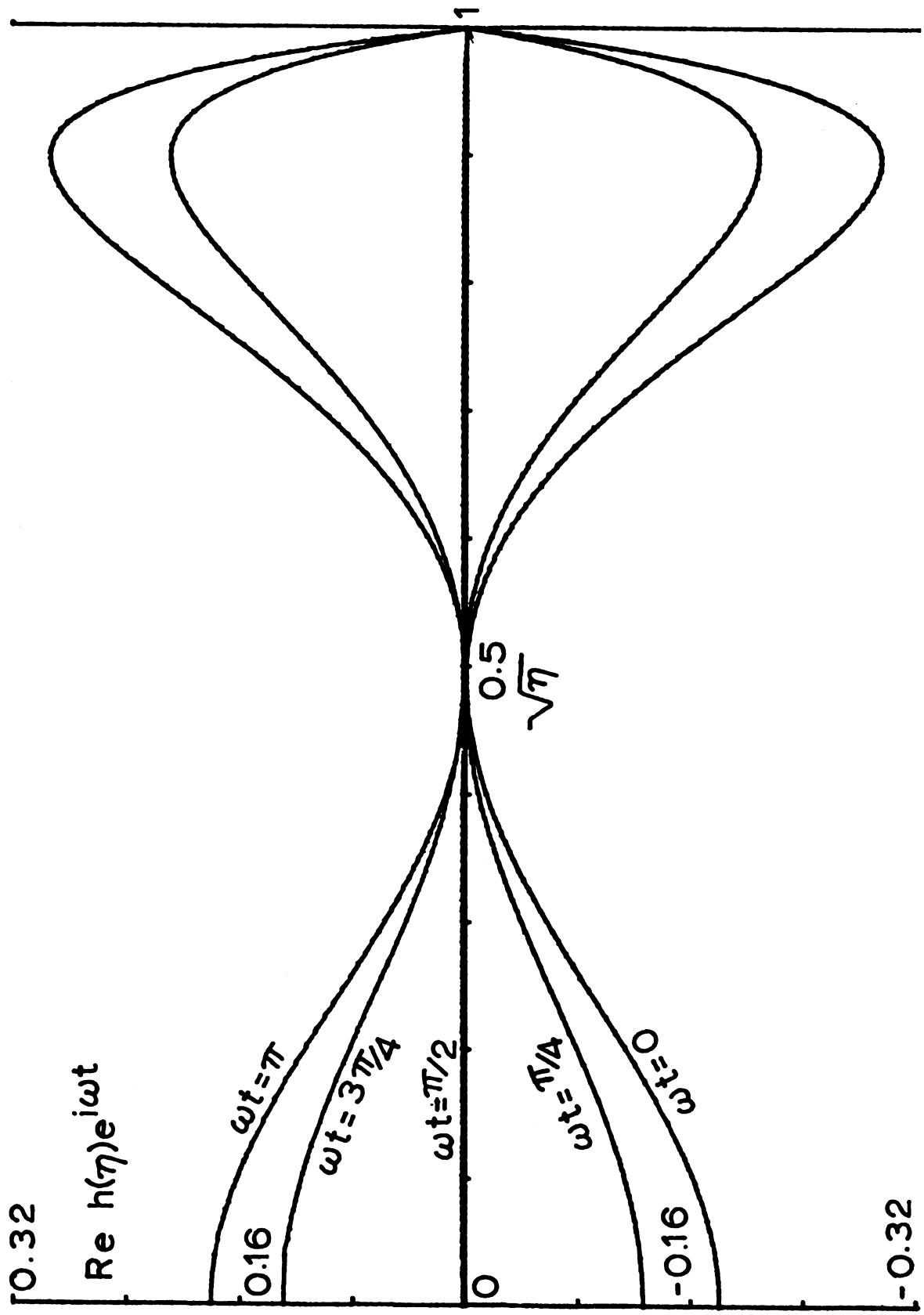

Figure 4.1.24. Axial velocity profile for a Section IV(ii) solution with R=23.7388 and α^2=0.2.

a change in the phase lag of the velocity profile relative to the pressure gradient, and a shift of the maximum velocity toward the wall. For α large and fixed and R first decreased for R = 23.7 to 20.6 and then increased results in the maximum veloctiy being shifted back toward the center of the tube.

Section IV(ii) Solutions

a) Maximum skin friction at the wall.

Case i) α small. (See Figure 4.1.17)

For this case as suction is increased skin friction increases to a maximum at R = 25.6 after which it decreases markedly.

Case ii) α large. (See Figure 4.1.18)

For a fixed amount of suction an increase in α results in a decrease in the magnitude of the skin friction However for α large and fixed increasing suction increases the skin friction.

b) Phase lag of the skin friction from the pulsatile pressure gradient.

Case i) α small. (See Figure 4.1.19)

In this case the maximum skin friction is almost π radians out of phase with the pressure gradient. Increasing suction results in a slight decrease in the phase lag until a

minimum is reached between $R = 35$ and $R = 40$. Any further increase in suction increases the phase lag.

Case ii) α large. (See Figure 4.1.21)

For a fixed amount of suction increasing α results in decreasing the phase lag and in suppressing the minimum phase lag between $R = 35$ and $R = 40$ until for α sufficiently large the minimum occurs at $R = 23.7$. For α large and fixed increasing the suction increases the phase lag.

c) Axial velocity profiles.

Case i) α small. (See Figures 4.1.24 - 4.1.25)

In this case increasing suction results in decreasing the magnitude of the velocity of the flow and in a flattening of the velocity profile.

Case ii) α large. (See Figures 4.1.26 - 4.1.27)

For a fixed amount of suction increasing α results in a decrease in the magnitude of the velocity of the flow, a change in the phase lag relative to the pressure gradient, and in a shifting of the maximum velocity toward the walls.

Section V(i) Solutions

a) Maximum skin friction at the wall.

Case i) α small. (See Figure 4.1.17)

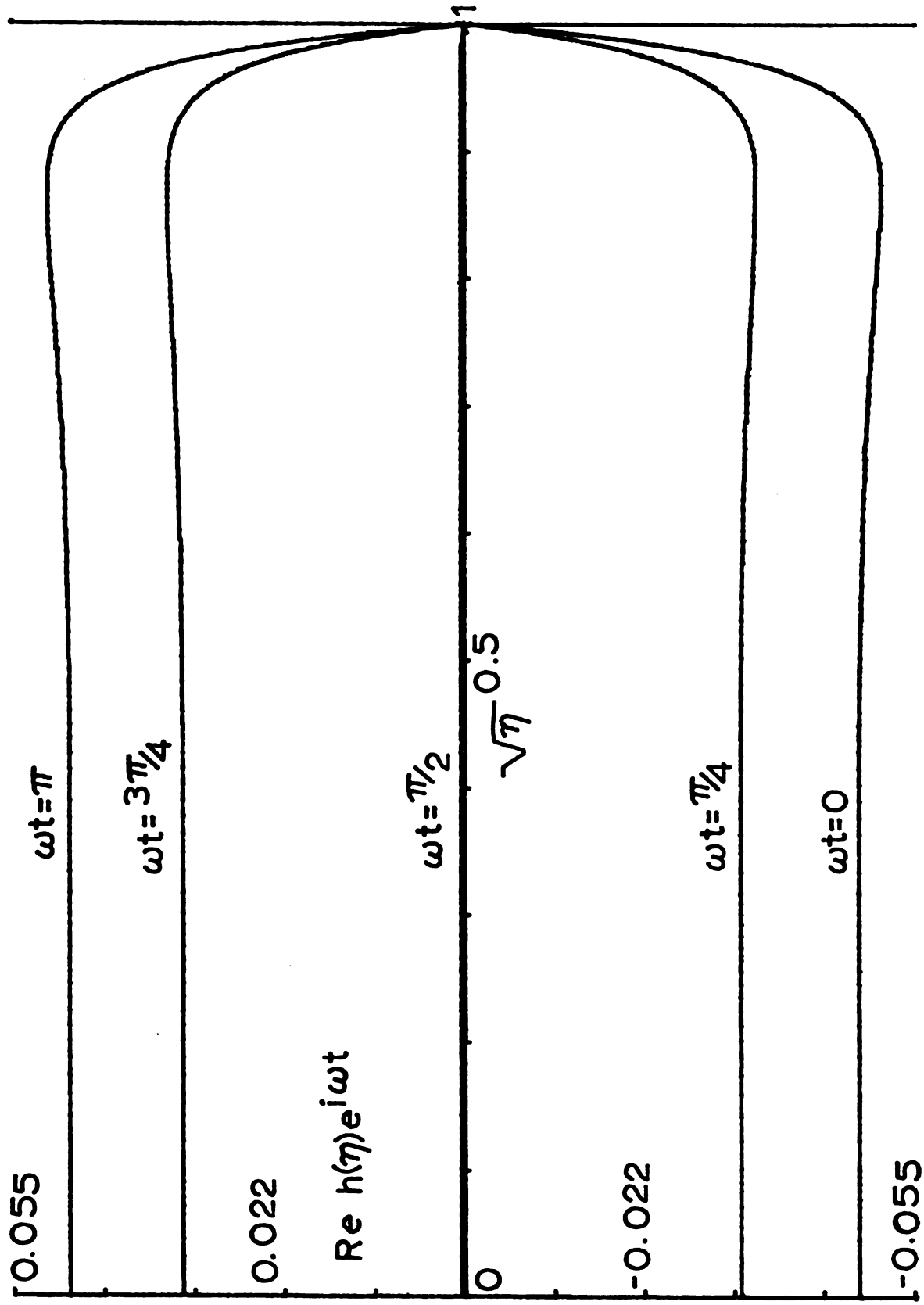

Figure 4.1.25. Axial velocity profile for a Section IV(ii) solution with R=40.5200 and α^2=0.2.

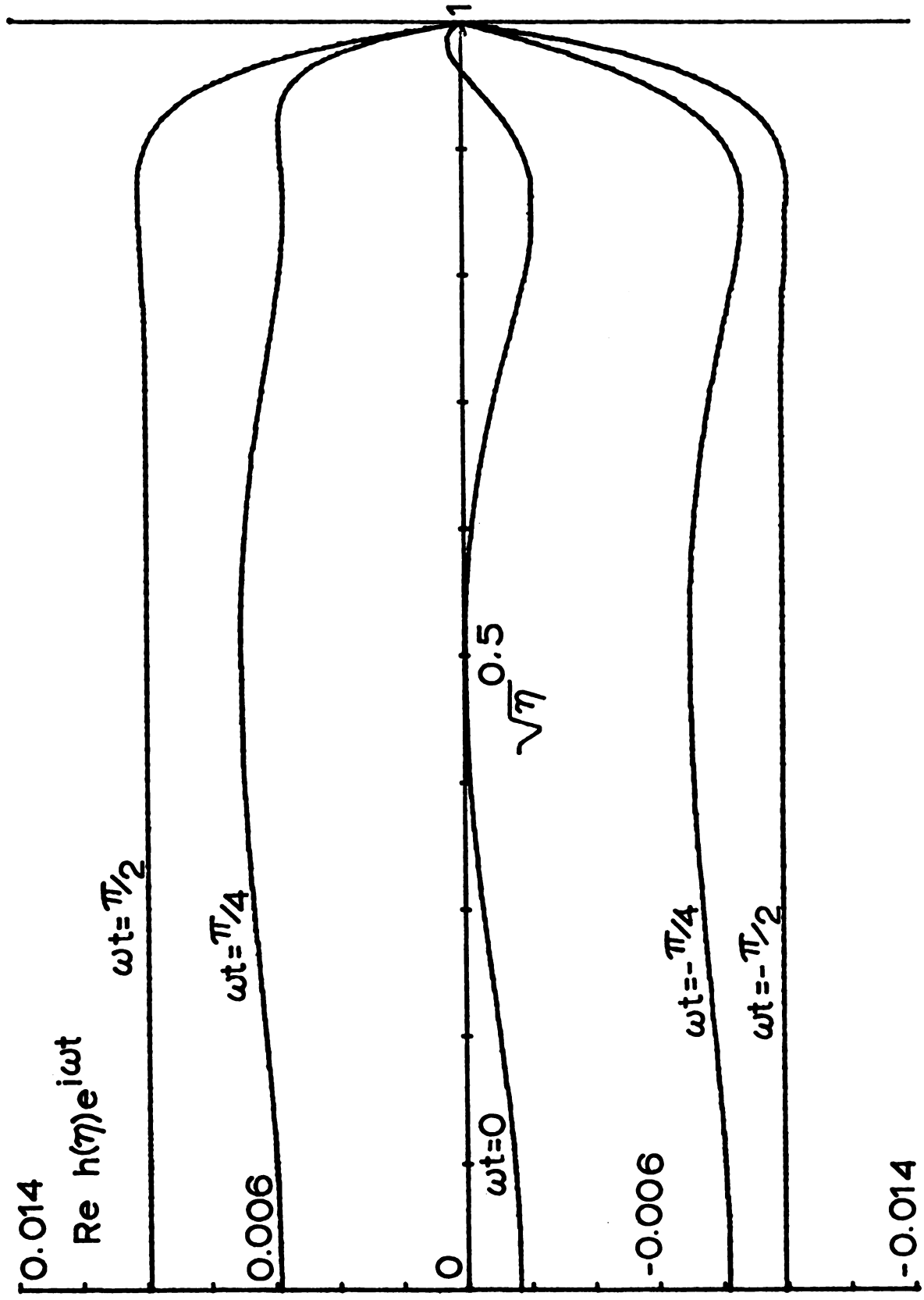

Figure 4.1.26. Axial velocity profile for a Section IV(ii) solution with R=23.7388 and α^2=100.0.

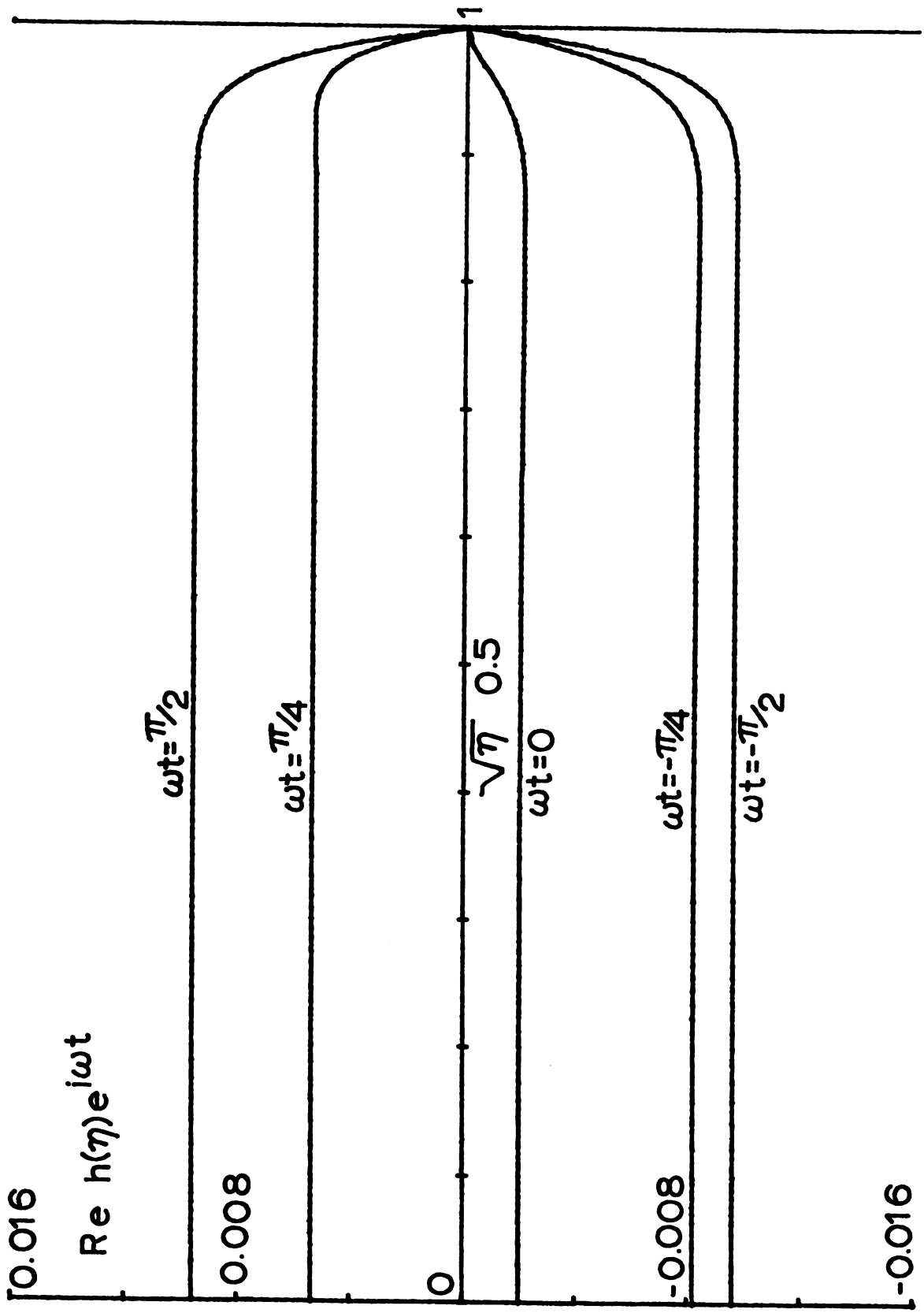

Figure 4.1.27. Axial velocity profile for a Section IV(ii) solution with R=40.5200 and α^2=100.0.

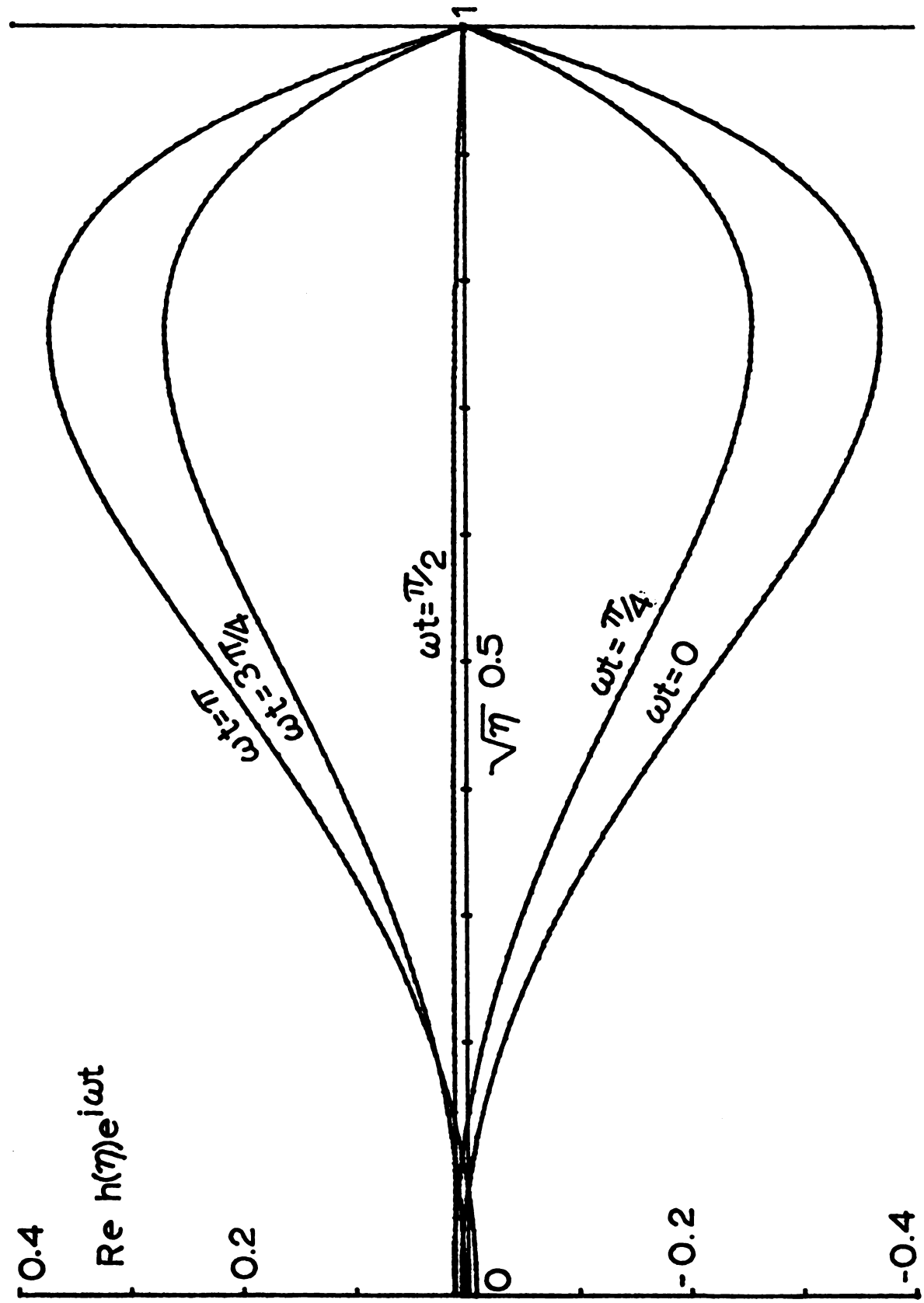

Figure 4.1.28. Axial velocity profile for a Section V(i) solution with R=10.0700 and α^2=0.2.

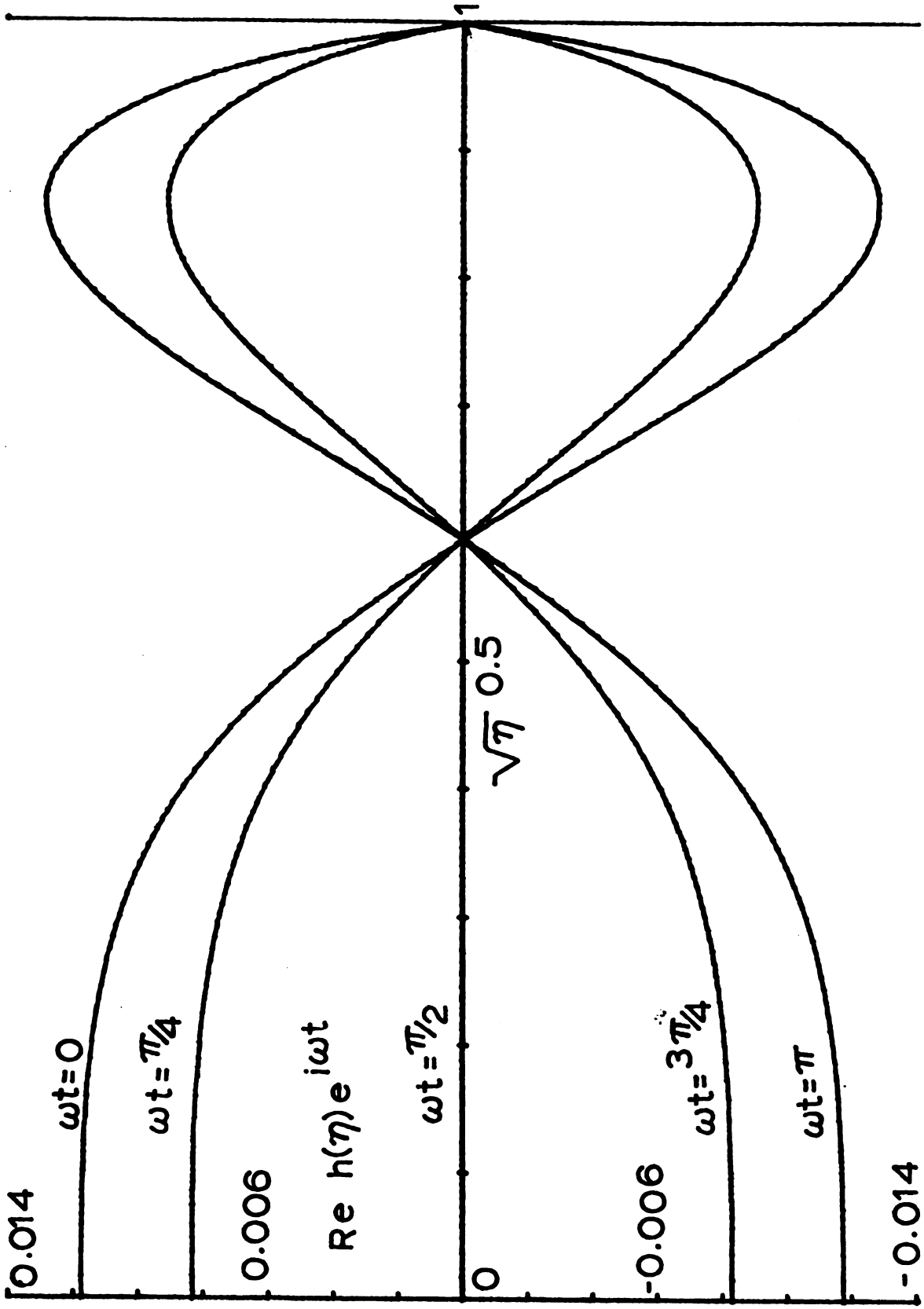

Figure 4.1.29. Axial velocity profile for a Section V(i) solution with R=41.8398 and α^2=0.2.

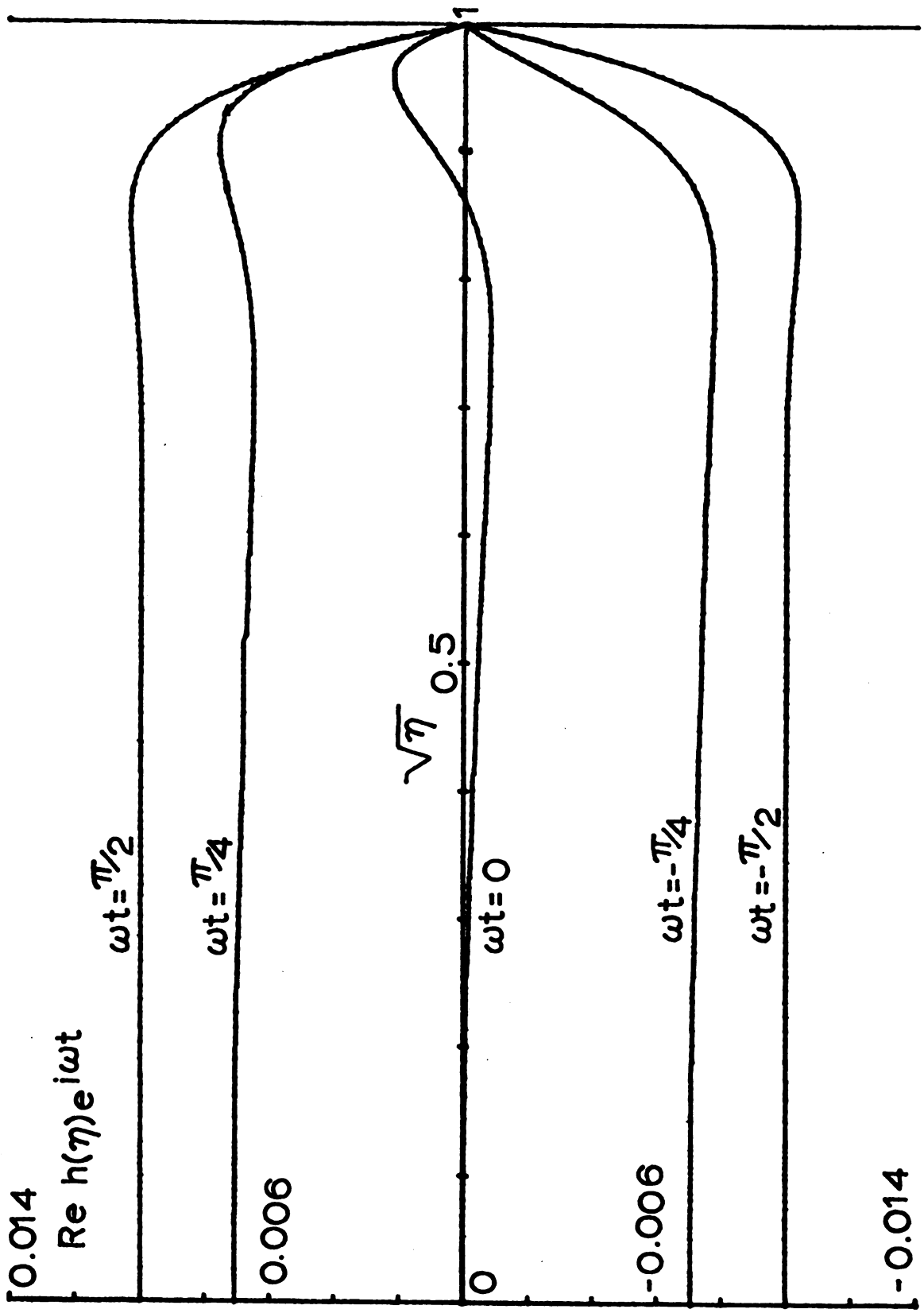

Figure 4.1.30. Axial velocity profile for a Section V(i) solution with R=10.0700 and α^2=100.0.

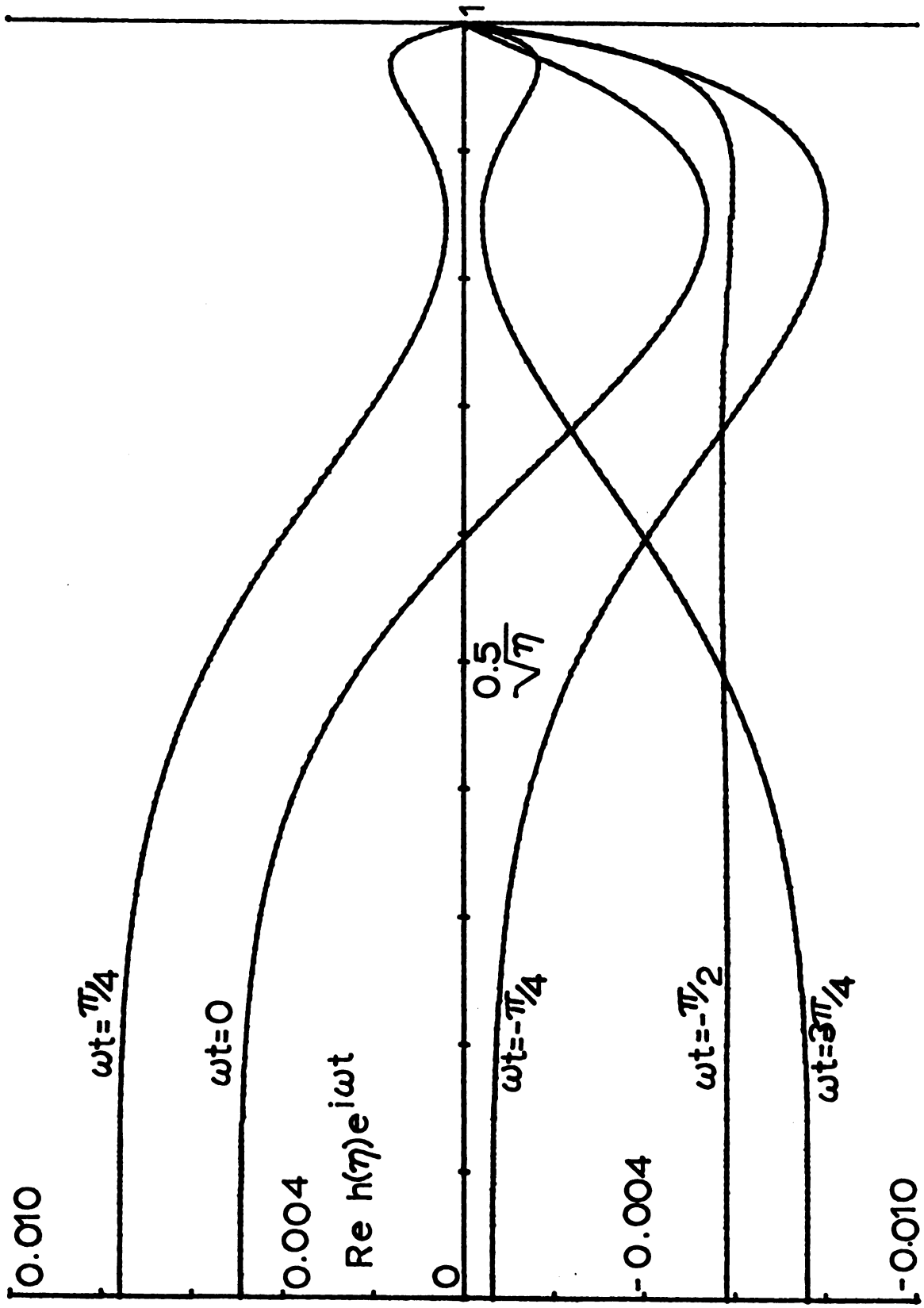

Figure 4.1.31. Axial velocity profile for a Section V(i) solution with R=41.8398 and α^2=100.0.

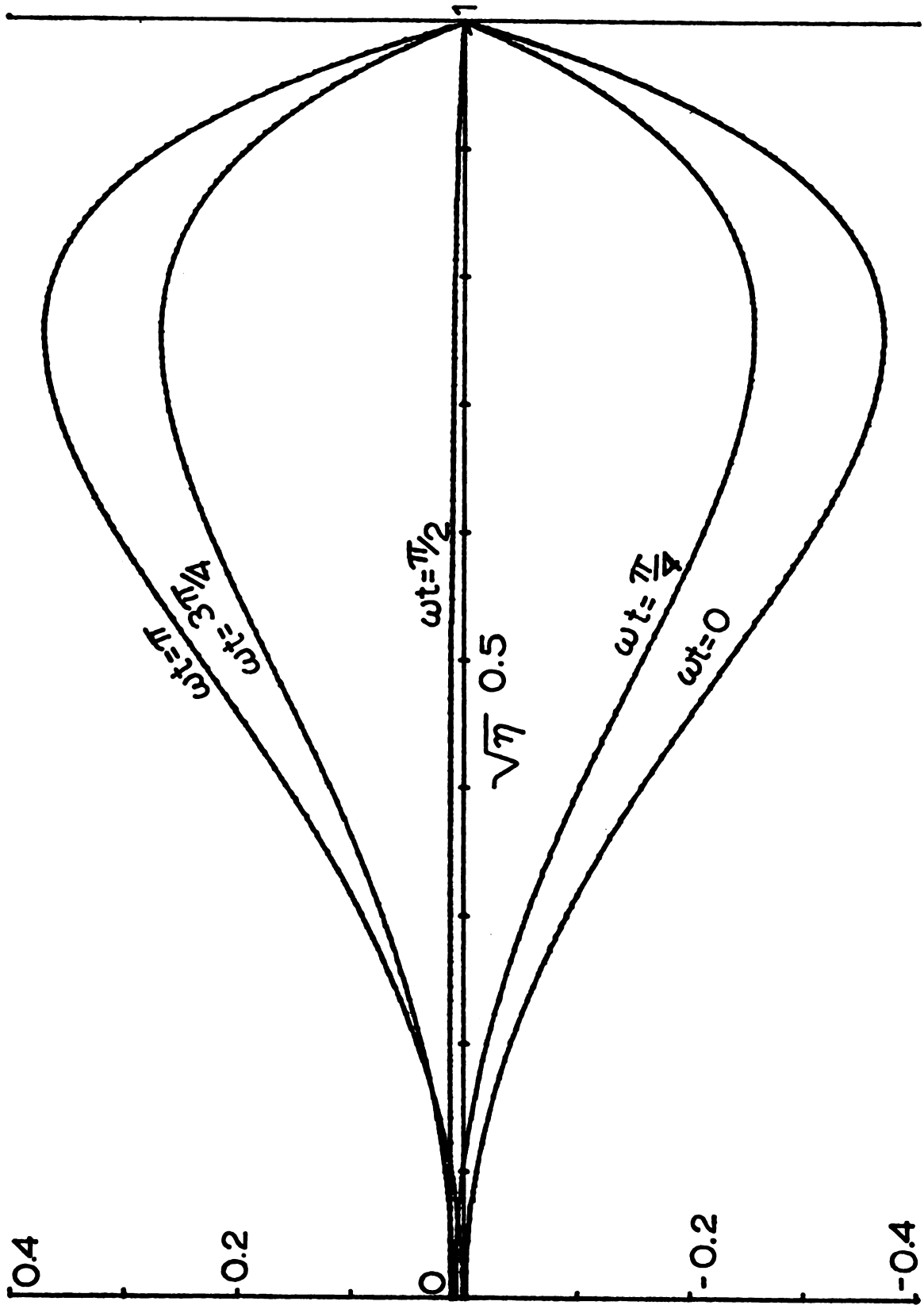

Figure 4.1.32. Axial velocity profile for a Section V(ii) solution with R = 9.9743 and $\alpha^2 = 0.2$.

In this case as suction is increased the skin friction first increases to a maximum at $R = 11.3$ and then decreases markedly. For large amounts of suction the maximum skin friction for the Section IV(i) and Section V(i) solutions apparently approach each other.

Case ii) α large. (See Figure 4.1.18)

For a fixed amount of suction, increasing α decreases the skin friction. For α large and fixed increasing suction results in at first an increase of skin friction until a maximum occurs after which skin friction decreases. For α sufficiently large the maximum no longer occurs near $R = 11.3$. For α large the maximum occurs at larger values of suction.

b) Phase lag of the skin friction from the pulsatile pressure gradient.

Case i) α small. (See Figure 4.1.20)

For this case there is a slight decrease in the phase lag for increasing suction.

Case ii) α large. (See Figure 4.1.21)

For a fixed amount of suction, increasing α decreases the phase lag. While for α large and fixed increasing the suction increases the phase lag.

c) Axial velocity profiles.

Case i) α small. (See Figures 4.1.28 - 4.1.29)

The flow in this case is divided into two regions separated by a point of velocity reversal. Increasing suction decreases the magnitude of the velocity while shifting the point of velocity reversal toward the wall of the tube.

Case ii) α large. (See Figures 4.1.30 - 4.1.31)

For a fixed amount of suction, increasing α results in decreasing the magnitude of the velocity profile, shifting the maximum velocity toward the wall, and in shifting the phase of the velocity profile relative to the pressure gradient. For α large and fixed, increasing suction decreases the magnitude of the velocity profile.

Section V(ii) Solutions

a) Maximum skin friction at the wall.

Case i) α small. (See Figure 4.1.17)

In this case as suction is first decreased to 9.1 and then increased the skin friction decreases markedly to a minimum at $R = 14.5$ and then increases.

Case ii) α large. (See Figure 4.1.18)

For a fixed amount of suction increasing α decreases the skin friction. For α fixed and large as suction first decreases to 9.1 and then increases the skin friction at first decreases to a minimum and then increases. As α gets larger the minimum occurs at smaller values of suction.

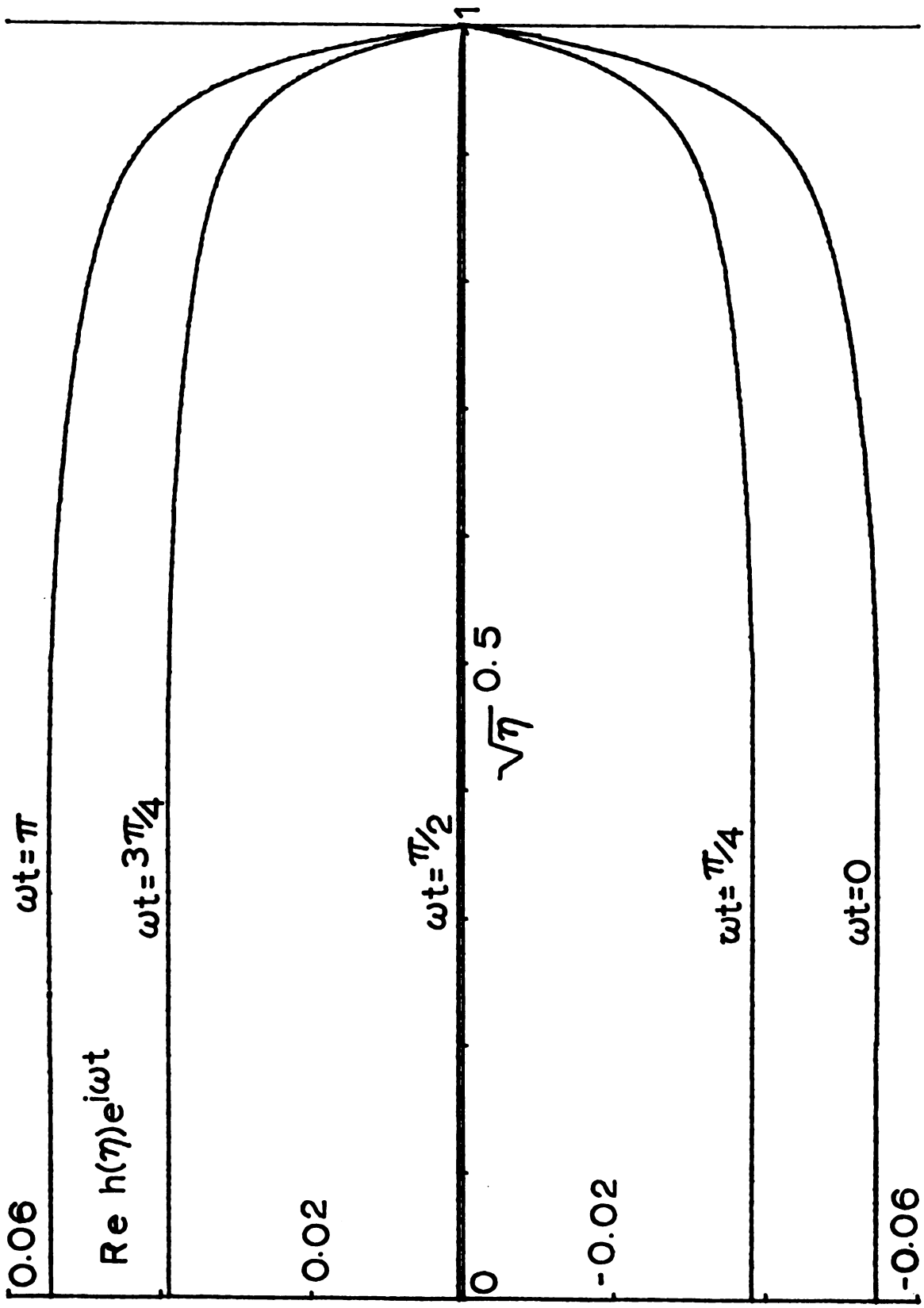

Figure 4.1.33. Axial velocity profile for a Section V(ii) solution with R=31.9268 and α^2=0.2.

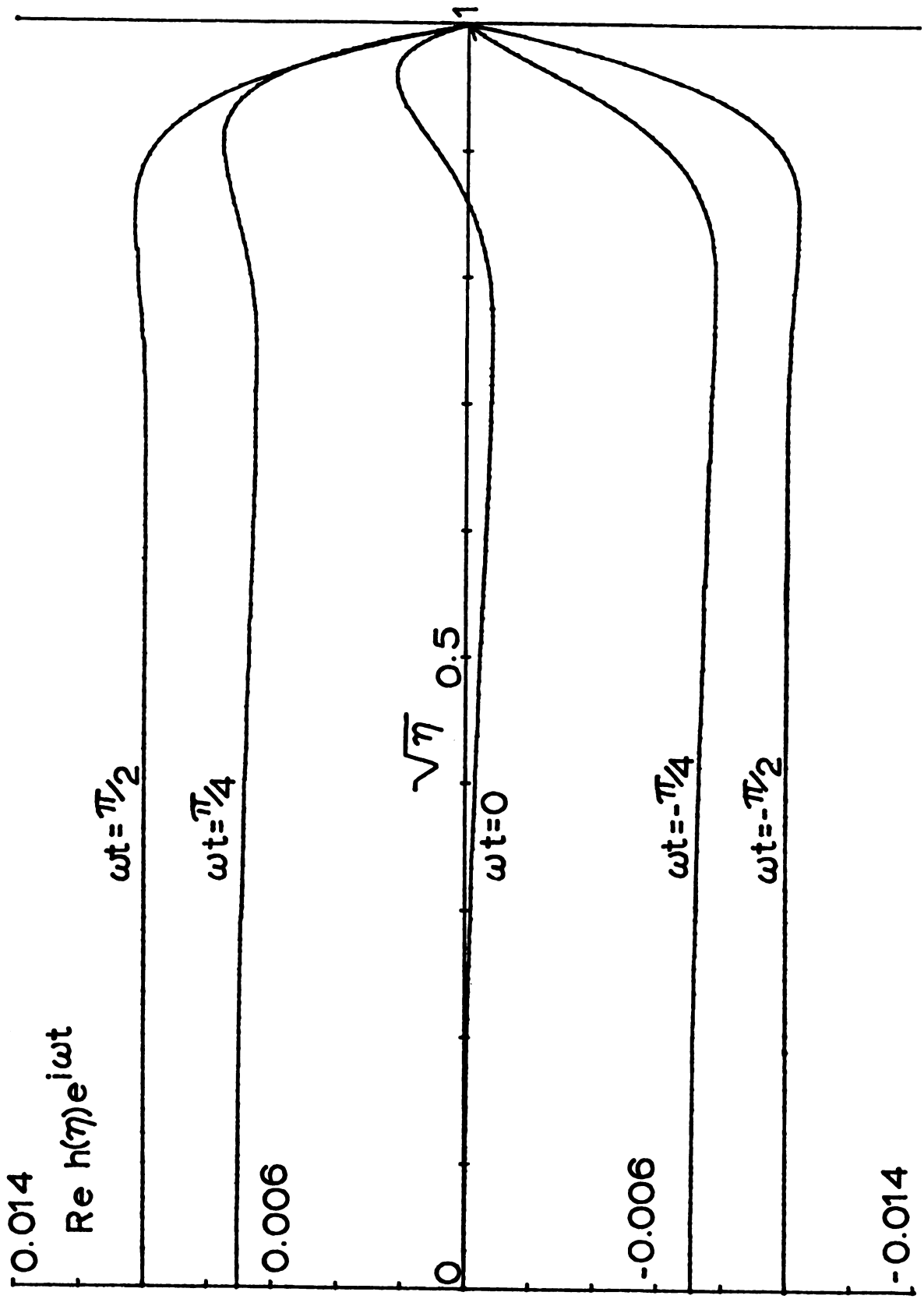

Figure 4.1.34. Axial velocity profile for a Section V(ii) solution with R=9.9743 and α^2=100.0.

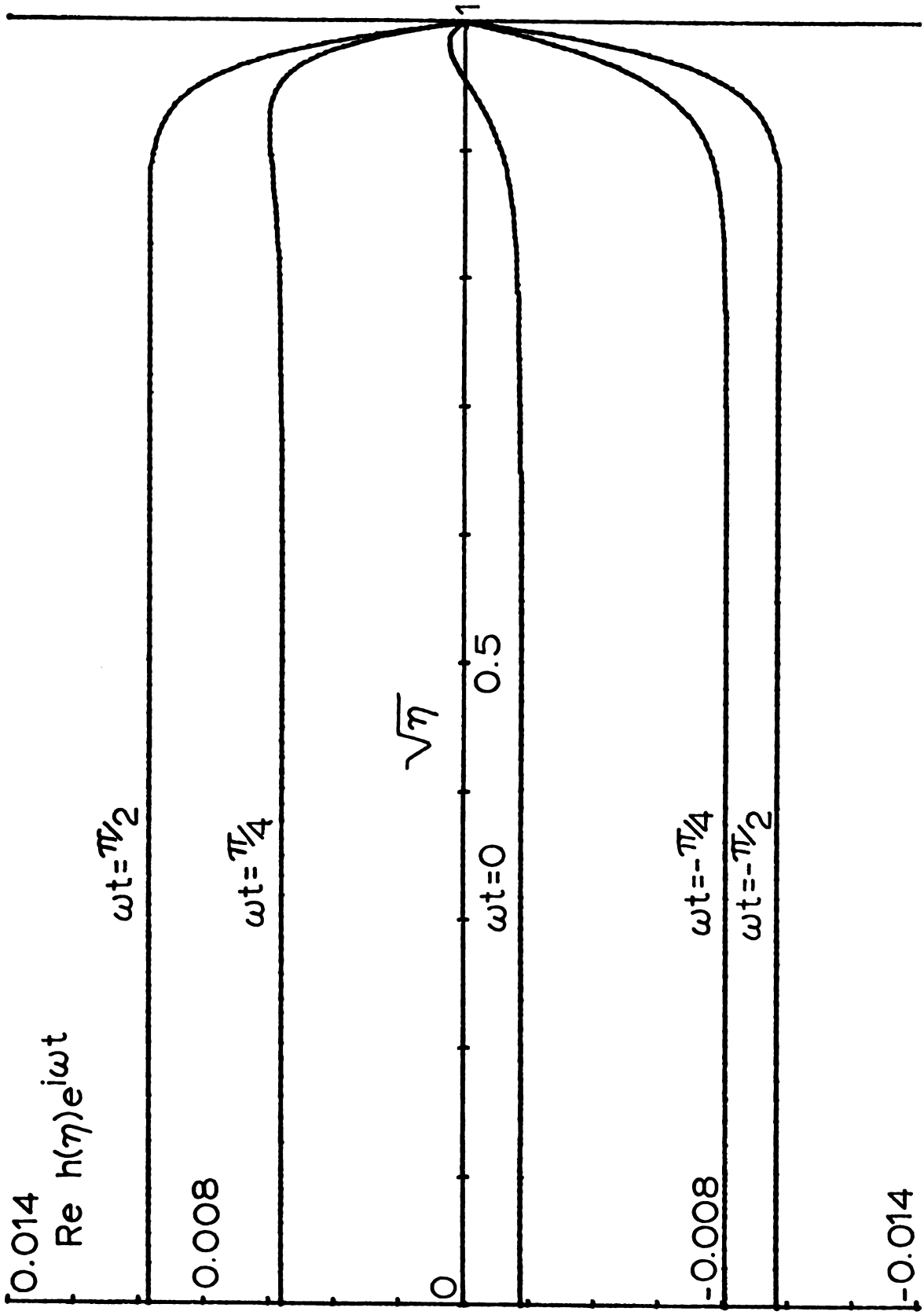

Figure 4.1.35. Axial velocity profile for a Section V(ii) solution with R=31.9268 and α^2=100.0.

b) Phase lag of the skin friction from the pulsatile pressure gradient.

Case i) α small. (See Figure 4.1.20)

In this case as suction is first decreased to 9.1 and then increased the phase lag decreases to a minimum at $R = 17.5$ and then increases.

Case ii) α large. (See Figure 4.1.21)

As α is increased for a fixed amount of suction the phase lag is decreased. For α fixed and large, as suction first decreases to 9.1 and then increases the phase lag first decreases to a minimum and then increases. As α increases the minimum occurs at smaller values of suction.

c) Axial velocity profiles

Case i) α small. (See Figures 4.1.32 - 4.1.33)

For this case as suction first decreases to 9.1 and then increases the magnitude of the velocity profile is decreased while the velocity profile becomes flatter.

Case ii) α large. (See Figures 4.1.34 - 4.1.35)

Increasing α for a fixed amount of suction results in a decrease in magnitude of the velocity profile, in a change in the phase of the velocity profile relative to the pressure gradient and a shifting of the maximum velocity

toward the wall of the tube. For α large and fixed, first decreasing the suction to 9.1 and then increasing suction results in a decrease in magnitude of the velocity profile and a flattening of the velocity profile.

From the numerical results we conclude the following: 1) The annular effect still occurs but the frequency at which it becomes important is increased by both suction and injection. 2) The phase lag of the velocity profile and the skin friction at the wall are decreased by injection but may be increased or decreased by suction. 3) The maximum skin friction at the wall is decreased by injection but may be increased or decreased by suction. 4) Small suction can cause resonance like effects. As Figure 4.1.1 shows, there is a sharp maximum in the skin friction at the wall at $R \doteq 1.25$. An examination of a typical velocity profile in this region of crossflow Reynolds numbers, such as given by Figure 4.1.6, shows this maximum is due to a large increase in the magnitude of the velocity at the center of the tube. Thus a small amount of suction in the case of a small frequency pulsatile pressure gradient can result in large velocity amplitudes at the center of the tube. At the present it is not clear exactly what causes this effect physically and this should be investigated further.

Section 4.2. Asymptotic Solutions for Large Injection.

In this section the asymptotic solutions in the case of large injection for the unsteady component of velocity will

be discussed. Letting $\varepsilon = -2/R$, where $\varepsilon << 1$, the problem for the unsteady component of velocity is formulated as follows:

4.2.1 $$\varepsilon(\eta h''(\eta) + h'(\eta)) + f(\eta)h'(\eta) - h(\eta)f'(\eta) - \varepsilon s^2 h(\eta) = -\varepsilon$$

$$\lim_{\eta \to 0} \eta^{1/2} h'(\eta) = 0 \qquad h(1) = 0$$

The case in which $f(\eta)$ is a Section I solution will be examined first. It was shown in Section 3.2 that $f(\eta)$ has a regular perturbation expansion of the form

4.2.2 $$f(\eta) = f_0(\eta) + \varepsilon f_1(\eta) + \cdots$$

where

4.2.3 $$f_0(\eta) = \sin \frac{\pi \eta}{2}$$

and $f_1(\eta)$ is given by equation 3.2.19.

Let

4.2.4 $$h(\eta) = \gamma_0(\varepsilon)h_0(\eta) + \gamma_1(\varepsilon)h_1(\eta) + \cdots$$

Substituting equations 4.2.2 and 4.2.4 into equation 4.2.1 and collecting terms gives

4.2.5 $$\varepsilon\gamma_0(\eta h_0'' + h_0') + \varepsilon\gamma_1(\eta h_1'' + h_1') + \gamma_0(f_0 h_0' - h_0 f_0')$$

$$+ \gamma_1(f_0 h_1' - h_1 f_0') + \varepsilon\gamma_0(f_1 h_0' - h_0 f_1') + \varepsilon\gamma_1(f_1 h_1' - h_1 f_1')$$

$$- \varepsilon s^2 \gamma_0 h_0 + \cdots = -\varepsilon$$

To find the equation for the leading term the relative sizes of γ_0, $\epsilon s^2 \gamma_0$ and ϵ must be examined. There are the following three cases to consider: 1) $a_0^2 = \epsilon s^2 = O(1)$ 2) $\epsilon s^2 << 1$ 3) $\epsilon s^2 >> 1$.

The following arguments will establish that case 2 can be included in case 1. Suppose $\epsilon s^2 << 1$, then we must have $\gamma_0 = \epsilon$ and the leading term of the expansion will be a solution of the following equation:

4.2.6 $$f_0 h_0' - h_0 f_0' = -1$$

Since the first order terms would need to include the unsteady effects we must set $\gamma_1 = \epsilon^2 s^2$. Then h_1 would be a solution of the following equation.

4.2.7 $$f_0 h_1' - h_1 f_0' = h_0$$

Since h_0 and h_1 both satisfy the same differential equation but with different forcing functions, we can, without loss of generality, include the unsteady effects in the leading term of the expansion in this case by assuming $\epsilon s^2 = a_0^2 = O(1)$. Thus case 2 is included in case 1. For both case 1 and case 2 we have $\gamma_0 = \epsilon$.

Using equation 4.2.3 we obtain that the leading term of the expansion in case 1 and case 2 is the solution of the following problem.

4.2.8 $$\sin \frac{\pi \eta}{2} h_0' - (\frac{\pi}{2} \cos \frac{\pi \eta}{2} + a_0^2) h_0 = -1$$

$$h_0(1) = 0 \qquad \lim_{\eta \to 0} \eta^{1/2} h_0'(\eta) = 0$$

By observing that

$$4.2.9 \qquad h_p = \frac{1}{\left(\frac{\pi^2}{4} - a_o^2\right)} \left(-a_o^2 + \frac{\pi}{2} \cos \frac{\pi\eta}{2}\right)$$

was a particular solution of 4.2.6, the following solution of equation 4.2.6 satisfying both boundary condition was obtained.

$$4.2.10 \qquad h_o = \frac{1}{\frac{\pi^2}{4} - a_o^2} \left(-a_o^2 + \frac{a_o^2 \sin \frac{\pi\eta}{2}}{(\csc \frac{\pi\eta}{2} + \cot \frac{\pi\eta}{2}) \frac{2a_o^2}{\pi}} + \frac{\pi}{2} \cos \frac{\pi\eta}{2}\right)$$

Since this solution satisfies both boundary conditions it should be observed that the Section I unsteady solutions like the Section I steady solutions have a regular perturbation expansion.

The most general first order term is obtained by setting $\gamma_1 = \epsilon^2$. This gives the following problem for $h_1(\eta)$.

$$4.2.11 \qquad \eta h_o'' + h_o' + f_o h_1' - h_1 f_o' + f_1 h_o' - h_o f_1' - a_o^2 h_1 = 0$$

$$h_1(1) = 0 \qquad \lim_{\eta \to 0} \sqrt{\eta}\, h_1'(\eta) = 0$$

Since equation 4.2.11 is a first order linear differential equation it could be solved for $h_1(\eta)$. But due to the complexity of the solutions for h_o and f_1, the solution would be in such a form as to yield little information about the asymptotic properties of the solution.

Using $a_0^2 = i\epsilon\alpha^2$ and separating equation 4.2.10 into real and imaginary parts we have then

4.2.12
$$h(\eta) = \frac{\epsilon}{\frac{\pi^2}{4} + \epsilon^2\alpha^4}\left(\epsilon\alpha^2 \sin\frac{\pi\eta}{2} \sin\left(\frac{2\epsilon\alpha^2}{\pi} \ln\left|\cot\frac{\pi\eta}{4}\right|\right)\right.$$
$$\left. + \frac{\pi}{2}\cos\frac{\pi\eta}{2} + i\epsilon\alpha^2\left(-1 + \sin\frac{\pi\eta}{2}\cos\left(\frac{2\epsilon}{\pi}\alpha^2 \ln\left|\cot\frac{\pi\eta}{4}\right|\right)\right)\right)$$
$$+ O(\epsilon^2).$$

However the asymptotic character of the maximum skin friction at the wall given by $|h'(1)|$ can be examined further without solving for $h_1(\eta)$ or higher order corrections. From equation 4.2.4 we have

4.2.13
$$h'(1) = \gamma_0 h_0'(1) + \gamma_1 h_1'(1) + \cdots$$

Equation 4.2.6 gives

4.2.14
$$h_0'(1) = -1$$

Setting $\eta = 1$ in equation 4.2.11 gives

4.2.15
$$h_1'(1) = -h_0''(1) - h_0'(1)$$

Differentiating equation 4.2.6 and evaluating it at $\eta = 1$ gives

4.2.16
$$h_0''(1) = a_0^2 h_0'(1)$$

Combining equation 4.2.14, 4.2.15, and 4.2.16 gives

$$4.2.17 \qquad h_1'(1) = a_0^2 + 1$$

By setting $\gamma_2 = \epsilon^3$ and by the same procedure as above we obtain

$$4.2.18 \qquad h_2'(1) = -2a_0^4 - 4a_0^2 - 1 + \frac{\pi^2}{4}$$

Using $a_0^2 = i\epsilon\alpha^2$ and combining equation 4.2.14, 4.2.17, 4.2.18, and 4.2.13 we obtain

$$4.2.19 \qquad h'(1) \sim -\epsilon + \epsilon^2 - \epsilon^3(1 - \frac{\pi^2}{4}) + 2\epsilon^5\alpha^4 + i\epsilon^3\alpha^2(1 - 4\epsilon)$$

Further terms of this series could be calculated by the same technique. This series shows that as long as $\epsilon\alpha^2 = O(1)$, α has very little effect on the magnitude of the skin friction at the wall or the phase shift of the maximum skin friction at the wall relative to the pressure gradient. To examine the accuracy of equation 4.2.19 the values of $|h'(1)|$ given by this equation are compared with the exact values computed numerically in Table 4.2.1.

Table 4.2.1

	$\lvert h'(1)\rvert$ (Eqn. 4.2.19)		$\lvert h'(1)\rvert$ (Exact)	
ϵ	$\alpha^2 = 0.2$	$\alpha^2 = 100.0$	$\alpha^2 = 0.2$	$\alpha^2 = 100.0$
0.02545	0.02478	0.02466	0.02478	0.02466
0.04038	0.03865	0.03692	0.03869	0.03766
0.05361	0.05051	0.04338	0.05062	0.04736
0.13562	0.11355	0.81216	0.11695	0.07510

As Table 4.2.1 shows the asymptotic and numerical results agree well for large values of injection. The large discrepancy between the asymptotic and exact values in the case where $\epsilon = 0.13562$ and $\alpha^2 = 100.0$ is due to the fact that in this case $\epsilon\alpha^2$ is not $O(1)$.

Consider now case 3 when $\epsilon s^2 \gg 1$. In the case we must set $\gamma_0 = \frac{1}{s^2}$ and therefore the leading term satisfies

4.2.20
$$h_0 = 1$$

$$\lim_{\eta \to 0} \sqrt{\eta}\, h_0'(\eta) = 0$$

Since h_0 cannot satisfy the boundary condition at the wall there must be an inner region near the wall. To examine the solution in this region let $\nu = \frac{1}{s^2}$, $\eta = 1 - \delta(\nu)\lambda$, $H(\lambda) = h(\eta)$ and $F(\lambda) = f(\eta)$. Substituting these into equation 4.2.1 we obtain

4.2.21
$$\nu\epsilon\left((1 - \delta\lambda)\frac{H''(\lambda)}{\delta^2} - \frac{1}{\delta} H'(\lambda)\right) + \frac{\nu}{\delta}(H(\lambda)F'(\lambda) - F(\lambda)H'(\lambda))$$

$$- \epsilon H(\lambda) = -\epsilon\nu$$

$$H(0) = 0$$

Let

4.2.21
$$H(\lambda) = \mu_0(\nu)H_0(\lambda) + \mu_1(\nu)H_1(\lambda) + \cdots$$

4.2.23
$$F(\lambda) = \alpha_0(\nu)F_0(\lambda) + \alpha_1(\nu)F_1(\lambda) + \cdots$$

Substituting equations 4.2.21 and 4.2.23 into equation 4.2.21 and collecting terms gives

$$4.2.24 \qquad \frac{\nu\varepsilon\mu_0}{\delta^2} H_0'' + \frac{\nu\varepsilon\mu_1}{\delta^2} H_1'' - \frac{\mu_0\nu\varepsilon}{\delta}(\lambda H_0'' + H_0')$$

$$- \frac{\mu_1\nu\varepsilon}{\delta}(\lambda H_1'' + H_1') + \frac{\nu}{\delta}\mu_0\alpha_0(H_0F_0' - F_0H_0')$$

$$+ \frac{\nu}{\delta}\mu_0\alpha_1(H_0F_1' - H_0'F_1) + \frac{\nu\mu_1\alpha_0}{\delta}(H_1F_0' - H_1'F_0)$$

$$+ \frac{\nu\mu_1\alpha_1}{\delta}(H_1F_1' - H_1'F_1) - \varepsilon\mu_0H_0 - \varepsilon\mu_1H_1 + \cdots = -\varepsilon\nu$$

Since in the outer region

$$4.2.25 \qquad h(\eta) \sim \nu$$

we see that $\mu_0 = \nu$ and hence that $\delta = \sqrt{\nu}$. This gives the following problem for the leading term of the inner expansion

$$4.2.26 \qquad H_0'' - H_0 = -1$$

$$H_0(0) = 0 \qquad H_0(\infty) = 1$$

Solving equation 4.2.26 gives

$$4.2.27 \qquad H_0 = 1 - e^{-\lambda}$$

Therefore near the wall we have that

$$4.2.28 \qquad h(\eta) \sim \nu\left(1 - e^{\frac{\eta - 1}{\sqrt{\nu}}}\right)$$

Again to examine the accuracy of this expansion the asymptotic and exact values of the maximum skin friction at the wall, given by $|h'(1)|$, will be compared. Differentiating equation

4.2.28, evaluating at one, and using $\nu = \frac{1}{i\alpha^2}$ we obtain

4.2.29 $$h'(1) \sim -\frac{\sqrt{2}}{2\alpha}(1 - i).$$

This gives then

4.2.30 $$|h'(1)| \sim \frac{1}{\alpha}$$

Table 4.2.2 compares the asymptotic and the exact values of $|h'(1)|$ for a large value of α.

Table 4.2.2

$\alpha^2 = 100.0$

ϵ	$\epsilon\alpha^2$	$\lvert h'(1)\rvert$ (Eqn. 4.2.30)	$\lvert h'(1)\rvert$ (Exact)
0.05361	5.36059	0.10000	0.04736
0.13562	13.56224	0.10000	0.07510
0.33347	33.34733	0.10000	0.08843
0.65441	65.44112	0.10000	0.09316

As Table 4.2.2 shows the agreement is good when $\epsilon\alpha^2$ is large. This expansion shows that the annular effect occurs for large values of injection but that it does not become important until $\epsilon\alpha^2 >> 1$.

Consider now the case where $f(\eta)$ is a Section III solution. In this case in Section 3.2 it was shown equation 4.2.2 was valid only as an outer solution in the region near the wall. Thus equation 4.2.4 for $h(\eta)$ will also be valid only in the region near the wall. It was also shown that the

width of the inner region or boundary layer was ϵ. Therefore setting $H(\lambda) = h(\eta)$ and $F(\lambda) = f(\eta)$ where $\lambda = \eta/\epsilon$ and substituting into equation 4.2.1 the following problem for the unsteady component of velocity in the inner region is obtained.

$$4.2.31 \quad \epsilon(\lambda H''(\lambda) + H'(\lambda)) + F(\lambda)H'(\lambda) - H(\lambda)F'(\lambda) - \epsilon^2 s^2 H(\lambda) = -\epsilon^2$$

$$\lim_{\lambda \to 0} \sqrt{\lambda}\, H'(\lambda) = 0$$

In Section 3.2 it was shown that the expansion for $F(\lambda)$ in the inner region was of the form

$$4.2.32 \qquad F(\lambda) = \epsilon F_0(\lambda) + \epsilon^2 F_1(\lambda) + \cdots$$

Let

$$4.2.33 \qquad H(\lambda) = \nu_0(\epsilon)H_0(\lambda) + \nu_1(\epsilon)H_1(\lambda) + \cdots$$

Substituting equations 4.2.32 and 4.2.33 into equation 4.2.31 and collecting terms gives

$$4.2.34 \quad \epsilon\nu_0(\lambda H_0'' + H_0' + F_0H_0' - H_0F_0') + \epsilon\nu_1(\lambda H_1'' + H_1' + F_0H_1' - F_0'H_1) + \epsilon^2\nu_0(F_1H_0' - H_0F_1') + \epsilon^2\nu_1(F_1H_1' - H_1F_1') - \epsilon^2 s^2 \nu_0 H_0 - \epsilon^2 s^2 \nu_1 H_1 + \cdots = -\epsilon^2$$

Consider first the case where $\epsilon s^2 = a_0^2 = O(1)$. In this case the outer solution is given by

$$4.2.35 \qquad h(\eta) \sim \epsilon h_0(\eta)$$

where $h_0(\eta)$ is given by equation 4.2.10. Expanding the outer solution in inner variables gives

4.2.36 $$h(\eta) \sim \frac{\epsilon}{\frac{\pi}{2} + a_0^2}$$

This gives that $\nu_0(\epsilon) = \epsilon$ and hence that the leading term of the inner expansion for the unsteady component of velocity is the solution of the following problem

4.2.37 $$\lambda H_0'' + H_0' + F_0 H_0' - H_0 F_0' - a_0^2 H_0 = -1$$

$$\lim_{\lambda \to 0} \sqrt{\lambda}\ H_0'(\lambda) = 0 \qquad H_0(\infty) = \frac{1}{\frac{\pi}{2} + a_0^2}$$

Since $F_0(\lambda) = \frac{\pi}{2}\lambda - 3 + 3e^{\frac{-\pi\lambda}{2}}$ by equation 3.2.27, equation 4.2.37 becomes

4.2.38 $$\lambda H_0'' + (-2 + \frac{\pi\lambda}{2} + 3e^{\frac{-\pi\lambda}{2}})H_0' - (\frac{\pi}{2} - \frac{3\pi}{2}e^{\frac{-\pi\lambda}{2}} + a_0^2)H_0 = -1$$

$$\lim_{\lambda \to 0} \sqrt{\lambda}\ H_0'(\lambda) = 0 \qquad H_0(\infty) = \frac{1}{\frac{\pi}{2} + a_0^2}$$

By inspection the solution of equation 4.2.38 was found to be

4.2.39 $$H_0(\lambda) = \frac{1}{a_0^2 + \frac{\pi}{2}} - \frac{3\pi e^{\frac{-\pi\lambda}{2}}}{2(\frac{\pi^2}{4} - a_0^4)}$$

Since $F_1(\lambda)$ is unknown $H_1(\lambda)$ could not be found.

Since the Section I and Section III solutions have the same expansion near the wall, the asymptotic values for $|h'(1)|$, the maximum skin friction at the wall, for Section

III solutions will also be computed from equation 4.2.19. As Table 4.2.3 shows the agreement between the asymptotic and numerical values in this case in similar to the case of Section I solutions.

Table 4.2.3

	$\lvert h'(1)\rvert$ (Eqn. 4.2.17)		$\lvert h'(1)\rvert$ (Exact)	
ϵ	$\alpha^2 = 0.2$	$\alpha^2 = 100.0$	$\alpha^2 = 0.2$	$\alpha^2 = 100.0$
0.032	0.031	0.030	0.031	0.031
0.05295	0.04993	0.04322	0.04998	0.04689
0.07467	0.06848	0.03659	0.06869	0.05875
0.10042	0.09484	0.05654	0.08951	0.06772

To examine the accuracy of the asymptotic solution in the inner region the asymptotic values of the maximum velocity at the center of the tube, given by $|h(0)|$, will be compared with the exact values obtained from numerical integration.

From equations 4.2.23 and 4.2.39 is obtained

4.2.40 $$h(0) \sim \epsilon\left(\frac{1}{a_0^2 + \frac{\pi}{2}} - \frac{3\pi}{2\left(\frac{\pi^2}{4} - a_0^4\right)}\right)$$

This gives, using $a_0^2 = i\epsilon\alpha^2$,

4.2.41 $$|h(0)| \sim \frac{\epsilon}{\frac{\pi^2}{4} + \epsilon^2\alpha^4}\left(\pi^2 + \epsilon^2\alpha^4\right)^{1/2}$$

Table 4.2.4 compares the asymptotic values of $|h(0)|$ with the exact values.

Table 4.2.4

	$\lvert h(0)\rvert$ (Eqn. 4.2.28)		$\lvert h(0)\rvert$ (Exact)	
ϵ	$\alpha^2 = 0.2$	$\alpha^2 = 100.0$	$\alpha^2 = 0.2$	$\alpha^2 = 100.0$
0.032	0.041	0.011	0.038	0.011
0.05295	0.06741	0.01069	0.05951	0.01082
0.07467	0.09506	0.01039	0.07995	0.01052
0.10042	0.12784	0.01023	0.10171	0.01034

As Table 4.2.3 shows the agreement between the exact and asymptotic values of $|h(0)|$ is good.

Consider now the case where $\epsilon s^2 \gg 1$ and let $\nu = \frac{1}{s^2}$. In this case the outer solution expanded into the inner region is given by

4.2.42 $$h(\eta) \sim \nu .$$

This gives then that $\nu_0 = \nu$ and therefore the leading term of the inner expansion for the unsteady component of velocity is the solution of the following problem.

4.2.43 $$H_0 = 1$$

$$\lim_{\lambda \to 0} \sqrt{\lambda}\, H_0'(\lambda) = 0 \qquad H_0(\infty) = 1$$

The solution of equation 4.2.43 is clearly $H_0 \equiv 1$. Therefore near zero we have

4.2.44 $$h(\eta) \sim \nu$$

It should be observed that this is the same expansion that was obtained for Section I solutions near zero for

$\epsilon s^2 \gg 1$. Thus we conclude that, if $\epsilon s^2 \gg 1$, the boundary layer has only a secondary effect at zero and, as for Section I solutions, the annular effect becomes important.

To examine the accuracy of the expansion the exact and asymptotic values of the maximum velocity at the center of the tube, given by $|h(0)|$, will be compared. From equation 4.2.44 and by using $\nu = \frac{1}{i\alpha^2}$ we obtain

4.2.45 $$|h(0)| \sim \frac{1}{\alpha^2}$$

Table 4.2.5 compares the asymptotic values of $|h(0)|$ with the exact values for a large value of α.

Table 4.2.5

$\alpha^2 = 100.0$

ϵ	$\epsilon\alpha^2$	$\lvert h(0)\rvert$(Eqn. 4.2.45)	$\lvert h(0)\rvert$(Exact)
0.07467	7.46677	0.01000	0.01052
0.10042	10.04177	0.01000	0.01034
0.82038	82.03849	0.01000	0.01004

As Table 4.2.5 shows the agreement is good if $\epsilon\alpha^2$ is large.

In this section asymptotic solutions have been found in the case of large injection for both the Section I and Section III solutions. In both cases the asymptotic solutions were in good agreement with the numerical solutions. It was also shown that for large injection the annular effect does occur but only if $\epsilon s^2 \gg 1$.

Section 4.3. Asymptotic Solutions for Small Injection and Suction.

In this section asymptotic solutions for the unsteady component of the velocity for the case of small injection and suction will be discussed. Let $\epsilon = -R/2$, where $|\epsilon| << 1$, then the problem for this case will have the following formulation:

4.3.1 $$\eta h''(\eta) + h'(\eta) = s^2 h(\eta) - 1 - \epsilon(f(\eta)h'(\eta) - h(\eta)f'(\eta))$$

$$\lim_{\eta \to 0} \sqrt{\eta}\, h'(\eta) = 0 \qquad h(1) = 0$$

Consider first the case where $f(\eta)$ is a Section I solution. In this case it was shown in Section 3.3 that $f(\eta)$ had a regular perturbation expansion of the form

4.3.2 $$f(\eta) = f_0(\eta) + \epsilon f_1(\eta) + \cdots$$

where

4.3.3 $$f_0(\eta) = 2\eta - \eta^2$$

4.3.4 $$f_1(\eta) = \frac{\eta^4}{18} - \frac{\eta^3}{3} + \frac{\eta^2}{2} - \frac{2}{9}\eta$$

Let

4.3.5 $$h(\eta) = \gamma_0(\epsilon)h_0(\eta) + \gamma_1(\epsilon)h_1(\eta) + \cdots$$

Substituting equations 4.3.2 and 4.3.5 into equation 4.3.1 and collecting terms gives

4.3.6 $$\gamma_0(\eta h_0'' + h_0') + \gamma_1(\eta h_1'' + h_1') + \cdots = \gamma_0 s^2 h_0 + \gamma_1 s^2 h_1 - 1$$
$$+ \varepsilon\gamma_0(-f_0 h_0' + h_0 f_0') + \varepsilon\gamma_1(-f_0 h_1' + f_0' h_1) + \varepsilon^2\gamma_0(-h_0' f_1$$
$$+ h_0 f_1') + \varepsilon^2\gamma_1(-f_1 h_1' + h_1 f_1') + \cdots$$

Since in this case ε and s^2 do not occur as a product, the leading term of the expansion is independent of the size of s^2. Therefore we set, without loss of generality, $\gamma_0 = 1$ and obtain the following problem for h_0:

4.3.7 $$\eta h_0'' + h_0' = s^2 h_0 - 1$$

$$h_0(1) = 0 \qquad \lim_{\eta \to 0} \sqrt{\eta}\, h_0'(\eta) = 0$$

Since the first order solution must take into account the effects of the leading inertial terms, we set $\gamma_1 = \varepsilon$. This gives the following problem for $h_1(\eta)$.

4.3.8 $$\eta h_1'' + h_1' = s^2 h_1 - f_0 h_0' + h_0 f_0'$$

$$h_1(1) = 0 \qquad \lim_{\eta \to 0} \sqrt{\eta}\, h_1'(\eta) = 0$$

Equation 4.3.7 can be solved exactly and its solution is given by

4.3.9 $$h_0(\eta) = \frac{1}{s^2}\left(1 - \frac{J_0(2B\sqrt{\eta})}{J_0(2B)}\right)$$

where $B = \sqrt{-s^2}$. This is the solution for pulsatile flow in a non-porous tube. The properties of this solution have been studied thoroughly by Womersley [31] and Uchida [26]. To examine the effects of small amounts of suction and

injection on pulsatile flow $h_1(\eta)$ must be solved. Since two linearly independent solutions of the homogenous part of equation 4.3.8 can be found in terms of Bessel functions, equations 4.3.8 could be solved exactly by using variation of parameters. However the solution obtained is complex and more information can be obtained by examining the solutions of equation 4.3.8 for small and large values of s^2. To do this, however, we must first expand the solution of equation 4.3.7 for small and large values of s^2. Consider first the case where $|s^2| << 1$. Letting $\nu = s^2$ equation 4.3.7 becomes

4.3.10 $$\eta h_0'' + h_0' = \nu h_0 - 1$$

$$h_0(1) = 0 \qquad \lim_{\eta \to 0} \sqrt{\eta}\, h_0'(\eta) = 0$$

Let

4.3.11 $$h_0(\eta) = k_0(\eta) + \nu k_1(\eta) + \nu^2 k_2(\eta) + \nu^3 k_3(\eta) + \cdots$$

Substituting equation 4.3.11 into equation 4.3.10 and collecting terms gives

4.3.12 $$\eta k_0'' + k_0' + \nu(\eta k_1'' + k_1') + \nu^2(\eta k_2'' + k_2') + \nu^3(\eta k_3'' + k_3')$$

$$+ \cdots = \nu k_0 + \nu^2 k_1 + \nu^3 k_2 + \cdots - 1$$

Equating powers of ν gives the following

4.3.13 $$\eta k_0'' + k_0' = -1$$

$$k_0(1) = 0 \qquad \lim_{\eta \to 0} \sqrt{\eta}\, k_0'(\eta) = 0$$

4.3.14 $$\eta k_r'' + k_r' = k_{r-1} \qquad r > 0$$

$$k_r(1) = 0 \qquad \lim_{\eta \to 0} \sqrt{\eta}\, k_r'(\eta) = 0$$

Solving gives

4.3.15 $$k_0 = 1 - \eta$$

4.3.16 $$k_1 = \eta - \frac{\eta^2}{4} - \frac{3}{4}$$

4.3.17 $$k_2 = \frac{\eta^2}{4} - \frac{\eta^3}{36} - \frac{3}{4}\eta + \frac{19}{36}$$

4.3.18 $$k_3 = \frac{\eta^3}{36} - \frac{\eta^4}{576} - \frac{3\eta^2}{16} + \frac{19\eta}{36} - \frac{211}{576}$$

Setting $\nu = s^2$, equation 4.3.8 becomes

4.3.19 $$\eta h_1'' + h_1' = \nu h_1 - f_0 h_0' + h_0 f_0'$$

Let

4.3.20 $$h_1(\eta) = \ell_0(\eta) + \nu \ell_1(\eta) + \nu^2 \ell_2(\eta) + \nu^3 \ell_3(\eta) + \cdots$$

Substituting equations 4.3.20 and 4.3.11 into equation 4.3.19 and collecting terms gives

4.3.21 $$\eta \ell_0'' + \ell_0' + \nu(\eta \ell_1'' + \ell_1') + \nu^2(\eta \ell_2'' + \ell_2') + \nu^3(\eta \ell_3'' + \ell_3')$$
$$+ \cdots = \nu \ell_0 + \nu^2 \ell_1 + \nu^3 \ell_2 + \nu^4 \ell_3 - f_0 k_0' + f_0' k_0$$
$$+ \nu(-f_0 k_1' + f_0' k_1) + \nu^2(-f_0 k_2' + f_0' k_2) + \nu^3(-f_0 k_3' + f_0' k_3)$$
$$+ \cdots$$

Equating powers of ν gives the following equations

4.3.22 $$\eta \ell_0'' + \ell_0' = -f_0 k_0' + f_0' k_0$$

$$\ell_0(1) = 0 \qquad \lim_{\eta \to 0} \sqrt{\eta}\ \ell_0'(\eta) = 0$$

4.3.23 $$\eta \ell_r'' + \ell_r' = \ell_{r-1} - f_0 k_r' + f_0' k_r$$

$$\ell_r(1) = 0 \qquad \lim_{\eta \to 0} \sqrt{\eta}\ \ell_r'(\eta) = 0$$

Solving gives

4.3.24 $$\ell_0 = \frac{\eta^3}{9} - \frac{\eta^2}{2} + 2\eta - \frac{29}{18}$$

4.3.25 $$\ell_1 = \frac{\eta^4}{144} - \frac{\eta^3}{9} + \frac{7\eta^2}{8} - \frac{28\eta}{9} + \frac{337}{144}$$

4.3.26 $$\ell_2 = \frac{-\eta^5}{1200} + \frac{\eta^3}{8} - \frac{25\eta^2}{24} + \frac{163\eta}{48} - \frac{1487}{600}$$

4.3.27 $$\ell_3 = \frac{-31\eta^6}{259200} + \frac{11\eta^5}{7200} + \frac{\eta^4}{1152} - \frac{43\eta^3}{324} + \frac{1189\eta^2}{1152}$$

$$- \frac{23119\eta}{7200} + \frac{199523}{86400}$$

Combining equations 4.3.5 and 4.3.20 we have for small values of s^2

4.3.28 $$h(\eta) \sim h_0(\eta) + \epsilon(\ell_0 + \nu\ell_1 + \nu^2\ell_2 + \nu^3\ell_3)$$

To examine the accurary of this expansion the maximum skin friction at the wall, given by $|h'(1)|$, computed from equation 4.3.28 will be compared with the exact values obtained from numerical integration. Differentiating equation 4.3.28, evaluating at one, and using $\nu = i\alpha^2$ gives

4.3.29 $$h'(1) \sim \frac{\sqrt{-i\alpha^2}\, J_1(2\sqrt{-i\alpha^2})}{i\alpha^2\, J_0(2\sqrt{-i\alpha^2})} + \epsilon\left(\frac{4}{3} - \frac{101}{60}\alpha^4 - \frac{55\alpha^2}{3} i + \frac{6629\alpha^6 i}{4320}\right)$$

Table 4.3.1 compares the exact values of $|h'(1)|$ with the asymptotic values for a small value of α.

Table 4.3.1

$\alpha^2 = 0.2$

ϵ	$\lvert h'(1)\rvert$ (Eqn. 4.3.29)	$\lvert h'(1)\rvert$ (Exact)
0.00000	0.99179	0.99179
0.10061	0.86206	0.87861
0.20445	0.72881	0.78883
0.47737	0.38651	0.62836
-0.02518	1.02432	1.02564
-0.03153	1.03253	1.03460
-0.18849	1.23578	1.33328
-0.34613	1.44041	1.94270

As Table 4.3.1 shows the asymptotic and exact values agree well for small amounts of injection and suction.

Let us turn now to the case where $\frac{1}{|s^2|} << 1$.

Setting $\nu = \frac{1}{s^2}$ equation 4.3.7 becomes

4.3.30 $$\nu(\eta h_0'' + h_0') = h_0 - \nu$$

Let

4.3.31 $$h_0 = \alpha_0(\nu)k_0(\eta) + \alpha_1(\nu)k_1(\eta) + \alpha_2(\nu)k_2(\eta) + \cdots$$

Substituting equation 4.3.31 into equation 4.3.30 and collecting terms gives

4.3.32 $$\nu\alpha_0(\eta k_0'' + k_0') + \nu\alpha_1(\eta k_2'' + k_2') + \nu\alpha_2(\eta k_2'' + k_2') + \cdots = \alpha_0 k_0 + \alpha_1 k_1 + \alpha_2 k_2 + \cdots - \nu$$

Without loss of generality we set $\alpha_0 = \nu$, $\alpha_1 = \nu^2$ and $\alpha_2 = \nu^3$. This gives the following problems

4.3.33 $$k_0 - 1 = 0$$

$$\lim_{\eta \to 0} \sqrt{\eta}\, k_0'(\eta) = 0$$

4.3.34 $$\eta k_r'' + k_r' = k_{r-1} \qquad r > 0$$

$$\lim_{\eta \to 0} \sqrt{\eta}\, k_r'(\eta) = 0$$

Solving equation 4.3.33 and 4.3.34 gives

4.3.35 $$k_0 = 1$$

4.3.36 $$k_r = 0 \qquad r > 0$$

Since k_0 cannot satisfy the boundary conditons near the wall there must be an inner region near the wall. To examine the solution in the inner region let $\eta = 1 - \delta(\nu)\lambda$ and $H_0(\lambda) = h_0(\eta)$. Substituting these into equation 4.3.30 gives

4.3.37 $$\frac{\nu}{\delta^2}\left((1 - \delta\lambda)H_0'' - \delta H_0'\right) = H_0 - \nu$$

Let

4.3.38 $$H_0(\lambda) = \gamma_0(\nu)K_0(\lambda) + \gamma_1(\nu)K_1(\lambda) + \gamma_2(\nu)K_2(\lambda) + \cdots$$

Substituting equation 4.3.38 into equation 4.3.37 and collecting terms gives

4.3.39 $$\frac{\nu}{\delta^2}(\gamma_0 K_0'' + \gamma_1 K_1'' + \gamma_2 K_2'' - \delta\gamma_0\lambda K_0'' - \delta\gamma_1\lambda K_1'' - \delta\gamma_2\lambda K_2''$$
$$- \delta\gamma_2\lambda K_2'' - \delta\gamma_0 K_0' - \delta\gamma_1 K_1' - \delta\gamma_2 K_2' + \cdots) = \gamma_0 K_0$$
$$+ \gamma_1 K_1 + \gamma_2 K_2 + \cdots - \nu$$

Since in the outer region

4.3.40 $$h(\eta) \sim \nu$$

we see that we must set $\gamma_0 = \nu$ and hence that $\delta = \sqrt{\nu}$. This gives that the leading term of the inner expansion is a solution of the following problem

4.3.41 $$K_0'' = K_0 - 1$$

$$K_0(0) = 0 \qquad K_0(\infty) = 1$$

Solving equation 4.3.41 gives

4.3.42 $$K_0 = 1 - e^{-\lambda}$$

Setting $\gamma_1 = \nu^{3/2}$ and $\gamma_2 = \nu^2$ we obtain the following problems for K_1 and K_2

4.3.43 $$K_1'' - K_1 = \lambda K_0'' + K_0'$$

$$K_1(0) = 0 \qquad K_1(\infty) = 0$$

4.3.44 $$K_2'' - K_2 = \lambda K_1'' + K_1'$$

$$K_2(0) = 0 \qquad K_2(\infty) = 0$$

Solving equations 4.3.43 and 4.3.44 gives

4.3.45 $$K_1 = \frac{\lambda}{4}(\lambda - 1)e^{-\lambda}$$

4.3.46 $$K_2 = (\frac{-\lambda^4}{32} + \frac{3\lambda^3}{16} - \frac{5\lambda^2}{32} - \frac{\lambda}{32})e^{-\lambda}$$

Setting $\nu = \frac{1}{s^2}$ equation 4.3.8 for $h_1(\eta)$ becomes

4.3.47 $$\nu(\eta h_1'' + h_1') = h_1 - \nu(f_0 h_0' - h_0 f_0')$$

Let

4.3.48 $$h_1 = \alpha_0(\nu)k_0 + \alpha_1(\nu)k_1 + \cdots$$

Since in the outer region $h_0 = \nu$, substituting equation 4.3.49 into equation 4.3.47 and collecting terms gives

4.3.49 $$\nu\alpha_0(\eta k_0'' + k_0') + \nu\alpha_1(\eta k_1'' + k_1') + \cdots = \alpha_0 k_0 + \alpha_1 k_1 + \cdots - \nu^2(2 - 2\eta)$$

Setting $\alpha_0 = \nu^2$ and $\alpha_1 = \nu^3$ gives the following problems for k_0 and k_1.

4.3.50 $$k_0 + 2 - 2\eta = 0$$

$$\lim_{\eta \to 0} \sqrt{\eta}\, k_0'(\eta) = 0$$

4.3.51 $$\eta k_0'' + k_0' = k_1$$

$$\lim_{\eta \to 0} \sqrt{\eta}\, k_1'(\eta) = 0$$

Solving equations 4.3.50 and 4.3.51 gives

4.3.52 $$k_0 = 2\eta - 2$$

4.3.54 $$k_1 = 2$$

Therefore in the outer region

4.3.54 $$h_1(\eta) \sim (2\eta - 2)\nu^2 + 2\nu^3$$

To examine the solution in the inner region let $H_1(\lambda) = h_1(\eta)$, $H_0(\lambda) = h_0(\eta)$, and $F_0(\lambda) = f_0(\eta)$ where $\eta = 1 - \sqrt{\nu}\,\lambda$ and substitute into equation 4.3.42. This gives

4.3.55 $$(1 - \sqrt{\nu}\,\lambda)H_1'' - \sqrt{\nu}\,H_1' = H_1 + \sqrt{\nu}\,(F_0H_0' - H_0F_0')$$

Let

4.3.56 $$H(\lambda) = \gamma_0(\nu)L_0(\lambda) + \gamma_1(\nu)L_1(\lambda) + \gamma_2(\nu)L_2(\lambda) + \cdots$$

Equation 4.3.3 gives

4.3.57 $$F_0(\lambda) = 1 - \nu\lambda^2$$

Substituting equations 4.3.56, 4.3.57 and 4.3.38 into equation 4.3.55 and collecting terms gives

4.3.58 $$\gamma_0L_0'' + \sqrt{\nu}\,\gamma_0(-\lambda L_0'' - L_0') + \gamma_1L_1'' + \sqrt{\nu}\,\gamma_1(-\lambda L_1'' - L_1')$$
$$+ \gamma_2L_2'' + \sqrt{\nu}\,\gamma_2(-\lambda L_2'' - L_2') + \cdots = \gamma_0L_0 + \gamma_1L_1 + \gamma_2L_2$$
$$+ \cdots + \nu^{3/2}K_0' + \nu^2K_1' + \nu^{5/2}(K_2' - \lambda^2K_0' + 2\lambda K_0) + \cdots$$

Expanding the outer solution given by equation 4.3.54 in inner variables gives

4.3.59 $$h_1 \sim -2\lambda\nu^{5/2}$$

Since $\nu^{3/2}$ and ν^2 are both larger than $\nu^{5/2}$ we set $\gamma_0 = \nu^{3/2}$, $\gamma_1 = \nu^2$ and $\gamma_2 = \nu^{5/2}$. This gives the following problems for L_0, L_1 and L_2

4.3.60 $$L_0'' - L_0 = K_0'$$

$$L_0(0) = 0 \qquad L_0(\infty) = 0$$

4.3.61 $$L_1'' - L_1 = \lambda L_0'' + L_0' + K_1'$$

$$L_1(0) = 0 \qquad L_1(\infty) = 0$$

4.3.62 $$L_2'' - L_2 = K_2' - \lambda^2 K_0' + 2\lambda K_0 + \lambda L_1'' + L_1'$$

$$L_2(0) = 0 \qquad L_2'(\infty) = -2$$

Solving gives

4.3.63 $$L_0 = \frac{-\lambda e^{-\lambda}}{2}$$

4.3.64 $$L_1 = \frac{1}{8}(\lambda^3 - 3\lambda^2)e^{-\lambda}$$

4.3.65 $$L_2 = -2\lambda + e^{-\lambda}\left(\frac{-\lambda^5}{64} + \frac{5\lambda^4}{32} - \frac{9}{64}\lambda^3 + \frac{47}{64}\lambda^2 + \frac{47}{64}\lambda\right)$$

Combining equations 4.3.5 and 4.3.56 gives that near the wall for large values of s^2

4.3.66 $$h(\eta) \sim h_0(\eta) + \varepsilon\left(\nu^{3/2}L_0\left(\frac{1-\eta}{\sqrt{\nu}}\right) + \nu^2 L_1\left(\frac{1-\eta}{\sqrt{\nu}}\right) + \nu^{5/2}L_2\left(\frac{1-\eta}{\sqrt{\nu}}\right)\right)$$

Again to examine the accuracy of this expansion the asymptotic and exact values of the maximum skin friction at the wall,

given by $|h'(1)|$, will be compared. Differentiating equation 4.3.66, evaluating at one, and using $\nu = \frac{1}{i\alpha^2}$ gives

$$4.3.67 \qquad h'(1) \sim \frac{\sqrt{-i\alpha^2}}{i\alpha^2} \frac{J_1(2\sqrt{-i\alpha^2})}{J_0(2\sqrt{-i\alpha^2})} - \epsilon \left(\frac{81}{64\alpha^4} + \frac{i}{2\alpha^2}\right)$$

Table 4.3.2 compares the exact and asymptotic values of $|h'(1)|$ for a large value of α.

Table 4.3.2

$\alpha^2 = 100.0$

ϵ	$\lvert h'(1)\rvert$ (Egn. 4.3.67)	$\lvert h'(1)\rvert$ (Exact)
0.00000	0.09825	0.09825
0.101	0.098	0.098
0.2044	0.0976	0.0976
0.4774	0.0967	0.0966
-0.02518	0.09834	0.09834
-0.03153	0.09836	0.09836
-0.18849	0.09889	0.09889
-0.34613	0.09943	0.09943
-0.81633	0.10105	0.10106

As Table 4.3.2 shows the agreement between the asymptotic and exact values in excellent. Comparing Tables 4.3.1 and 4.3.2 shows that for large values of α suction and injection have very little effect on skin friction but that for small values of α suction and injection have very pronounced effects in skin friction.

Consider now the case where $f(\eta)$ is a Section II or Section III solution. In this case it was shown that $f(\eta)$ had an expansion of the form

4.3.68 $$f(\eta) = \frac{1}{\epsilon} f_0(\eta) + \cdots$$

where $f_0(\eta)$ is the solution of 3.3.11. Let

4.3.69 $$h(\eta) = \gamma_0(\epsilon)h_0(\eta) + \gamma_1(\epsilon)h_1(\eta) + \cdots$$

Substituting equations 4.3.68 and 4.3.69 into equation 4.3.1 and collecting terms gives

4.3.70 $$\gamma_0(\eta h_0'' + h_0') + \gamma_1(\eta h_1'' + h_1') + \cdots = \gamma_0 s^2 h_0 + \gamma_1 s^2 h_1$$

$$- 1 + \gamma_0(-f_0 h_0' + h_0 f_0') + \gamma_1(-f_0 h_1' + f_0 h_1') + \cdots$$

Without loss of generality we set $\gamma_0 = 1$. Thus unlike the steady state component of velocity the pulsatile velocity component remains finite as $\epsilon \to 0$. This gives the following problem for the leading term of the expansion.

4.3.71 $$\eta h_0''(\eta) + h_0'(\eta) = s^2 h_0(\eta) - 1 + h_0(\eta) f_0'(\eta) - f_0(\eta) h_0'(\eta)$$

$$\lim_{\eta \to 0} \sqrt{\eta}\, h_0'(\eta) = 0 \qquad h_0(1) = 0$$

In Section 3.3 it was noted that on the interval $[0, \eta^*]$, where $\eta^* = 0.262$, an approximate solution for $f_0(\eta)$ was given by

4.3.72 $$f_0(\eta) = \beta\eta - 3 + 3e^{-\beta\eta}$$

where $\beta = 4.196$

Thus in the interval $[0, \eta^*]$ an approximate solution of $h_0(\eta)$ is obtained by solving

4.3.73 $$\eta h_0'' + h_0' = s^2 h_0 - 1 + (\beta - 3\beta e^{-\beta\eta}) h_0 - h_0'(\beta\eta - 3 + 3e^{-\beta\eta})$$

$$\lim_{\eta \to 0} \sqrt{\eta}\ h_0'(\eta) = 0$$

It was found that

4.3.74 $$h_p(\eta) = \frac{1}{s^2 + \beta} + \frac{3\beta e^{-\beta\eta}}{s^4 - \beta^2}$$

is a particular solution of 4.3.73. However no solution of the homogeneous equation was found. Thus to solve equation 4.3.73 in the interval $[0, \eta^*]$ a power series was used. The power series solution is given as follows:

4.3.75 $$h_0(\eta) = \sum_{k=0}^{\infty} b_k \eta^k$$

where $b_1 = (s^2 - 2\beta) b_0 - 1$; b_0 is arbitrary,

$$(k+1)^2 b_{k+1} + b_k(\beta k - s^2 - \beta) + 3L_k = 0 \qquad k \geq 1$$

where $$L_k = \sum_{r=1}^{k+1} b_{k+1-r} \frac{(-1)^r \beta^r (k + 1 - 2r)}{r!}$$

In the interval $[\eta^*, 1]$ $h_0(\eta)$ is a solution of 4.3.71 with $h_0(1) = 0$. If the inertial terms are neglected then in this interval $h_0(\eta)$ satisfies

4.3.76 $$\eta h_0''(\eta) + h_0'(\eta) = s^2 h_0 - 1$$

$$h_0(1) = 0$$

The solution of 4.3.76 is given by

4.3.77 $$h_0(\eta) = C_1 J_0(2B\sqrt{\eta}) + C_2 Y_0(2B\sqrt{\eta}) + \frac{1}{s^2}$$

where

4.3.78 $$C_1 J_0(2B) + C_2 Y_0(2B) + \frac{1}{s^2} = 0$$

and $B = \sqrt{-s^2}$.

This is a valid approximation near one since at one the inertial terms are zero. But to find an approximation valid on the interval $[\eta^*,1]$ the effects of the inertial terms must be considered. This will be done by examining the power series for $h_0(\eta)$ at one. Letting $h_0'(1) = D$ the power series solution of 4.3.71 expanded about one is given by

4.3.79
$$\begin{aligned} h_0(\eta) = -D[(\eta - 1) &- \frac{(\eta-1)^2}{2!} + (s^2 + 2)\frac{(\eta-1)^3}{3!} \\ &- (4s^2 + 6)\frac{(\eta-1)^4}{4!} + (18s^2 + s^4 + 24)\frac{(\eta-1)^5}{5!} \\ &- (96s^2 + 9s^4 + 120)\frac{(\eta-1)^6}{6!} - \frac{(\eta-1)^2}{2!} + \frac{2(\eta-1)^3}{3!} \\ &- (6 + s^2)\frac{(\eta-1)^4}{4!} + (24 + 6s^2)\frac{(\eta-1)^5}{5!} - (120 + 36s^2 \\ &+ s^4)\frac{(\eta-1)^6}{6!}] - Df_0''(1)\frac{(\eta-1)^4}{4!} + (4Df_0''(1) - 2Df_0'''(1))\frac{(\eta-1)^5}{5!} \\ &+ [f_0''(1)(-16D + Ds^2 - 4 + f_0'''(1)(12D - 2) - 3Df_0^{IV}(1)]\frac{(\eta-1)^6}{6!} \\ &+ O[(\eta-1)^7] \end{aligned}$$

where $f_0''(1)$, $f_0'''(1)$ and $f_0^{IV}(1)$ are computed from equation 3.3.13.

Expanding the approximate solution given by equation 4.3.77 in a power series about one gives

$$4.3.80 \quad h_0(\eta) = -B(C_1J_1(2B) + C_2Y_1(2B))((\eta-1) - \frac{(\eta-1)^2}{2!} + (2 + s^2)\frac{(\eta-1)^3}{3!} - (6 + 4s^2)\frac{(\eta-1)^4}{4!} + (18s^2 + s^4 + 24)\frac{(\eta-1)^5}{5!} - (96s^2 + 9s^4 + 120)\frac{(\eta-1)^6}{6!} - \frac{(\eta-1)^2}{2!} + \frac{2(\eta-1)^3}{3!} - (6 + s^2)\frac{(\eta-1)^4}{4!} + (24 + 6s^2)\frac{(\eta-1)^5}{5!} - (120 + 36s^2 + s^4)\frac{(\eta-1)^6}{6!} + O[(\eta-1)^7]$$

By comparing equations 4.3.79 and 4.3.80 and setting

$$4.3.81 \quad D = B(C_1J_1(2B) + C_2Y_1(2B))$$

an approximate solution of equation 4.3.71 on $[\eta^*,1]$ is given by the following equation.

$$4.3.82 \quad h_0(\eta) = C_1J_0(2B\sqrt{\eta}) + C_2Y_0(2B\sqrt{\eta}) + \frac{1}{s^2} - Df_0''(1)\frac{(\eta-1)^4}{4!} + (4Df_0''(1) - 2Df_0'''(1))\frac{(\eta-1)^5}{5!} + [f_0''(1)(-16D + Ds^2 - 4) + f_0'''(1)(12D - 2) - 3Df_0^{IV}(1)]\frac{(\eta-1)^6}{6!} + O[(\eta-1)^7]$$

The four unknown constants C_1, C_2, b_0 and D were determined from equations 4.3.81 and 4.3.78 and by requiring equation 4.3.75 and equation 4.3.80 and their first derivatives agree at η^*. For this procedure thirty terms of equation 4.3.75 were used.

Table 4.3.3 tabulates the results obtained for these constants for three different values of α.

Table 4.3.3

	ReC_1	ImC_1	ReC_2	ImC_2	Reb_0	Imb_0	ReD	ImD
$\alpha^2 = 0.2$	1.22	6.09	1.94	0.113	-0.402	-0.008	-0.380	0.012
$\alpha^2 = 1.0$	-0.051	2.18	1.82	0.546	-0.384	-0.039	-0.374	0.059
$\alpha^2 = 100.0$	-3760	7040	7040	3760	0.000	-0.005	-0.050	0.052

To examine the accuracy of these results the approximate value of the maximum velocity at the center of the tube given by $|b_0|$ will be compared with the exact values, given by $|h(0)|$, for small amounts of injection or suction obtained from numerical integration. A similar comparison will be made between the approximate value of the maximum skin friction at the wall given by $|D|$ and the exact values given by $|h'(1)|$. These comparisons are contained in Table 4.3.4.

Table 4.3.4

	$\alpha^2 = 0.2$		$\alpha^2 = 100.0$	
	$\|b_0\| = 0.402$	$\|D\| = 0.380$	$\|b_0\| = 0.005$	$\|D\| = 0.072$
ϵ	$\|h(0)\|$	$\|h'(1)\|$	$\|h(0)\|$	$\|h'(1)\|$
0.360	0.370	0.372	0.010	0.097
0.056	0.399	0.386	0.010	0.098
-0.091	0.415	0.390	0.010	0.099
-0.344	0.445	0.390	0.010	0.100

From Table 4.3.4 it is seen that the accuracy of the approximation is fairly good for small values of α, but decreases for large values of α. To increase the accuracy of this approximation three things can be done. First more accurate values of β and η^* must be obtained. As Terrill and Thomas [24] pointed out there is a 3% error in their evaluation of β. Secondly more terms in the series in equation 4.3.82 would have to be calculated. Thirdly more accurate values for $f_0''(1)$, $f_0'''(1)$, $f_0^{IV}(1)$, ... would have to be found by computing more terms in equation 3.3.13.

In this section we have obtained asymptotic solutions in the case of small injection and suction and have compared these solutions with the exact solutions obtained by numerical integration. In the case of Section I solutions good agreement was found between the asymptotic and exact values. In the case of Section II and Section III solutions the agreement was not as good since only an approximate solution could be obtained for the leading term of the expansion. Also it was observed that for large values of s^2 suction and injection have very little effect on pulsatile flow.

Section 4.4. Asymptotic Solutions for Large Suction

In this section asymptotic solutions for large suction for the Section IV(ii) and Section V(ii) solutions will be discussed. No asymptotic solutions can be obtained for the Section IV(i) and Section V(i) solutions since none have

been obtained for the respective steady state components of velocity. Any information about these solutions will have to be obtained from the numerical results given in Section 4.1. Letting $\epsilon = R/2$, where $\epsilon \ll 1$, the problem for this case has the following formulation.

$$4.4.1 \quad \epsilon(\eta h''(\eta) + h'(\eta)) + h(\eta)f'(\eta) - f(\eta)h'(\eta) - \epsilon s^2 h(\eta) = -\epsilon$$

$$\lim_{\eta \to 0} \sqrt{\eta}\, h'(\eta) = 0 \qquad h(1) = 0$$

In Section 3.4 it was shown that the Section IV(ii) and Section V(ii) steady state solutions have a boundary layer of width ϵ at the wall. It was shown that if exponentially small terms were neglected in matching the inner and outer expansions that both solutions were asymptotic to the same series. Using this series a solution for equation 4.4.1 will be sought which is also asymptotic to both the Section IV(ii) and Section V(ii) solutions for the unsteady component of velocity. In Section 3.4 it was shown that in the region near the center of the tube the Section IV(ii) and Section V(ii) solutions for the steady state component of velocity were both asymptotic to the following series.

$$4.4.2 \qquad f(\eta) = f_0(\eta) + \epsilon f_1(\eta) + \epsilon^2 f_2(\eta) + \cdots$$

where

$$4.4.3 \quad \text{a)} \ f_0(\eta) = \eta \qquad \text{b)} \ f_1(\eta) = \eta \qquad \text{c)} \ f_2(\eta) = 3\eta$$

Let

4.4.4 $$h(\eta) = \gamma_0(\varepsilon)h_0(\eta) + \gamma_1(\varepsilon)h_1(\eta) + \gamma_2(\varepsilon)h_2(\eta) + \cdots$$

Substituting equations 4.4.4 and 4.4.2 into equation 4.4.1 and collecting terms gives

4.4.5 $$\varepsilon\gamma_0(\eta h_0'' + h_0') + \varepsilon\gamma_1(\eta h_1'' + h_1') + \varepsilon\gamma_2(\eta h_2'' + h_2')$$
$$+ \gamma_0(h_0 f_0' - f_0 h_0') + \gamma_1(h_1 f_0' - f_0 h_1') + \gamma_2(h_2 f_0' - f_0 h_2')$$
$$+ \varepsilon\gamma_0(f_1'h_0 - f_1 h_0') + \varepsilon\gamma_1(f_1'h_1 - f_1 h_1') + \varepsilon\gamma_2(f_1'h_2 - f_1 h_2')$$
$$+ \varepsilon^2\gamma_0(h_0 f_2' - f_2 h_0') + \varepsilon\gamma_1(h_1 f_2' - f_2 h_1') + \varepsilon^2\gamma_2(f_2'h_2 - h_2'f_2)$$
$$- \varepsilon\gamma_0 s^2 h_0 - \varepsilon\gamma_1 s^2 h_1 - \varepsilon\gamma_2 s^2 h_2 + \cdots = -\varepsilon$$

As in the case of large injection the leading term in the outer region near the center of the tube is determined by the relative sizes of γ_0, $\varepsilon s^2\gamma_0$, and ε. This gives again the following three cases to consider. 1) $a_0^2 = \varepsilon s^2 = O(1)$ 2) $\varepsilon s^2 << 1$ 3) $\varepsilon s^2 >> 1$. By using the same arguments as for large injection it can be shown case 2 is included in case 1. Thus only case 1 and case 3 need to be examined. Let us consider first the case where $\varepsilon s^2 = a_0^2 = O(1)$. For this case we must have $\gamma_0 = \varepsilon$. Since the higher order terms must include the effects of the lower order viscous terms we set, without loss of generality, $\gamma_1 = \varepsilon^2$ and $\gamma_2 = \varepsilon^3$. This gives the following problems for h_0, h_1, and h_2.

4.4.6 $$h_0 f_0' - f_0 h_0' - a_0^2 h_0 = 1$$
$$\lim_{\eta \to 0} \sqrt{\eta}\, h_0'(\eta) = 0$$

4.4.7 $$\eta h_0'' + h_0' + h_0 f_1' - f_1 h_0' + h_1 f_0' - f_0 h_1' - a_0^2 h_1 = 0$$

$$\lim_{\eta \to 0} \sqrt{\eta}\, h_1'(\eta) = 0$$

4.4.8 $$\eta h_1'' + h_1' + h_2 f_0' - f_0 h_2' + h_1 f_1' - f_1 h_1' + h_0 f_2' - f_2 h_0' - a_0^2 h_2 = 0$$

$$\lim_{\eta \to 0} \sqrt{\eta}\, h_2'(\eta) = 0$$

Solving equations 4.4.6, 4.4.7, and 4.4.8 gives

4.4.9 $$h_0 = \frac{1}{a_0^2 - 1}$$

4.4.10 $$h_1 = \frac{1}{(a_0^2 - 1)^2}$$

4.4.11 $$h_2 = \frac{3a_0^2 - 2}{(a_0^2 - 1)^3}$$

Therefore in the outer region we have

4.4.12 $$h(\eta) \sim \frac{\epsilon}{a_0^2 - 1} + \frac{\epsilon^2}{(a_0^2 - 1)^2} + \frac{(3a_0^2 - 2)\epsilon^3}{(a_0^2 - 1)^3}$$

To examine the solution in the inner region at the wall let $H(\lambda) = h(\eta)$ and $F(\lambda) = f(\eta)$ where $\eta = 1 - \epsilon\lambda$. Substituting these into equation 4.4.1 gives the following problem in the inner region:

4.4.13 $$(1 - \epsilon\lambda)H''(\lambda) - \epsilon H'(\lambda) + F(\lambda)H'(\lambda) - H(\lambda)F(\lambda) - \epsilon a_0^2 H(\lambda) = -\epsilon^2$$

$$H(0) = 0$$

In Section 3.4 it was shown that in this region the Section IV(ii) and Section V(ii) steady solutions were both asymptotic to the following series:

$$4.4.14 \qquad F(\lambda) = F_0(\lambda) + \epsilon F_1(\lambda) + \epsilon^2 F_2(\lambda) + \cdots$$

where

$$4.4.15 \quad a) \quad F_0(\lambda) \equiv 1 \qquad b) \quad F_1(\lambda) = 1 - \lambda - e^{-\lambda}$$

$$c) \quad F_2(\lambda) = 3 - \lambda - (2\lambda + 3)e^{-\lambda}$$

Let

$$4.4.16 \qquad H(\lambda) = \nu_0(\epsilon)H_0(\lambda) + \nu_1(\epsilon)H_1(\lambda) + \nu_2(\epsilon)H_2(\lambda) + \cdots$$

Substituting equations 4.4.14 and 4.4.16 into equation 4.4.13 and collecting terms gives

$$4.4.17 \quad \nu_0(H_0'' + F_0H_0' - H_0F_0') + \nu_1(H_1'' + F_0H_1' - H_1F_0') + \nu_2(H_2'' + F_0H_2' - H_2F_0') + \epsilon\nu_0(-\lambda H_0'' - H_0' - a_0^2H_0 + F_1H_0' - H_0F_1') + \epsilon\nu_1(-\lambda H_1'' - H_1' - a_0^2H_1 + F_1H_1' - H_1F_1') + \epsilon\nu_2(-\lambda H_2'' - H_2' - a_0^2H_2 + F_1H_2' - H_2F_1') + \epsilon^2\nu_0(F_2H_0' - H_0F_2') + \epsilon^2\nu_1(F_2H_1' - H_1F_2') + \epsilon^2\nu_2(F_2H_2' - H_2F_2') + \cdots = -\epsilon^2$$

Expanding the outer solution given by equation 4.4.12 in inner variables shows that $\nu_0 = \epsilon$, $\nu_1 = \epsilon^2$, and $\nu_2 = \epsilon^3$. This gives the following problems for H_0, H_1 and H_2:

4.4.18 $$H_o'' + F_oH_o' - H_oF_o' = 0$$

$$H_o(0) = 0 \qquad H_o(\infty) = \frac{1}{a_o^2 - 1}$$

4.4.19 $$-\lambda H_o'' - H_o' - a_o^2 H_o + H_1'' + F_oH_1' - H_1F_o' + F_1H_o' - H_oF_1' = -1$$

$$H_1(0) = 0 \qquad H_1(\infty) = \frac{1}{(a_o^2 - 1)^2}$$

4.4.20 $$H_2'' + F_oH_o' - H_oF_o' - \lambda H_1'' - H_1' - a_o^2 H_1 + F_1H_1' - H_1F_1'$$

$$+ F_2H_o' - H_oF_2' = 0$$

$$H_2(0) = 0 \qquad H_2(\infty) = \frac{3a_o^2 - 2}{(a_o^2 - 1)^3}$$

The condition at infinity comes from matching the inner and outer solutions. Solving equations 4.4.18, 4.4.19, and 4.4.20 we obtain

4.4.21 $$H_o = \frac{1}{a_o^2 - 1}(1 - e^{-\lambda})$$

4.4.22 $$H_1 = \frac{(a_o^2 - 2)}{(a_o^2 - 1)} \lambda e^{-\lambda} + \frac{1}{(a_o^2 - 1)^2}(1 - e^{-\lambda})$$

4.4.23 $$H_2 = \frac{((a_o^2 - 2)^2 + 3)}{(1 - a_o^2)} (\frac{\lambda^2}{2} + \lambda)e^{-\lambda} + \frac{(2a_o^2 - 1)\lambda e^{-\lambda}}{(a_o^2 - 1)^2}$$

$$+ \frac{a_o^2}{2(a_o^2 - 1)}(e^{-2\lambda} - e^{-\lambda}) + \frac{(3a_o^2 - 2)(1 - e^{-\lambda})}{(a_o^2 - 1)^3}$$

The accuracy of these expansions will be examined by comparing the asymptotic values for the maximum velocity at the center

of the tube, given by $|h(0)|$, and the maximum skin friction at the wall, given by $|h'(1)|$, with the exact values computed from numerical integration for both Section IV(ii) and Section V(ii) solutions. Substituting equations 4.4.21, 4.4.22, and 4.4.23 into equation 4.4.16, setting $\lambda = \frac{1 - \eta}{\varepsilon}$, differentiating, and evaluating at one gives

$$4.4.24 \qquad h'(1) \sim \frac{1}{1 - a_o^2} + \varepsilon\left(\frac{2 - a_o^2}{a_o^2 - 1} - \frac{1}{(a_o^2 - 1)^2}\right) + \varepsilon^2\left(\frac{(1 - 2a_o^2)}{(a_o^2 - 1)^2} + \frac{((a_o^2 - 2)^2 + 3 + a_o^2)}{(a_o^2 - 1)} + \frac{(2 - 3a_o^2)}{(a_o^2 - 1)^3}\right)$$

The comparison between the exact and asymptotic values for $|h(0)|$ and $|h'(1)|$ are contained in Tables 4.4.1 and 4.4.2 respectively.

Table 4.4.1

	$\lvert h(0)\rvert$ (Egn. 4.4.12)		$\lvert h(0)\rvert$ (Exact)	
ε	$\alpha^2 = 0.2$	$\alpha^2 = 100.0$	$\alpha^2 = 0.2$	$\alpha^2 = 100.0$
0.037 (IV(ii))	0.036	0.010	0.036	0.010
0.049 (IV(ii))	0.047	0.010	0.048	0.010
0.0576(IV(ii))	0.0539	0.010	0.0592	0.010
0.0680(IV(ii))	0.0628	0.0099	0.0881	0.0099
0.0738(IV(ii))	0.0675	0.0099	0.1416	0.0100
0.044 (V(ii))	0.042	0.010	0.042	0.010
0.0626(V(ii))	0.0582	0.010	0.0545	0.010
0.0819(V(ii))	0.0741	0.0099	0.0664	0.0099
0.0920(V(ii))	0.0820	0.0099	0.0729	0.0099
0.1140(V(ii))	0.0980	0.0100	0.0876	0.0099

Table 4.4.1(cont'd.)

0.1373(V(ii))	0.1133	0.0100	0.1044	0.0100
0.1794(V(ii))	0.1356	0.0100	0.1357	0.0100
0.2067(V(ii))	0.1463	0.0100	0.1509	0.0100
0.2184(V(ii))	0.1498	0.0100	0.1415	0.0100

Table 4.4.2

	$\lvert h'(1)\rvert$(Egn. 4.4.24)		$\lvert h'(1)\rvert$(Exact)	
ϵ	$\alpha^2 = 0.2$	$\alpha^2 = 100.0$	$\alpha^2 = 0.2$	$\alpha^2 = 100.0$
0.037 (IV(ii))	0.876	0.244	0.889	--
0.049 (IV(ii))	0.832	0.195	0.952	0.195
0.058 (IV(ii))	0.801	0.179	1.158	0.177
0.0680(IV(ii))	0.7588	0.1724	2.3077	0.1593
0.0738(IV(ii))	0.7350	0.1740	4.6948	0.1510
0.044 (V(ii))	0.851	0.212	0.806	--
0.063 (V(ii))	0.781	0.174	0.595	0.169
0.082 (V(ii))	0.701	0.181	0.444	0.148
0.092 (V(ii))	0.656	0.198	0.402	0.141

Several things should be noted about these comparisons. Since the numerical technique used required integrating into a boundary layer for these solutions we were unable to obtain accurate exact solutions for small values of ϵ especially at large values of α^2. Thus relatively large values of ϵ were used in making the comparison. However the comparisons made in Tables 4.4.1 and 4.4.2 still show the series obtained

is asymptotic to both Section IV(ii) and Section V(ii) solutions. The discrepancies between the series solution and the exact solution for small α^2 and relatively large ϵ is due to ignoring the exponentially small terms in matching the inner and outer solutions. The discrepancies between the series solution and the exact values for large α^2 and large ϵ is due to the fact that ϵs^2 is no longer of order one.

Let us consider now case 3 when $\epsilon s^2 >> 1$. In this case we must set $\gamma_0 = \frac{1}{s^2}$ and therefore the leading term satisfies the following:

4.4.25
$$h_0 = 1$$

$$\lim_{\eta \to 0} \sqrt{\eta}\ h'''(\eta) = 0$$

Since h_0 cannot satisfy the boundary condition at the wall there must be an inner region near the wall. To examine the solutions in this region let $\nu = \frac{1}{s^2}$, $\eta = 1 - \delta\lambda$, $H(\lambda) = h(\eta)$, and $F(\lambda) = f(\eta)$ where δ is the width of the boundary layer. Substituting these into equation 4.4.1 we obtain

4.4.26
$$\nu\epsilon\left((1 - \delta\lambda)\frac{H''(\lambda)}{\delta^2} - \frac{1}{\delta} H'(\lambda)\right) + \frac{\nu}{\delta}(F(\lambda)H'(\lambda) - F'(\lambda)H(\lambda) - \epsilon H(\lambda) = -\epsilon\nu$$

Let

4.4.27
$$H(\lambda) = \mu_0 H_0(\lambda) + \mu_1 H_1(\lambda) + \cdots$$

and

4.4.28 $$F(\lambda) = \alpha_0 F_0(\lambda) + \alpha_1 F_1(\lambda) + \cdots$$

Substituting equations 4.4.27 and 4.4.28 into equation 4.4.26 and collecting terms gives

4.4.29 $$\frac{\nu\varepsilon\mu_0}{\delta^2} H_0'' + \frac{\nu\varepsilon\mu_1}{\delta^2} H_1'' - \frac{\mu\nu\varepsilon}{\delta} (\lambda H_0'' + H_0') - \frac{\mu_1\nu\varepsilon}{\delta} (\lambda H_1'' + H_1')$$

$$+ \frac{\nu}{\delta} \mu_0\alpha_0(F_0H_0' - \mu_0F_0') + \frac{\nu\mu_0\alpha_1}{\delta} (H_0'F_1 - F_1'H_0)$$

$$+ \frac{\nu\mu_1\alpha_0}{\delta} (H_1'F_0 - H_1F_0') + \frac{\nu\mu_1\alpha_1}{\delta} (H_1F_1' - H_1'F_1) - \varepsilon\mu_0H_0$$

$$- \varepsilon\mu_1H_1 + \cdots = -\varepsilon\nu .$$

Since in the outer region

4.4.30 $$h(\eta) \sim \nu$$

we have that $\mu_0 = \nu$ and from equation 4.4.14 we have $\alpha_0 = 1$. The equation for the leading term in the inner expansion depends on the relative magnitude of $\frac{\nu^2\varepsilon}{\delta^2}$, $\frac{\nu^2}{\delta}$ and $\varepsilon\nu$. This leads us to consider the following three cases: 1) $\varepsilon^2\nu << 1$. 2) $\varepsilon^2\nu = a_0^2 = O(1)$. 3) $\varepsilon^2\nu >> 1$. As before case one is included in case 2. Let us examine now case 2 where $\varepsilon^2\nu = a_0^2 = O(1)$. In this case we must have $\delta = \varepsilon$ and that the leading term in the inner region is the solution of the following problem:

4.4.31 $$H_0'' + F_0H_0' - H_0F_0' - a_0^2H_0 = -a_0^2$$

$$H_0(0) = 0 \qquad H_0(\infty) = 1$$

Since $F_0 \equiv 1$ this becomes

4.4.32 $$H_0'' + H_0' - a_0^2 H_0 = a_0^2$$

$$H_0(0) = 0 \qquad H_0(\infty) = 1$$

Solving equation 4.4.32 we obtain

4.4.33 $$H_0 = 1 - e^{-D\lambda}$$

where

4.4.34 $$D = -\frac{1}{2}(1 + \sqrt{1 + 4a_0^2})$$

Therefore in this case we have that near the wall

4.4.35 $$h(\eta) \sim \nu(1 - e^{\frac{-D(1-\eta)}{\epsilon}})$$

Let us examine now case 3 where $\epsilon^2 \nu >> 1$. In this case we must set $\delta = \sqrt{\nu}$. This gives the leading term of the inner expansion as the solution of the following problem:

4.4.36 $$H_0'' - H_0 = -1$$

$$H_0(0) = 0 \qquad H_0(\infty) = 1$$

Solving equation 4.4.36 gives

4.4.37 $$H_0 = 1 - e^{-\lambda}$$

Therefore in this case we have that near the wall

4.4.38 $$h(\eta) \sim \nu(1 - e^{\frac{\eta - 1}{\sqrt{\nu}}})$$

This expansion shows the annular effect does occur for large values of suction but does not become important until $\epsilon^2 s^2 >> 1$. To examine the accuracy of the above expansions we will compare the asymptotic values of the maximum skin friction at the wall, given by $|h'(1)|$, with the exact values. Differentiating equation 4.4.33, evaluating at one, and using equation 4.4.34 we obtain

4.4.39 $$h'(1) \sim \frac{-\nu}{2\epsilon} \left(1 + \sqrt{1 + a_0^2}\right)$$

Using $\nu = \frac{1}{s^2}$, $s^2 = i\alpha^2$, and $a_0^2 = \epsilon^2 \nu$ and separating real and imaginary parts equation 4.4.39 becomes

4.4.40 $$h'(1) \sim \frac{r \sin \theta/2}{2\epsilon\alpha^2} + \frac{i(1 + r \cos \theta/2)}{2\epsilon\alpha^2}$$

where

4.4.41 $$r = (1 + 16\epsilon^4\alpha^4)^{1/4}$$

and

4.4.42 $$\theta = \text{Arctan } (4\epsilon^2\alpha^2)$$

Differentiating equation 4.4.38, evaluating at one, and using $\nu = \frac{1}{i\alpha^2}$, we obtain

4.4.43 $$h'(1) \sim -\frac{\sqrt{2}}{2\alpha} (1 - i)$$

Table 4.4.43 compares the asymptotic and the exact values of $|h'(1)|$ for a large value of α.

Table 4.4.3

$\alpha^2 = 100.0$

ϵ	$\epsilon^2\alpha^2$	$\lvert h'(1)\rvert$ (Eqn. 4.4.39)	$\lvert h'(1)\rvert$ (Eqn. 4.4.43)	$\lvert h'(1)\rvert$ (Exact)
0.0738 (IV(ii))	0.5446	0.1660	0.1000	0.1510
0.07824(IV(ii))	0.61215	0.16097	0.10000	0.14580
0.08425(IV(ii))	0.70981	0.15563	0.10000	0.14014
0.092 (V(ii))	0.848	0.149	0.100	0.141
0.11399(V(ii))	1.29937	0.13760	0.10000	0.13180
0.13731(V(ii))	1.88537	0.13006	0.10000	0.12539
0.17943(V(ii))	3.21956	0.12208	0.10000	0.11840

Because of difficulties in obtaining accurate numerical solutions for large values of α^2, in Table 4.4.3 we were only able to make a limited comparison between the exact and asymptotic values. However Table 4.4.3 still does show that there is good agreement between the asymptotic solutions in their range of validity and the exact solutions.

In this section we were able to obtain a series which was asymptotic to both the Section IV(ii) and Section V(ii) solutions and differed from them by exponentially small terms. These exponentially small terms were not included in the expansion because, as noted previously, these terms were important only for relatively large ϵ and small α^2 and were unimportant if ϵ was small or $\epsilon\alpha^2 \gg 1$ and because the equations involved in obtaining these terms were quite

complex. We were also able to show that the annular effect does occur for large suction but only if $\epsilon^2\alpha^2 \gg 1$.

CHAPTER V

DISCUSSION

Section 5.1. Summary and Comments.

In this section the preceding work will be reviewed and the results summarized. The problem that has been treated is the effect of suction and injection on pulsatile flow in a tube. It was shown that the system of partial differential equations governing the flow could be reduced to a system of two ordinary differential equations. It was observed that the equation for the unsteady component of velocity was coupled to the equation for the steady component of velocity, but not conversely. Thus we were able to examine the two equations separately. The solutions of the equation for the steady component of velocity were studied and it was shown that for injection and small suction two solutions were possible for each crossflow Reynolds number, while for large suction four solutions were possible, and that for $R = 4$ no solutions were possible. The qualitive behavior of all the possible solutions was also given. The equation for the steady component of the velocity was then integrated numerically and all the theoretically possible solutions were found including two solutions for large

suction which had not previously been reported. The asymptotic solutions for large and small crossflow Reynolds number for the steady component of velocity were rederived and examined in the light of the theoretical results obtained. We were able to show that in the case of large injection there could be no boundary layer at the wall and that in the case of large suction there could be no boundary at the center of the tube. By examining the diffusion of vorticity in the flow this phenomena would be expected but it has not been shown mathematically that it does occur for the tube. Also it was shown that for large suction there is no regular perturbation solution as there is in the case of large injection. But we were unable to obtain any asymptotic solutions for the two new large suction solutions we found.

Having examined the solutions for the steady component of velocity we were able to study the solutions for the unsteady component of velocity. Before proceeding with this discussion we would like to again point out that, due to linearity of the equation for the unsteady component of velocity, although only a sinusoidally varying pressure gradient was examined the results will be applicable to any time dependent pressure gradient that has a Fourier series expansion. Using the previously obtained solutions for the steady component of the velocity numerical solutions were obtained for the unsteady component of velocity. These solutions were used to examine various aspects of the effects of suction and

injection on the flow and the following results were found: 1) Injection decreases the maximum skin friction at the wall while suction could result in either increasing or decreasing it. 2) The phase lag of the velocity profile and the skin friction at the wall relative to the pulsatile pressure gradient is decreased by injection but could be increased or decreased by suction. 3) The annular effect still occurs for both suction and injection. 4) Suction can cause resonance like effects for small frequency pulsatile pressure gradients. Also asymptotic solutions were found for the unsteady component of velocity. The results were compared with the numerical solutions and the agreement was generally found to be good.

Section 5.2. Final Considerations.

In this section we discuss the aspects of our present problem which should be considered further and the assumptions about the flow that would be interesting to modify and study. The facets of our present problem which should be examined further come under the two broad headings of analytical and numerical problems. The analytical problems that would be interesting to examine further are the following: 1) In the case where $\alpha = g'(0) > 0$ and $\beta = g''(0) < 0$, what conditions on α and β will guarantee $g'(\xi)$, where $g(\xi)$ is the solution of equation 1.3.4, have exactly one or exactly three zeroes. 2) What is the relationship between the magnitude of α and β and the resulting value of R obtained.

3) What can be said about the zeroes of $g'(\xi)$ if weaker assumptions are made about the solutions of equation 1.3.4 such as not assuming $g(\xi)$ is analytic at zero. 4) Are there any eigenvalue solutions of equation 1.2.13 if $f(\eta)$ is not a Section I injection solution. 5) Whether asymptotic solutions can be found for the Section IV(i) and V(i) solutions. 6) How the inclusion of exponentially small terms modify the asymptotic expansion obtained for the Section IV(ii) and Section V(ii) unsteady component of velocity. 7) Why resonance like effects occur for small frequency pulsatile pressure gradients at certain values of suction. The main numerical problem that needs further consideration is how to modify the numerical technique used to obtain more accurate solutions for the unsteady component of velocity for large suction.

Although there are many possibilities for varying the assumptions about the flow, we discuss here only the following three which are of particular interest or importance: 1) The introduction of an angular velocity component into the flow. Terrill and Thomas [25] have already shown the angular velocity component has some marked effects on the steady component of the flow in a uniformly porous tube. It would be interesting to examine how the unsteady component is effected. 2) The walls are not uniformly porous. A steady flow of this type has been discussed by Kozinski, Schmidt, and Lightfoot [9]. The problem for unsteady flow in this case

would be important for studying dialysis in the kidney. 3) The density is not constant. Unsteady flow in this case would be especially important to examine for its application to filtration problems.

APPENDIX A

COMMENTS ON STEADY FLOW IN A UNIFORMLY POROUS CHANNEL

Section A.1. Introduction.

In Section 1.1 it was noted Berman [2] was able to reduce the system of partial differential equations governing flow in a uniformly porous channel to an ordinary differential equation. Berman and others examined the solutions of this equation for various values of the crossflow Reynolds number R, where $R = \frac{Vd}{\nu}$ and where V is the velocity at which the fluid is being injected or extracted from the top and bottom of the channel, d is one-half the width of the channel, and ν is the viscosity of the fluid. The case of R negative indicates injection while the case of R positive indicates suction. Until 1970 only one solution for each crossflow Reynolds number had been reported. However in that year Raithby [16] reported obtaining numerically a second solution for large suction. Since for the tube problem, none, two or four solutions are possible for a given crossflow Reynolds number, it is of interest to examine the number of solutions possible for the channel problem.

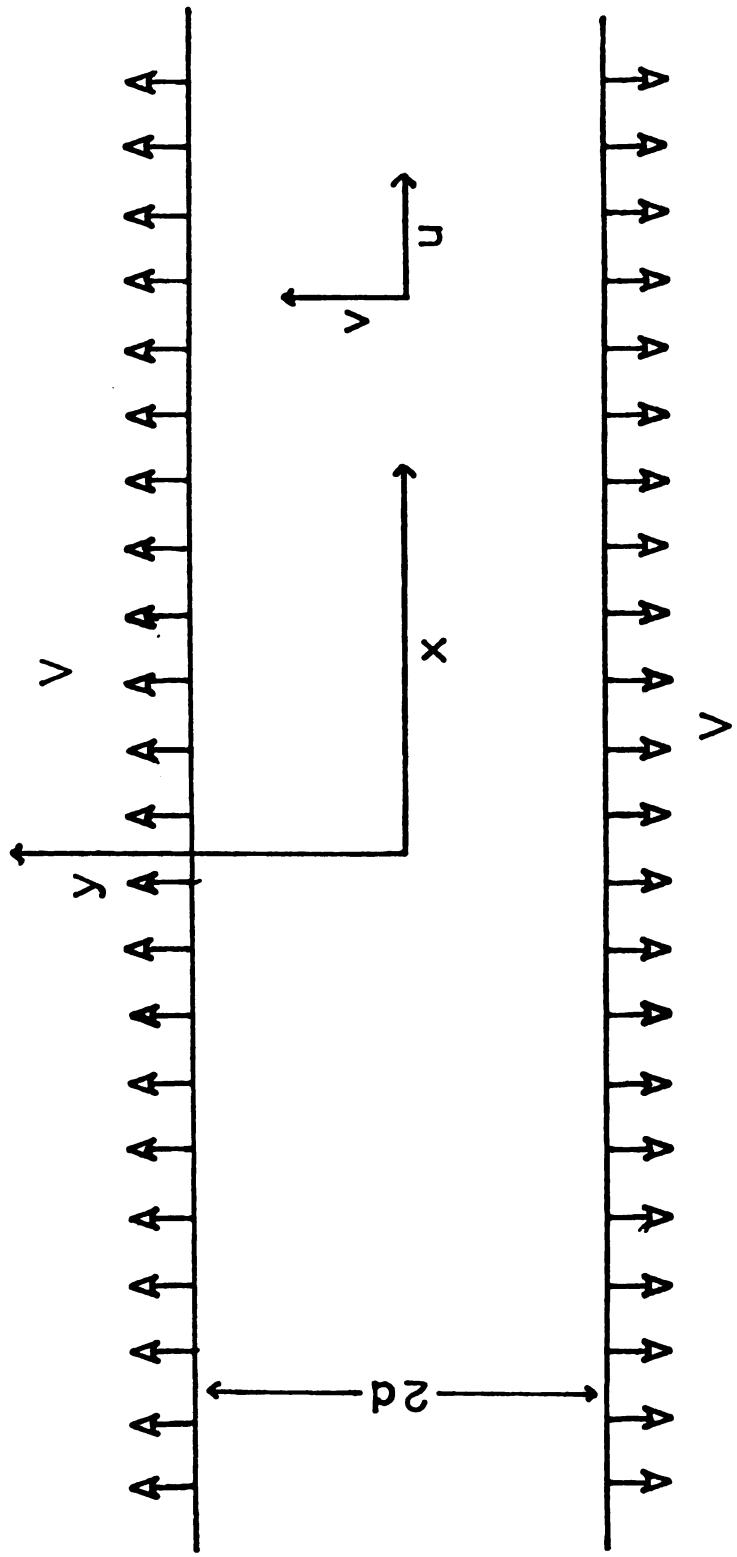

Figure A.1.1. Uniformly porous channel.

Consider flow in a long two dimensional channel from which fluid is being extracted or into which fluid is being injected at the same rate at top and bottom. (See Figure A.1.1). As in the case of the tube we assume the flow is laminar, the walls are uniformly porous, the flow is fully developed, and the density is constant. Under these assumptions the Navier-Stokes equations become:

A.1.1 $$uu_x + vu_y = -\frac{1}{\rho}p_x + \nu(u_{xx} + u_{yy})$$

$$uv_x + vv_y = -\frac{1}{\rho}p_y + \nu(v_{xx} + v_{yy})$$

and the equation of continuity becomes

A.1.2 $$u_x + u_y = 0$$

The boundary conditions are

A.1.3 $$u(x,\pm d) = 0 \qquad v(x,0) = 0$$

$$v(x,\pm d) = \pm V \qquad u_y(x,0) = 0$$

Since the flow is assumed to be fully developed v will be a function of y alone. This allows us to obtain from equation of continuity, equations of the following form for the velocity components:

A.1.4 $$u = -\frac{Vx}{d} f'(\eta) + u_0(\eta)$$

A.1.5 $$v = Vf(\eta)$$

where $\eta = y/d$.

Substituting equations A.1.4 and A.1.5 into the Navier-Stokes equations and applying the boundary conditions gives

A.1.6 $$f''' + R(f'^2 - ff'') = k$$

$$f(0) = 0 \qquad f(1) = 1$$

$$f''(0) = 0 \qquad f'(1) = 0$$

A.1.7 $$u_0'' + R(u_0 f' - u_0' f) = \ell$$

$$u_0'(0) = 0 \qquad u_0(1) = 0$$

where k and ℓ are constants determined from the pressure gradient. A particular solution of A.1.7 is obtained by setting

A.1.8 $$u_0(\eta) = \frac{\ell}{k} f'(\eta).$$

As in the case of the tube all other solutions of this equation may be considered as eigenvalues solutions. Therefore the important equation for describing flow in a uniformly porous channel is equation A.1.6 and the solutions of this equation are the ones we will examine here.

Using equations A.1.4, A.1.5 and A.1.8 we get that the shear stress or skin friction at the wall is given by

A.1.9 $$\tau_{xy} = \rho\nu\left(\frac{-Vx}{d^2} + \frac{\ell}{kd}\right) f''(1).$$

Section A.2. Completeness of the Problem of Steady Flow in a Uniformly Porous Channel.

By making the transformation

A.2.1 $$f(\eta) = \frac{b}{R}\, g(\xi)$$

where $x = b\eta$ equation A.1.6 becomes

A.2.2 $$g'''(\xi) + g'^{2}(\xi) - g(\xi)g''(\xi) = K$$

A.2.3 a) $g(0) = 0$ c) $bg(b) = R$

b) $g''(0) = 0$ d) $g'(b) = 0$

where $K = \frac{Rk}{b^4}$.

Since the transformation given by equation A.2.1 is nonsingular and from equations A.2.2 and A.2.3 it is seen that solutions of equation A.1.6 can be examined by studying the zeroes of $g'(\xi)$ for the solutions of the following initial value problem:

A.2.4 $$g''' = g''g - g'^{2} + K$$

a) $g(0) = 0$ c) $g'(0) = \alpha$ e) $K = \beta + \alpha^2$

b) $g''(0) = 0$ d) $g''(0) = \beta$

where α and β are non-zero real constants.

In the following discussion of this equation it will be assumed $g^{V}(\xi)$ is continuous.

Differentiating equation A.2.4 twice gives

A.2.5 $$g^{IV} = g'''g - g'g''$$

A.2.6 $$g^{V} = g^{IV}g - g''^{2}$$

Theorem A.2.1. For any solution $g(\xi)$ of equation A.2.4 $g'''(\xi)$ is a decreasing function of ξ.

Proof: It is sufficient to show $g^{IV}(\xi) \leq 0$ for all $\xi \geq 0$. Let $c \geq 0$ be any point such that $g^{IV}(c) = 0$. Then, by equation A.2.6, $g^{V}(c) = -g''^{2}(c) \leq 0$. Therefore at any point that g^{IV} is zero its slope is zero or decreasing. Therefore since $g^{IV}(0) = 0$, $g^{IV}(\xi) \leq 0$ for all $\xi \geq 0$. Q.E.D.

Theorem A.2.2. If $g'(0) = \alpha < 0$ and $g'''(0) = \beta < 0$ then for any solutions $g(\xi)$ of equation A.2.4 $g'(\xi) < 0$ for all $\xi \geq 0$.

Proof: Since $g'''(0) < 0$ and by Theorem A.2.1 $g''(\xi)$ is decreasing and concave down for all $\xi \geq 0$. Since $g''(0) = 0$, $g'(\xi)$ is also decreasing and concave down for all $\xi \geq 0$. Thus since $g'(0) < 0$, $g'(\xi) < 0$ for all $\xi \geq 0$. Q.E.D.

Theorem A.2.3. If $g'(0) = \alpha > 0$ and $g'''(0) = \beta > 0$ then for any solution $g(\xi)$ of equation A.2.4 $g'(\xi)$ has one and only one zero. See Figure A.2.1. for a qualitative description of this solution.

The proof will be contained in the following two lemmas.

Lemma A.2.1. In this case $g'(\xi)$ has at least one zero.

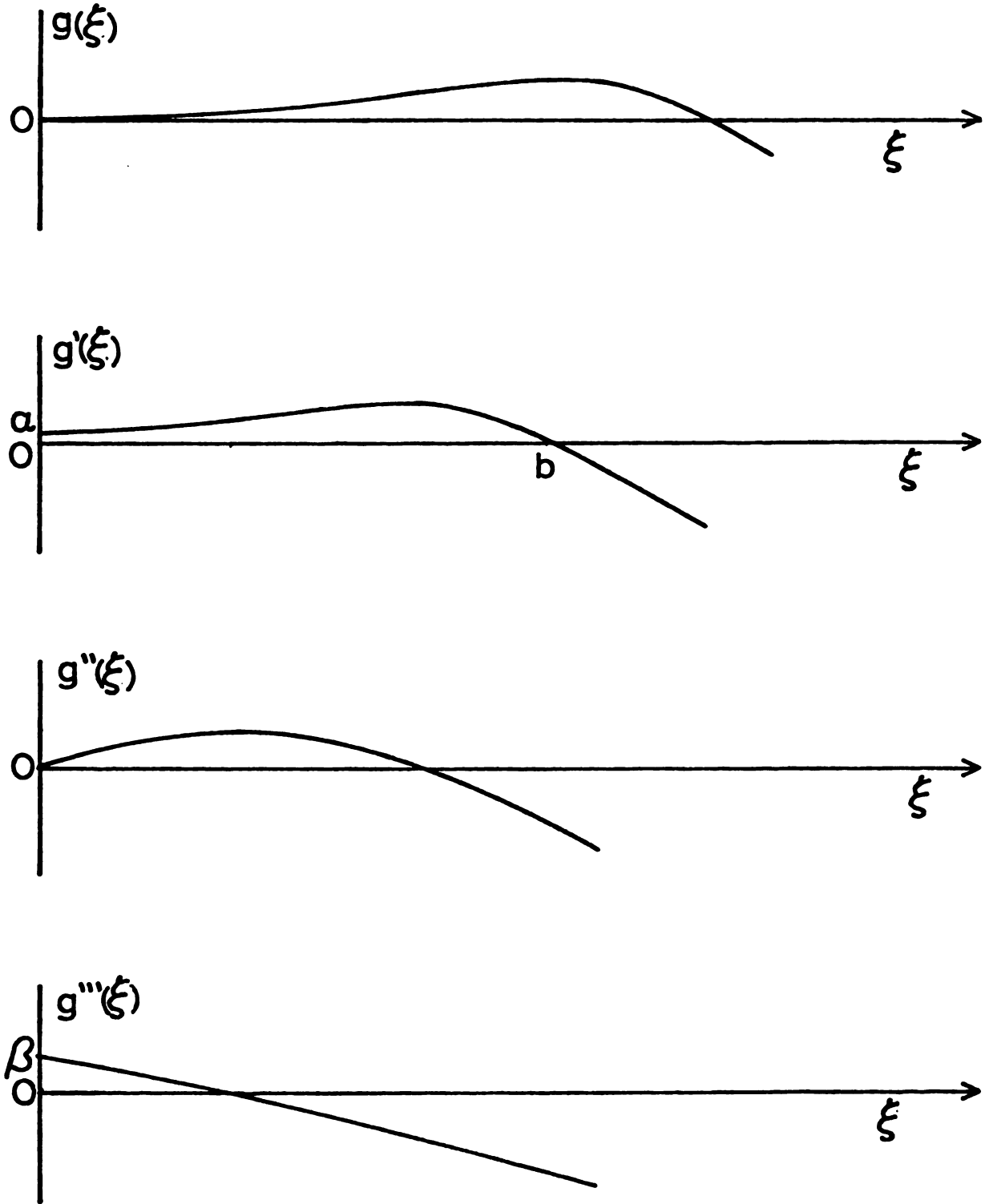

Figure A.2.1.
The solution of equation A.2.2. for $\alpha>0$ and $\beta>0$. The concavity of $g'''(\xi)$ is undetermined.

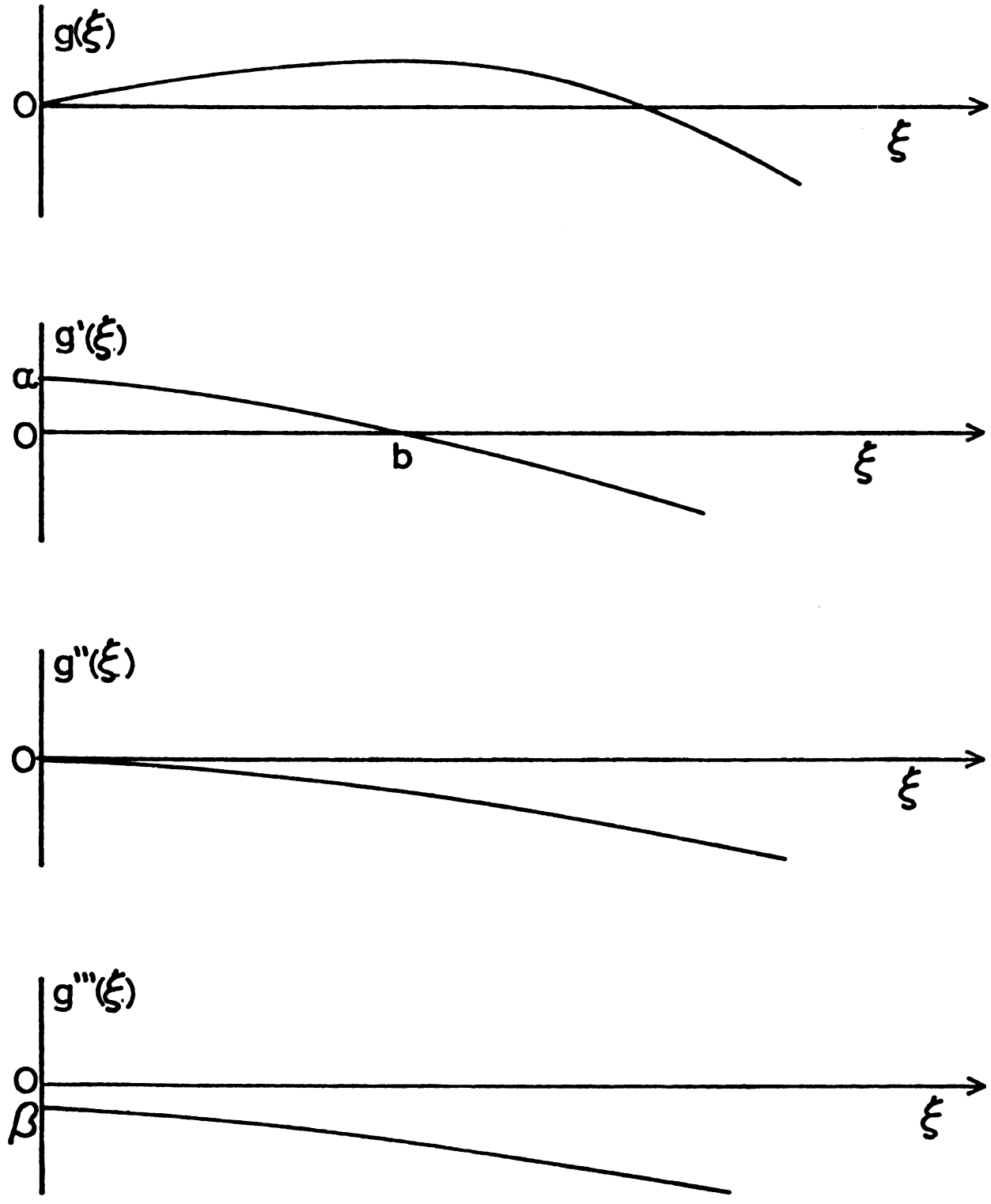

Figure A.2.2.
The solution of equation A.2.2. for $\alpha>0$ and $\beta<0$. The concavity of $g'''(\xi)$ is undetermined.

Proof: Suppose $g'(\xi) > 0$ for all $\xi \geq 0$. Then since $g(0) = 0$, $g(\xi) \geq 0$ for all $\xi \geq 0$. Since $g^{IV}(\xi) = 0$ for all $\xi \geq 0$ by Theorem A.2.1, $g^{V}(\xi) = g^{IV}(\xi)g(\xi) - g''(\xi)^2 \leq 0$ for all $\xi \geq 0$. Therefore $g'''(\xi)$ is decreasing and concave down for all $\xi \geq 0$. Hence $g'''(\xi)$ must cross the ξ-axis. This would make $g''(\xi)$ decreasing and concave down and thus $g''(\xi)$ must cross the ξ-axis. This in turn makes $g'(\xi)$ decreasing and concave down and thus it too must cross the ξ-axis. This contradicts the assumption $g'(\xi) > 0$ for all $\xi \geq 0$. Therefore there is a point b such that $g'(b) = 0$. Q.E.D.

At b $g(\xi)$ and its derivatives have the following properties

$g(b) > 0$ $\quad$ $g'(b) = 0$ $\quad$ $g''(b) < 0$ $\quad$ $g'''(b) < 0$

By equation A.2.3c this gives $R > 0$. The solutions of equation A.1.6 corresponding to this zero will be designated a Section II(ii) solution. By equation A.2.4e we have also that in this case $K > 0$.

Lemma A.2.2. In this case there are no further zeroes of $g'(\xi)$.

Proof: Since $g'''(b) < 0$, $g''(b) < 0$ and by Theorem A.2.1 $g''(\xi) < 0$ for all $\xi \geq b$. Therefore since $g'(b) = 0$, $g'(\xi) < 0$ for all $\xi \geq b$. Q.E.D.

Theorem A.2.4. If $g'(0) > 0$ and $g'''(0) < 0$ then for any solution $g(\xi)$ of equation A.2.4 $g'(\xi)$ has exactly one zero. See Figure A.2.3 for a qualitative description of this solution.

Proof: Since $g'''(0) < 0$ and by Theorem A.2.1 $g'''(\xi) < 0$ for all $\xi \geq 0$. Thus since $g''(0) = 0$, $g''(\xi) < 0$ for all $\xi > 0$. Hence since $g'(0) > 0$ and $g'(\xi)$ is decreasing and concave down there is a point b such that $g''(b) = 0$. That $g'(\xi)$ has no further zeroes follows by the same arguments as used in the proof of Lemma A.2.2. Q.E.D.

At b $g(\xi)$ and its derivatives have the following properties.

$g(b) > 0$ $\quad$ $g'(b) = 0$ $\quad$ $g''(b) < 0$ $\quad$ $g'''(b) < 0$

By equation A.2.3d this gives $R > 0$. The solution of equation A.1.6 corresponding to this zero will be designated a Section I solution for suction.

Theorem A.2.5. If $g'(0) < 0$ and $g'''(0) > 0$ then for any solution $g(\xi)$ of equation A.2.4 $g'(\xi)$ has two zeroes. See Figure A.2.3 for a qualitative description of this case.

This theorem will be proven by a series of lemmas.

Lemma A.2.3. In this case there is a point c such that $g'''(c) = 0$.

Proof: Suppose $g'''(\xi) > 0$ for all $\xi \geq 0$. Then since $g''(0) = 0$, $g''(\xi) \geq 0$ for all $\xi \geq 0$. Thus $g'(\xi)$ is increasing and concave up for all $\xi \geq 0$. Thus $g'(\xi)$ must cross the ξ-axis making $g(\xi)$ increasing and concave up. Hence $g(\xi)$ must also cross the ξ-axis. This gives then

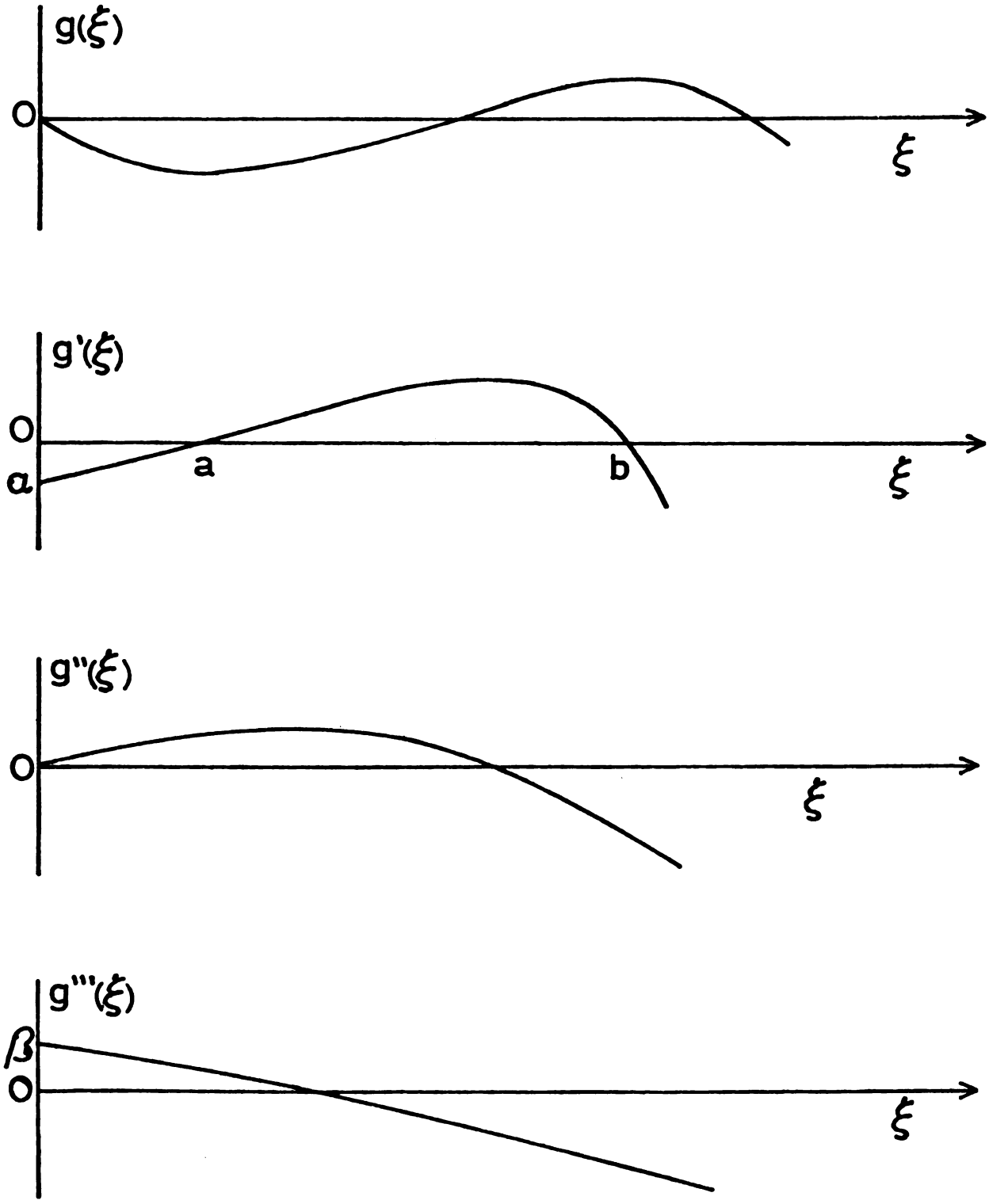

Figure A.2.3.

The solution of equation A.2.2. for $\alpha<0$ and $\beta>0$. The concavity of $g'''(\xi)$ is undetermined.

that $g^{V} = g^{IV}g - g''^{2} < 0$. Thus making $g'''(\xi)$ decreasing and concave down. Hence $g'''(\xi)$ must go negative. This contradicts the assumption $g'''(\xi) > 0$ for all $\xi \geq 0$. Therefore there is a point c such that $g'''(c) = 0$. Q.E.D.

Lemma A.2.4. There is a point $a < c$ such that $g'(a) = 0$.

Proof: Since at c $g'''(c) = 0$, equation A.2.5 gives $g^{IV}(c) = -g'(c)g''(c)$. Since $g''(c) > 0$ and $g^{IV}(c) < 0$, $g'(c) > 0$. Thus since $g'(0) < 0$ there is a point $a < c$ such that $g'(a) = 0$. Q.E.D.

At a $g(\xi)$ and its derivatives have the following properties.

$g(a) < 0$ $\quad$ $g'(a) = 0$ $\quad$ $g''(a) > 0$ $\quad$ $g'''(a) > 0$

By equation A.2.3c this gives $R < 0$. The solution of equation A.1.6 corresponding to this zero will be designated a Section I solution for injection. By equation A.2.4e we have also that in this case $K > 0$.

Lemma A.2.5. There is a point $b > c$ such that $g'(b) = 0$.

Proof: Since at c $g'''(c) = 0$ and by Theorem A.2.1 $g'''(\xi) < 0$ for all $\xi > c$. Therefore $g''(\xi)$ is decreasing and concave down and hence must cross the ξ-axis. This in turn makes $g'(\xi)$ decreasing and concave down. Hence there must be a point $b > c$ such that $g'(b) = 0$. Q.E.D.

From equation A.2.5 we have that at b $g^{IV}(b) = g'''(b)g(b)$. Since $g^{IV}(b) < 0$ and $g'''(b) < 0$ we have $g(b) \geq 0$.

Therefore at b $g(\xi)$ and its derivatives have the following properties.

$$g(b) > 0 \qquad g'(b) = 0 \qquad g''(b) < 0 \qquad g'''(b) < 0$$

By equation A.2.3c this gives $R > 0$. The solution of equation A.1.6 corresponding to this zero will be designated as a Section II(i) solution. In this case as above we also have $K > 0$.

Lemma A.2.6. There are no further zeroes for $g'(x)$.

Proof: The same as for Lemma A.2.2.

Section A.3. Numerical Results.

Numerical solutions were obtained for equation A.1.6 by a method similar to that discussed in Section 2.1. These results are summarized by plotting $-f''(1)$, which, as shown by equation A.1.9, is proportional to the skin friction at the wall. Only one solution was found for $R < 12.2$ but three solutions were found for $R \geq 12.2$. The Section I solutions have been found previously and discussed extensively in the literature and the Section II(ii) solution was found numerically by Raithby [16]. The Section II(i) solution has not been reported previously in the literature.

The characteristics of each solution will be discussed briefly here.

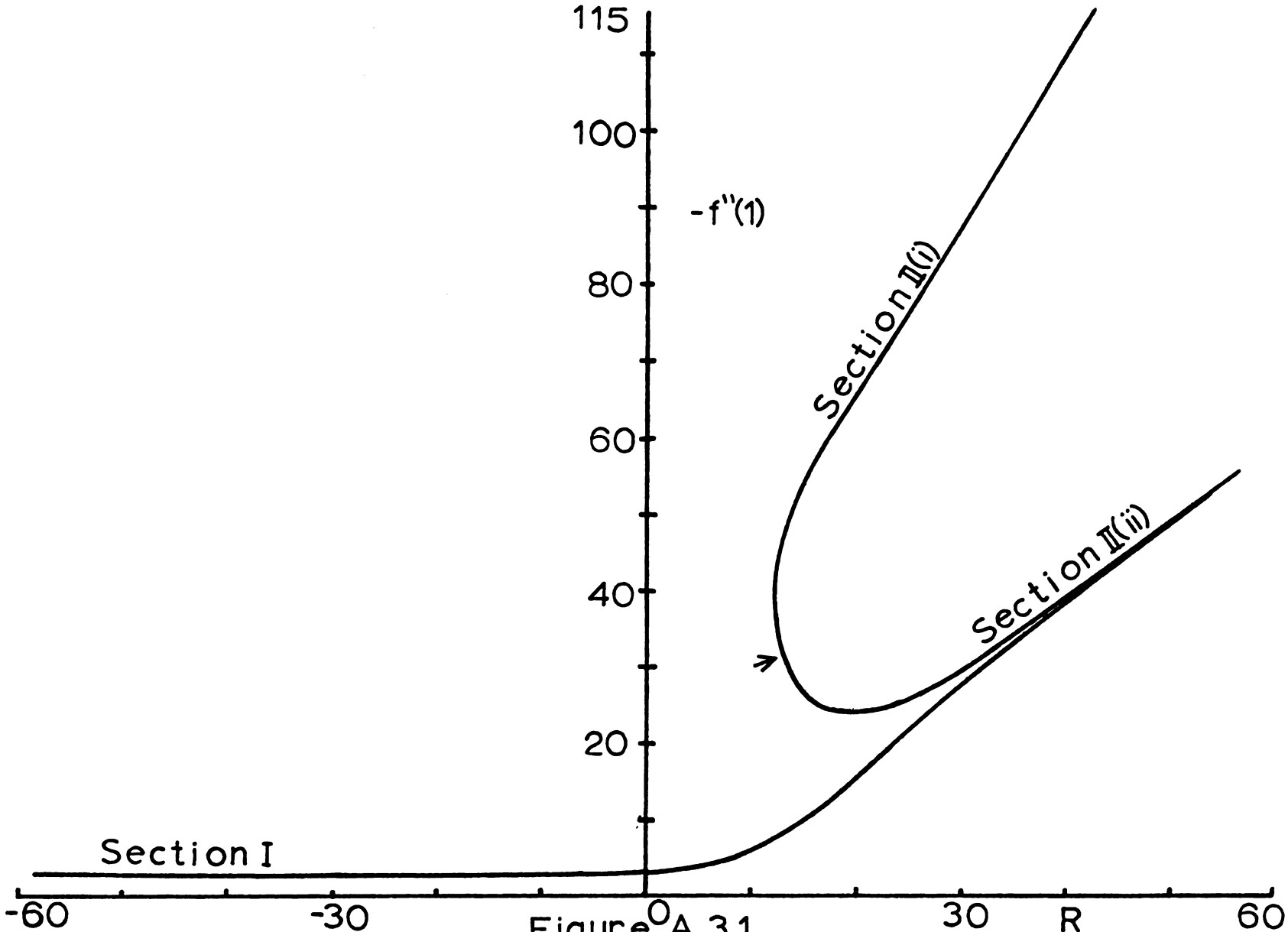

Figure A.3.1.
Skin friction at the wall.

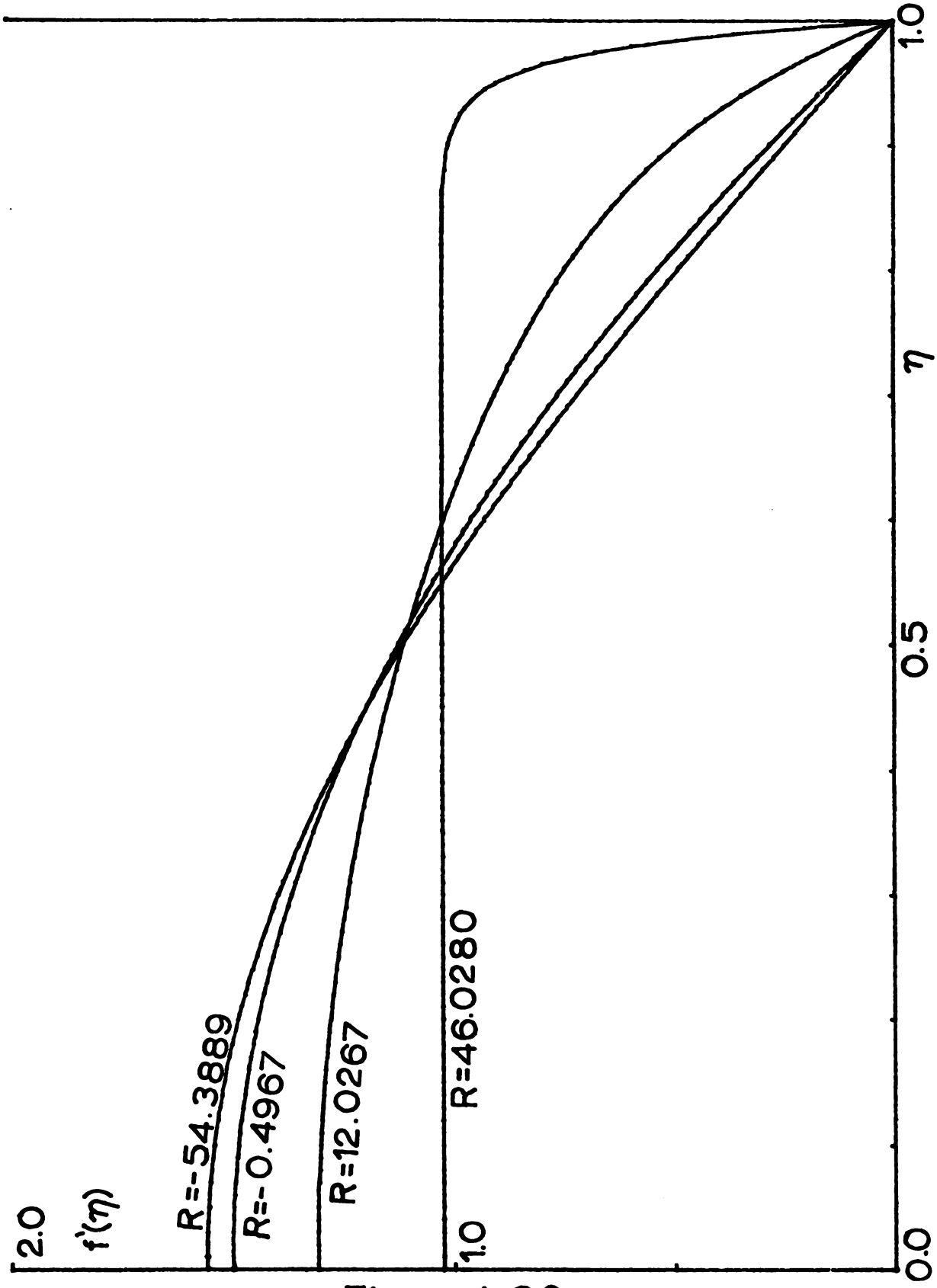

Figure A.3.2.

Axial velocity profiles for Section I solutions.

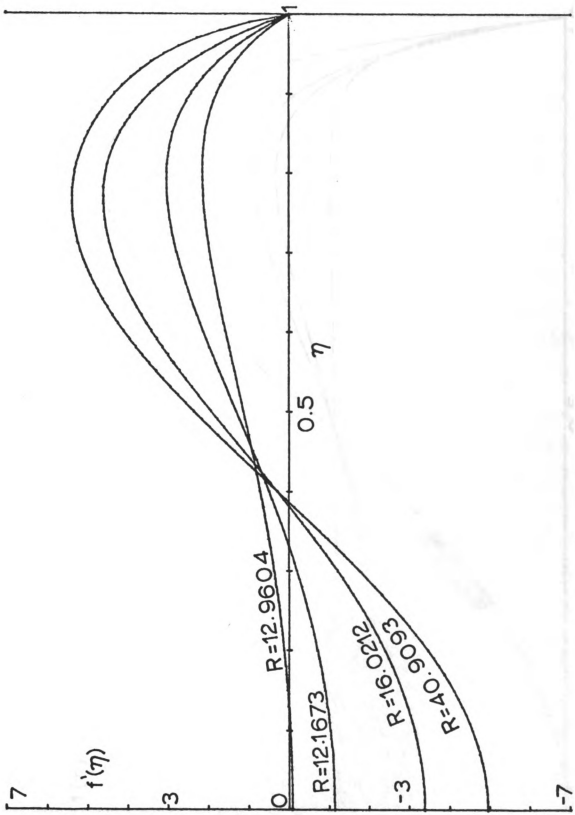

Figure A.3.3.
Axial velocity profiles for Section II(i) solutions.

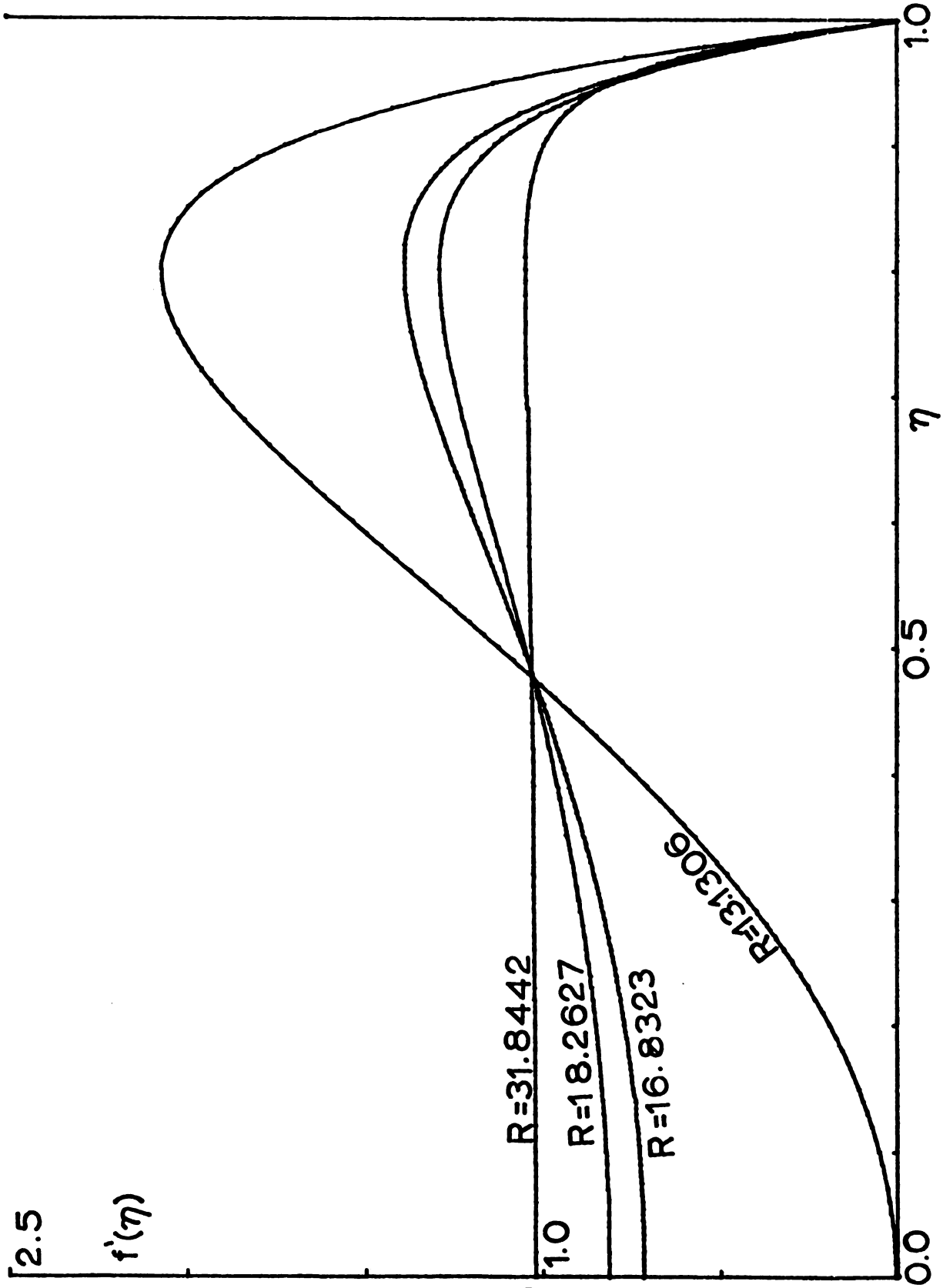

Figure A.3.4.

Axial velocity profiles for Section II(ii) solutions.

1) Section I solutions $(-\infty < R < \infty)$. In Figure A.3.2 several axial velocity profiles of Section I solutions are graphed. The Section I solutions are all well behaved and exhibit no reverse flow. These solutions are in many ways similar to the Section I and Section IV(ii) solutions for steady flow through a uniformly porous tube.

2) Section II(i) solutions $(12.2 < R < \infty)$. Several axial velocity profiles for these solutions are given in Figure A.3.3. For this case there are two solutions for $12.2 < R < 13.1$. These solutions exhibit a region of reverse flow near the center of the channel.

3) Section II(ii) solutions $(13.1 < R < \infty)$. Several axial velocity profiles for this case are given in Figure A.3.4. These solutions exhibit no reverse flow but do have an inflection point. It should be noted that as $R \to +\infty$ the Section II(ii) and Section I solutions approach the same axial velocity profile. This behavior is very similar to the case of Section IV(ii) and Section V(ii) solutions for steady flow in a uniformly porous tube. Also as $R \to 13.1$ the Section II(i) and Section II(ii) solutions approach the same axial velocity profile.

BIBLIOGRAPHY

BIBLIOGRAPHY

[1] Batchelor, G.K., An Introduction to Fluid Dynamics, Cambridge University Press, (1970).

[2] Berman, A.S., "Laminar Flow in Channels with Porous Walls", Journal of Applied Physics, Vol. 24, No. 9, (1953), pp. 1243-1235.

[3] Berman, A.S., "Effects of Porous Boundaries on the Flow of Fluids in Systems with Various Geometries", Proceedings Second United Nations International Conference on the Peaceful Uses of Atomic Energy, Geneva, Vol. 4, (1958), pp. 351-358.

[4] Bundy, R.D. and Weissberg, H.L., "Experimental Study of Fully Developed Laminar Flow in a Porous Pipe with Wall Injection", Physics of Fluids, Vol. 13, (1970), pp. 2613-2615.

[5] Carnahan, B., Luther, H.A. and Wilkes, J.O., Applied Numerical Methods, John Wiley and Sons, Inc., (1969).

[6] Eckert, E.R.G., Donoughe, P.L. and Moore, B.J., "Velocity and Friction Characteristics of Laminar Viscous Boundary-Layer and Channel Flow over Surfaces with Ejection or Suction", NACA TN 4102, (1957).

[7] Isaacson, E. and Keller, H.B., Analysis of Numerical Methods, John Wiley and Sons, Inc., (1966).

[8] Kinney, R.B., "Fully Developed Frictional and Heat Transfer Characteristics of Laminar Flow in Porous Tubes", International Journal of Heat and Mass Transfer, Vol. 11, (1968), pp. 1393-1401.

[9] Kozinski, A.A., Schmidt, F.P. and Lightfoot, E.N., "Velocity Profiles in Porous-Walled Ducts", Industrial Engineering and Chemical Fundamentals, Vol. 9, (1970), pp. 502-505.

[10] Lightfoot, E.N., Transport Phenomena and Living Systems, John Wiley and Sons, Inc., (1974).

[11] Morduchow, M., "On Laminar Flow through a Channel or Tube with Injection: Applications of Method of Averages", Quarterly Journal of Applied Mathematics, Vol. XIV, No. 4, (1957), pp. 361-368.

[12] Nayfeh, A., Perturbation Methods, John Wiley and Sons, Inc., (1973).

[13] Peng, Y. and Yuan, S.W., "Laminar Pipe Flow with Mass Transfer Cooling", Journal of Heat Transfer, Vol. 87, (1965), pp. 252-258.

[14] Prayer, S., "Spiral Flow in a Stationary Porous Pipe", Physics of Fluids, Vol. 7, (1964), pp. 907-908.

[15] Quaile, J.P. and Levy, E.K., "Laminar Flow in a Porous Tube with Suction", Journal of Heat Transfer, Vol. 97, (1975), pp. 66-71.

[16] Raithby, G., "Laminar Heat Transfer in the Thermal Entrance Region of Circular Tubes and Two-Dimensional Rectangular Ducts with Wall Suction and Injection", International Journal of Heat and Mass Transfer, Vol. 14, (1971), pp. 223-243.

[17] Richardson, E.G. and Tyler, E., "The Transverse Velocity Gradient Near the Mouths of Pipes in which an Alternating or Continuous Flow of Air is Established", The Proceedings of the Physical Society, Vol. 42, Part I, (1929), pp. 1-15.

[18] Schlichting, H., Boundary-Layer Theory, McGraw Hill Book Company, (1968).

[19] Sexl, T., "Über den von E.G. Richardson entdecken „Annulareffeckt"", Zeitschrift Physics, Vol. 61, (1930), pp. 349-362.

[20] System /360 Scientific Subroutine Package Version III Programmer's Manual, Program Number 360A-CM-03X, International Business Machines Corporation, fifth edition, (1966, 1967, 1968), pp. 333-336.

[21] Terrill, R.M., "Laminar Flow in a Uniformly Porous Channel", The Aeronautical Quarterly, Vol. XV, (1964), pp. 299-310.

[22] Terrill, R.M., "Laminar Flow in a Uniformly Porous Channel with Large Injection", The Aeronautical Quarterly, Vol. XVI, (1965), pp. 323-332.

[23] Terrill, R.M., "On Some Exponentially Small Terms Arising in Flow Through a Porous Pipe", Q. Jl. Mech. Appl. Math., Vol. XXVI, Pt. 3, (1973), pp. 347-354.

[24] Terrill, R.M. and Thomas, P.W., "On Laminar Flow Through a Uniformly Porous Pipe", Applied Scientific Research, Vol. 21, (1969), pp. 37-67.

[25] Terrill, R.M. and Thomas, P.W., "Spiral Flow in a Porous Pipe", The Physics of Fluids, Vol. 16, No. 3, (1973), pp. 356-359.

[26] Uchida, S., "The Pulsating Viscous Flow Superposed on the Steady Laminar Motion of Incompressible Fluid in a Circular Pipe", ZAMP, Vol. VII, (1956), pp. 403-422.

[27] Van Dyke, M., Perturbation Methods in Fluid Mechanics, Academic Press, (1964).

[28] Wang, C.-Y., "Pulsatile Flow in a Porous Channel", Journal of Applied Mechanics, Vol. 38, (1971), pp. 553-555.

[29] Weissberg, H.L., "Laminar FLow in the Entrance Region of a Porous Pipe", The Physics of Fluids, Vol. 2, No. 5, (1959), pp. 510-516.

[30] White, F.M., "Laminar Flow in a Uniformly Porous Tube", Journal of Applied Mechanics, Vol. 29, (1962), pp. 201-204.

[31] Womersley, J.R., "An Elastic Tube Theory of Pulse Transmission and Oscillatory Flow in Mammalian Arteries", WADC Technical Report TR 56-614, (1957).

[32] Yih, C.-S., Fluid Mechanics, McShaw Hill Book Company, (1969).

[33] Yuan, S.W. and Finkelstein, A.B., "Laminar Pipe Flow with Injection and Suction Through a Porous Wall", Transaction ASME, Vol. 87, (1956), pp. 719-724.